

สัปดาห์ที่มีประสิทธิภาพของคอนกรีตมวลหนักสำหรับการป้องกันรังสีแกมมาและคุณสมบัติ  
เชิงกลของคอนกรีต



บทคัดย่อและแฟ้มข้อมูลฉบับเต็มของวิทยานิพนธ์ตั้งแต่ปีการศึกษา 2554 ที่ให้บริการในคลังปัญญาจุฬาฯ (CUIR)  
เป็นแฟ้มข้อมูลของนิสิตเจ้าของวิทยานิพนธ์ ที่ส่งผ่านทางบัณฑิตวิทยาลัย

The abstract and full text of theses from the academic year 2011 in Chulalongkorn University Intellectual Repository (CUIR)  
are the thesis authors' files submitted through the University Graduate School.

วิทยานิพนธ์นี้เป็นส่วนหนึ่งของการศึกษาตามหลักสูตรปริญญาวิศวกรรมศาสตรมหาบัณฑิต  
สาขาวิชาวิศวกรรมโยธา ภาควิชาวิศวกรรมโยธา  
คณะวิศวกรรมศาสตร์ จุฬาลงกรณ์มหาวิทยาลัย  
ปีการศึกษา 2558  
ลิขสิทธิ์ของจุฬาลงกรณ์มหาวิทยาลัย

EFFECTIVE MIX DESIGN OF HEAVYWEIGHT CONCRETE FOR GAMMA-  
RAY SHIELDING AND MECHANICAL PROPERTIES OF CONCRETE

Mr. Pamuko Aditya Rahman



A Thesis Submitted in Partial Fulfillment of the Requirements  
for the Degree of Master of Engineering Program in Civil Engineering

Department of Civil Engineering

Faculty of Engineering

Chulalongkorn University

Academic Year 2015

Copyright of Chulalongkorn University



พามูโก อาดิทยา ราห์มาน : สัดส่วนผสมที่มีประสิทธิภาพของคอนกรีตมวลหนักสำหรับการป้องกันรังสีแกมมาและคุณสมบัติเชิงกลของคอนกรีต (EFFECTIVE MIX DESIGN OF HEAVYWEIGHT CONCRETE FOR GAMMA-RAY SHIELDING AND MECHANICAL PROPERTIES OF CONCRETE) อ.ที่ปรึกษาวิทยานิพนธ์หลัก: วิจิต ปานสุข, อ.ที่ปรึกษาวิทยานิพนธ์ร่วม: นเรศร์ จันทน์ขาว, 103 หน้า.

คอนกรีตมวลหนักที่ใช้เป็นวัสดุป้องกันรังสีสามารถใช้ประโยชน์โดยมิใช่เพียงแค่ว่าสำหรับโรงไฟฟ้าพลังงานนิวเคลียร์ แต่รวมไปถึงในด้านการแพทย์ อุตสาหกรรม และสำหรับแหล่งกำเนิดรังสีเพื่อการเกษตร และเนื่องจากการศึกษาวิจัยด้านงานโครงสร้างจากคอนกรีตมวลหนักมีไม่มากนักจึงเป็นที่มาของงานวิจัยนี้ โดยคอนกรีตมวลหนักในงานวิจัยนี้ใช้แบไรต์ (BaSO<sub>4</sub>) เป็นส่วนผสมหลักเนื่องจากหาได้ง่ายในประเทศ มีการปรับเปลี่ยนส่วนผสมระหว่างมวลรวมปกติและแบไรต์เพื่อหาสัดส่วนผสมที่ทำให้ได้วัสดุที่มีประสิทธิภาพสูงสุด โดยงานวิจัยนี้ได้ทำการหาคุณสมบัติเชิงกลและความสามารถในการป้องกันรังสีแกมมาสำหรับสัดส่วนผสมต่างๆทั้งหมด 20 สัดส่วนผสม โดยมีการเปลี่ยนแปลงค่าอัตราส่วนน้ำต่อปูนซีเมนต์ 2 อัตราส่วน และค่าเปอร์เซ็นต์การแทนที่มวลรวมปกติ 4 ค่า การทดสอบรังสีกระทำโดยใช้ ซีเซียม-137 และ โคบอลต์-60 เป็นแหล่งกำเนิดรังสี โดยทำการตรวจวัดสัมประสิทธิ์การลดทอนเชิงเส้น ( $\mu$ ) ของคอนกรีตมวลหนัก ด้วยการตรวจวัดที่การทดสอบด้วยพลังงาน 0.662 MeV และ ค่าเฉลี่ย 1.250 MeV (ระหว่าง 1.173 และ 1.332 MeV) ตามลำดับ งานวิจัยนี้สรุปได้ว่าการแทนที่มวลรวมหยาบด้วยมวลรวมปกติจะได้ผลดีที่สุดในด้านความสามารถทางสมการดังกล่าว ประเมินค่าได้ต่ำกว่าผลการทดลอง นอกจากนี้พบว่าการแทนที่ทรายปกติในสัดส่วนผสมมีผลต่อค่าสถิติฟเนสของคาน และเปอร์เซ็นต์ของแบไรต์ในสัดส่วนผสมเป็นตัวแปรหลักที่ส่งผลต่อค่าความเหนียว โดยไม่มีความสัมพันธ์กับอัตราส่วนน้ำต่อปูนซีเมนต์และชนิดการแทนที่มวลรวมในสัดส่วนผสม

ภาควิชา วิศวกรรมโยธา

สาขาวิชา วิศวกรรมโยธา

ปีการศึกษา 2558

ลายมือชื่อนิสิต .....

ลายมือชื่อ อ.ที่ปรึกษาหลัก .....

ลายมือชื่อ อ.ที่ปรึกษาร่วม .....

# # 5770505121 : MAJOR CIVIL ENGINEERING

KEYWORDS: HEAVYWEIGHT CONCRETE / GAMMA-RAY SHIELDING / MECHANICAL PROPERTIES / FLEXURAL BEHAVIORS RC BEAM

PAMUKO ADITYA RAHMAN: EFFECTIVE MIX DESIGN OF HEAVYWEIGHT CONCRETE FOR GAMMA-RAY SHIELDING AND MECHANICAL PROPERTIES OF CONCRETE. ADVISOR: ASSOC. PROF. WITHIT PANSUK, Ph.D., CO-ADVISOR: ASSOC. PROF. NARES CHANKOW, 103 pp.

Utilization of heavyweight concrete as radiation shielding has bringing benefits not only in energy for nuclear power plant, but also accelerators in medical and in industrial, then in radiation sources for agricultural field. The lack of experiment related to structural member in heavyweight concrete is a reason in performing this study. Concrete that were resulted for this study restricted to barite ( $BaSO_4$ ) as heavy material that highly available in Thailand. Modification experiment was expected to achieve effective barite concrete mixture using local material from Thailand. This experiment will evaluate mechanical properties of barite concrete, attenuation of gamma-ray, and barite reinforced concrete beam as parameter to determine the effectiveness of the mixture. 20 different barite concrete mixtures with 2 variations of w/c ratios and 4 classifications of replacement percentage aggregate will be examined. Using Cesium-137 and Cobalt-60 energy sources, linear attenuation coefficient ( $\mu$ ) of barite concrete will be measured at two different energies which are 0.662 MeV and average 1.250 MeV (combination 1.173 MeV and 1.332 MeV), respectively. We concluded that replacement coarse aggregate with normal aggregate deemed most advantageous in term of workability of concrete. In relation with provision standard, ACI 349-06 equation is not applied for barite concrete due to underestimated. Contribution replacement normal sand in mixture is affected in stiffness of the beam. Moreover, percentage barite in the mixture had main role in ductility factor and not correlated with number of w/c ratio and type of replacement aggregate in the mixture.

Department: Civil Engineering

Student's Signature .....

Field of Study: Civil Engineering

Advisor's Signature .....

Academic Year: 2015

Co-Advisor's Signature .....

## ACKNOWLEDGEMENTS

I would like to express my sincere appreciation to several peoples who supporting, assisting, and advising me to complete this thesis successfully.

My deepest gratitude goes to my supervisor, Associate Professor Withit Pansuk, Ph.D., whose continuous support, constructive comments, guidance, and encouragement throughout my master study and research. I would like to thank my committee members: Associate Professor Nares Chankow, Pitcha Jongvivatsakul, Ph.D., and Assistant Professor Dr. Meng Jing, for their suggestion, importance advices, and constructive comments for improving my research. I am also deeply grateful to Dr. Chalermpong Polee and Mr. Pongyuth Sriploy at Nuclear Engineering Laboratory for their assistance and Mr. Utis Thongklueang at Mining and Petroleum Engineering for providing raw materials.

I sincerely acknowledge the cooperation and support to Chulalongkorn University ASEAN Scholarship Programme to make possible studying here. I also appreciate PT. Wijaya Karya (Persero), Tbk for emotional supports and permission to continue my master degree.

I am grateful to all friends and fellow in Structural Engineering, Department of Civil Engineering, Mr. Chanachai Thongchom, Ms. Penpitcha Krittayakornnupong, Mr. Sakkasem Suwarnarat, Mr. Cao Nguyen Thi, Mr. Thuc Nguyen Nhu, Mr. Nguyen Thanh Tung, and Ms. Nguyen Thi Chung for their joyful, support, and their encouragement. I am also thankful to my Indonesia friends: Ms. Dyah Anantalia Widyastari, Mr. Doni Marisi Sinaga, and Mr. Beni Adi Trisna for their friendship, cheerful gathering, and emotional supports.

I would like to thank to my family; my parent: Lusdiyono and Cey Hetty, my siblings Rizkia Prabandini Rahmanita and Mufid Abdurrahman, and my aunt Cey Yully for their unlimited love, support, and encouragement.

Lastly, I would like to send gratitude to everyone whom I forget to mention to support and help me during my study.

## CONTENTS

	Page
THAI ABSTRACT .....	iv
ENGLISH ABSTRACT .....	v
ACKNOWLEDGEMENTS .....	vi
CONTENTS .....	vii
LIST OF FIGURES.....	x
LIST OF TABLES .....	xiv
CHAPTER 1 Introduction.....	1
1.1 General Review.....	1
1.2 Objectives and Scope of Works .....	3
1.3 Outlines.....	5
CHAPTER 2 Literature Review.....	6
2.1 Background .....	6
2.2 Heavyweight Concrete .....	7
2.3 Radiation Transmission.....	10
2.4 Mixed Design of Heavyweight Concrete and Radiation Testing.....	14
2.4.1 Mixture of Barium Minerals.....	14
2.4.2 Mixture of Combination Barium Mineral with Iron Minerals .....	19
2.4.3 Mixture of Iron Minerals.....	22
2.4.4 Mixture of Synthetic Aggregate .....	30
2.5 Mixture Based on American Concrete Institute (ACI) and American Society for Testing and Materials International (ASTM).....	32
CHAPTER 3 Research Methodology .....	36
3.1 Physical and Mechanical Properties of Aggregates .....	36

	Page
3.1.1 Gradation, Wear, and Organic Content.....	37
3.1.2 Specific Gravity and Water Absorption.....	37
3.1.3 Bulk Density (Unit Weight) and Void in Aggregates.....	38
3.2 Experiment Problems.....	39
3.2.1 Mix Design and Specimen.....	40
3.2.1.1 Material.....	40
3.2.1.2 Specimen.....	41
3.2.1.3 Mix Design.....	42
3.2.2 Radiation Attenuation Test.....	44
3.2.3 Heavyweight Reinforced Concrete Beam Test.....	46
CHAPTER 4 Result and Discussion.....	49
4.1 Physical and Chemical Properties of Aggregates.....	49
4.2 Workability of Concrete.....	53
4.3 Unit Weight of Concrete.....	54
4.4 Mechanical Properties of Barite Concrete.....	56
4.4.1 Compressive Strength.....	56
4.4.2 Stress-Strain Relationship.....	58
4.4.3 Modulus of Elasticity and Poisson's Ratio.....	60
4.4.3.1 Modulus of Elasticity.....	60
4.4.3.2 Poisson's Ratio.....	63
4.5 Attenuation of Gamma-ray.....	64
4.6 Heavyweight Reinforcement Concrete Beam.....	69
4.6.1 Failure Mode and Load-Deflection Characteristic.....	69

	Page
4.6.1.1 Load-Deflection Behaviour .....	69
4.6.1.2 Reinforcement Bar Behaviour .....	72
4.6.2 Flexural Stiffness.....	75
4.6.3 Ductility Index .....	76
4.6.4 Crack Pattern .....	78
4.6.4.1 Crack Pattern at Load 40 kN .....	78
4.6.4.2 Crack Pattern at Ultimate Load.....	81
4.7 Design Analysis ACI 349-06.....	86
4.7.1 Design for Flexural Strength of Barite Concrete.....	86
4.7.1.1 Basic Consideration.....	86
4.7.1.2 Flexural Behaviour .....	87
4.7.1.3 Design Calculation.....	88
Calculation of cracking load .....	89
Calculation of ultimate flexural capacity.....	89
4.7.2 Design for Shear Strength of Barite Concrete .....	91
CHAPTER 5 Conclusion and Recommendation .....	94
5.1 Conclusion of Experimental Result .....	94
5.2 Recommendation for Future Work.....	96
REFERENCES .....	97
VITA.....	103

## LIST OF FIGURES

<b>Figure 1.1</b> Absorption power in different types of radiation rays[3].....	2
<b>Figure 2.1</b> Distribution and variation heavyweight concrete in Thailand[8].....	9
<b>Figure 2.2</b> The Exponential Law of Radiation Attenuation[10] .....	10
<b>Figure 2.3</b> Gamma-rays propagation with different media absorbers and energies[10].....	11
<b>Figure 2.4</b> Interaction processes for obtaining Total Attenuation Coefficient[10].....	12
<b>Figure 2.5</b> Contribution of each interaction processes due to attenuation coefficient and density of material[11].....	13
<b>Figure 2.6</b> The value of mass attenuation coefficient several elements[10].....	13
<b>Figure 2.7</b> Linear Attenuation Coefficients Result of Combination Series by using photon energies 0.66 MeV and 1.33 MeV[12].....	15
<b>Figure 2.8</b> Distribution of compressive strength and Schmidt hardness by different w/c ratio[18].....	19
<b>Figure 2.9</b> Linear attenuation coefficient of different density of concrete by 0.622 MeV, 1.173 MeV, and 1.332 MeV energy resources[25].....	21
<b>Figure 2.10</b> Density impact on (a) modulus of elasticity, and (b) modulus of rupture[17] .....	24
<b>Figure 2.11</b> Gamma rays flow in varies energies for (a) hematite-serpentine concrete, and (b) ilmenite-limonite concrete[39].....	28
<b>Figure 2.12</b> Comparison result of impact strength between normal concrete (O.C) and ilmenite-serpentine concrete (I.S.C)[41].....	29
<b>Figure 2.13</b> Neutron flow ratio in varies thickness of normal and colemanite concrete[42].....	30

<b>Figure 2.14</b> Compressive strength response due to fly ash and ferrochromium[43].....	31
<b>Figure 3.1</b> Visualization of aggregates (a) Natural sand (b) Gravel (c) Barite sand, and (d) Barite stone.....	40
<b>Figure 3.2</b> Dimension and Detail of reinforcement steel in beam specimen .....	42
<b>Figure 3.3</b> Radiation testing (a) Cylinder sample with penetrated point, (b) Set-up radiation test in laboratory .....	45
<b>Figure 3.4</b> Scheme of set-up $\gamma$ -rays transmission test[60].....	45
<b>Figure 3.5</b> Scheme of set-up beam tested with (a) LVDTs and concrete strain gages, (b) steel strain gages location in beam.....	47
<b>Figure 3.6</b> Setting up experiment test with beam sample using four point testing... ..	48
<b>Figure 4.1</b> The morphology of aggregates in microstructure by SEM micrograph each aggregates (a) Natural sand (b) Gravel (c) Barite sand, and (d) Barite stone. ....	50
<b>Figure 4.2</b> Element composition of each aggregate by EDS analysis (a) Natural sand (b) Gravel (c) Barite sand, and (d) Barite stone.....	52
<b>Figure 4.3</b> Comparison slump value in varies percentage replacement of aggregate in barite concrete.....	53
<b>Figure 4.4</b> Comparison unit weight in varies percentage replacement of fine aggregate in barite concrete.....	55
<b>Figure 4.5</b> Comparison unit weight in varies percentage replacement of coarse aggregate in barite concrete.....	56
<b>Figure 4.6</b> Distribution of unit weight in barite concrete comparing with compressive strength.....	58
<b>Figure 4.7</b> Stress-strain relationship curvature barite mixture with (a) w/c 0.35 and replacement fine aggregate, (b) w/c 0.35 and replacement coarse aggregate, (c) w/c 0.55 and replacement fine aggregate (d) w/c 0.55 and replacement coarse aggregate.....	59

<b>Figure 4.8</b> Distribution normalized modulus of elasticity of barite concrete parallel with ACI 349-06 standard.....	62
<b>Figure 4.9</b> Influence of unit weight concrete on normalized modulus of elasticity compared with ACI 349-06 standard.....	63
<b>Figure 4.10</b> Comparison Half-Value Layer (HVL) at energy 0.662 MeV in varies percentage replacement aggregate for w/c 0.35 and w/c 0.55.....	67
<b>Figure 4.11</b> Comparison Half-Value Layer (HVL) at energy 1.250 MeV in varies percentage replacement aggregate for w/c 0.35 and w/c 0.55.....	68
<b>Figure 4.12</b> Influence of unit weight concrete on HVL for both energies emitted in concrete w/c 0.35.....	68
<b>Figure 4.13</b> Influence of unit weight concrete on HVL for both energies emitted in concrete w/c 0.55.....	69
<b>Figure 4.14</b> Normalized stress-deflection at mid span characteristics for all beam specimens.....	71
<b>Figure 4.15</b> Normalized stress-deflection at mid span characteristics of concrete with w/c ratio 0.35.....	71
<b>Figure 4.16</b> Normalized stress-deflection at mid span characteristics of concrete with w/c ratio 0.55.....	72
<b>Figure 4.17</b> Load-strain at tension rebar of normal concrete with (a) w/c ration 0.35 and (b) w/c ratio 0.55.....	73
<b>Figure 4.18</b> Load-strain at tension rebar of barite concrete with (a) w/c ration 0.35 and (b) w/c ratio 0.55.....	73
<b>Figure 4.19</b> Load-strain at tension rebar of barite concrete for w/c 0.35 with (a) replacement fine aggregate 25% and (b) replacement fine aggregate 50%.....	73
<b>Figure 4.20</b> Load-strain at tension rebar of barite concrete for w/c 0.55 with (a) replacement fine aggregate 75% and (b) replacement coarse aggregate 100%.....	74

<b>Figure 4.21</b> Load-strain at stirrup of barite concrete for w/c 0.35 at (a) left hand side and (b) right hand side.....	74
<b>Figure 4.22</b> Load-strain at stirrup of barite concrete for w/c 0.55 at (a) left hand side and (b) right hand side.....	75
<b>Figure 4.23</b> Crack pattern of beam NN1 at load 40kN.....	78
<b>Figure 4.24</b> Crack pattern of beam NN2 at load 40kN.....	78
<b>Figure 4.25</b> Crack pattern of beam BB1 at load 40kN.....	79
<b>Figure 4.26</b> Crack pattern of beam BB2 at load 40kN.....	79
<b>Figure 4.27</b> Crack pattern of beam RFA-251 at load 40kN.....	80
<b>Figure 4.28</b> Crack pattern of beam RFA-501 at load 40kN.....	80
<b>Figure 4.29</b> Crack pattern of beam RFA-752 at load 40kN.....	80
<b>Figure 4.30</b> Crack pattern of beam RCA-1002 at load 40kN .....	81
<b>Figure 4.31</b> Crack pattern of beam NN1 at ultimate load.....	82
<b>Figure 4.32</b> Crack pattern of beam NN2 at ultimate load.....	82
<b>Figure 4.33</b> Crack pattern of beam BB1 at ultimate load .....	83
<b>Figure 4.34</b> Crack pattern of beam BB2 at ultimate load .....	84
<b>Figure 4.35</b> Crack pattern of beam RFA-251 at ultimate load .....	84
<b>Figure 4.36</b> Crack pattern of beam RFA-501 at ultimate load .....	85
<b>Figure 4.37</b> Crack pattern of beam RFA-752 at ultimate load .....	85
<b>Figure 4.38</b> Crack pattern of beam RCA-1002 at ultimate load.....	86
<b>Figure 4.39</b> Distribution of stress-strain at ultimate stage.....	88
<b>Figure 4.40</b> Shear resistant of stirrup.....	91

## LIST OF TABLES

<b>Table 2.1</b> Characteristics and distribution heavyweight material in Thailand[7] .....	8
<b>Table 2.2</b> Combination series of all concrete (kg/m <sup>3</sup> )[12] .....	15
<b>Table 2.3</b> Compressive strength and gamma-ray attenuation coefficient from Cobalt-60 of varies percentage barite[15] .....	17
<b>Table 2.4</b> Variation mixture of barite concrete with different w/c ratio[18] .....	18
<b>Table 2.5</b> Variation mixture of magnetite concrete with different w/c ratio[17] .....	24
<b>Table 2.6</b> Combination mixture magnetite aggregate with silica fume[33] .....	25
<b>Table 2.7</b> Variation mixture percentage of ilmenite concrete with under investigation ( $\rho=3.5$ g/cm <sup>3</sup> ) and previous investigation ( $\rho=4.6$ g/cm <sup>3</sup> )[40] .....	27
<b>Table 2.8</b> Mixture of hematite-serpentine concrete ( $\rho=2.5$ g/cm <sup>3</sup> ) and ilmenite-limonite concrete ( $\rho=2.9$ g/cm <sup>3</sup> )[39] .....	27
<b>Table 2.9</b> Combination different steel fibre in ilmenite-serpentine concrete[41] .....	29
<b>Table 2.10</b> Mixture concrete with different percentage of steel fibre[44] .....	32
<b>Table 2.11</b> Characteristics heavyweight aggregate[50] .....	34
<b>Table 2.12</b> Characteristics mixture ratio of heavyweight concrete[31] .....	35
<b>Table 3.1</b> Mechanical Properties of Reinforcement Steel .....	41
<b>Table 3.2</b> Varies of heavyweight concrete mixture composition with replacement of normal aggregate and different w/c ratio .....	43
<b>Table 4.1</b> Physical Properties of aggregates .....	49
<b>Table 4.2</b> Chemical Composition of normal aggregates .....	52
<b>Table 4.3</b> Chemical Composition of barite aggregates .....	53
<b>Table 4.4</b> Unit weight of barite concrete and comparison each sample with normal concrete .....	54

<b>Table 4.5</b> Compression strength for 7 days and 28 days of cylinder concrete.....	57
<b>Table 4.6</b> Comparison modulus elasticity of barite concrete from experiment and estimation of ACI standard in varies of w/c ratio.....	61
<b>Table 4.7</b> Poisson's ratio and maximum stress of barite concrete with different w/c ratio .....	64
<b>Table 4.8</b> Analysis result of radiation test using sources Caesium-137 (0.662 MeV) and Cobalt-60 (1.250 MeV).....	65
<b>Table 4.9</b> Beam test result for all specimens.....	70
<b>Table 4.10</b> Analysis beam test result of flexural stiffness at elastic stage.....	76
<b>Table 4.11</b> Displacement ductility factor .....	77
<b>Table 4.12</b> Varies of cracking load for specimens .....	89
<b>Table 4.13</b> Comparison ultimate load of estimation provision and experimental results.....	91

## CHAPTER 1

### Introduction

#### 1.1 General Review

Nowadays, nuclear energy plays a key role in bringing benefits not only in energy for nuclear power plant, but also accelerators in medical and in industrial, then in radiation sources for agricultural field. For long-term existence in the future, nuclear energy may be the one solution to the scarcity of unrenovable resources such as the oil, natural gas, peat, coal, when the demand of energy is increasing. In addition, nuclear energy can be considered as the other forms of energy to produce electricity by reliable, safe, clean energy and pollution-free sources. Nuclear power plants—as an alternative to fossil energies—are also the source of sustainable energy[1]. There recorded at least 439 operating nuclear power plant producing net capacity almost 378 GW and also 69 in the construction phase with 30 countries user state worldwide including Asian countries e.g., China, India, Iran, Japan, Korea, Pakistan, and Vietnam[2]. But, many users especially Southeast Asia countries still do not understand and worry to use nuclear energy as the safety issue arise. Thus, the dissemination of nuclear safety has to be conducted to convince users and to enable the construction of power plant. In fact, the working principle of nuclear power plant is similar to conventional thermal power plant, but different fuels as a source of heat in the boiler water. However, producing energy with nuclear—both fission and fusion reaction—is emitting nuclear radiation that require special handling with some special material building to prevent space of radioactive rays.

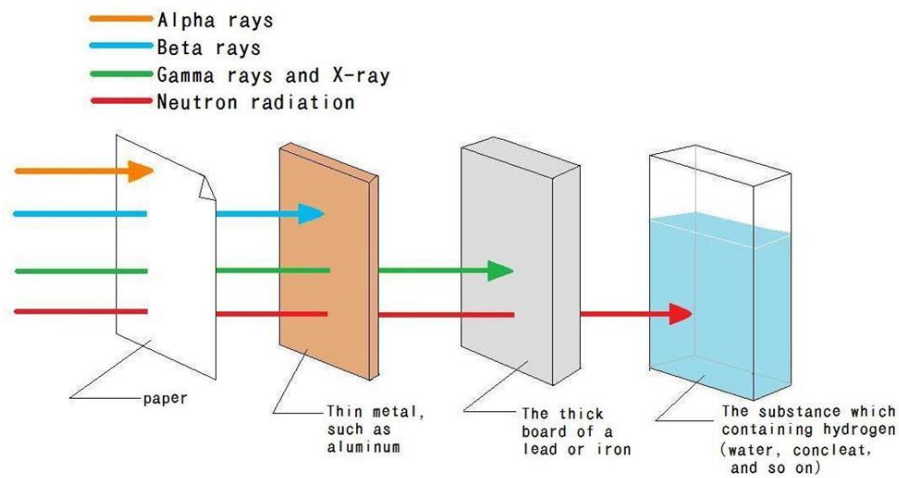


**Figure 1.1** Absorption power in different types of radiation rays[3]

Application of heavyweight concrete is not only in energy field area. In daily life, radiation has been used many years ago. In application for gamma-ray irradiation for example, radiation is used for sterilization in relation with food processing manufacture, pharmaceutical, and processing for medical device. Then, heavyweight concrete is needed to overcome protection in area that gamma-ray irradiator existed. Or even in hospital, heavyweight is applied for making radiography room become safety for worker and patients.

As we know, radiation has destroying effect invisibly and harmful for human being. Hence, it needs material that has capability to absorb radiation of radioactive especially gamma rays. Gamma rays have longer wavelength propagation, so that needs special material which more solid density and more thickness such as concrete. Moreover, not only normal fine aggregate like sand or normal coarse aggregate like gravel and granite, but also material that have high specific density or called heavyweight material such as barite ( $\text{BaSO}_4$ ), Magnetite ( $\text{Fe}_3\text{O}_4$ ), ilmenite ( $\text{FeTiO}_3$ ), etc. In term of nuclear power plant, heavyweight concrete is largely used as shielding of nuclear reactor which radioactive rays occurred. This shielding is not only preventing

from radioactive rays, but also has appropriate strength to resist pressures that happen in reactor.

Utilization of heavyweight concrete in Thailand has not been developed yet. An increasing power supply in nuclear energy based becomes one of the factors for starting heavyweight material exploration. As beginning stage with data collection of supply material existing bring through possibility of heavyweight material as mass production for industry occurs. Then, quality checking compares with standards which are used globally become heavyweight material properties similar in every area in Thailand. Furthermore, those combination heavyweight materials produce effective mixture for gamma rays attenuation and mechanical properties of concrete become major purpose of this research study. The prospective of heavyweight concrete application besides shielding based on mechanical properties become another allurements to be expanded.

## **1.2 Objectives and Scope of Works**

The purposes of this research as follow:

1. Study basic properties of heavyweight material especially barite types, consider appropriate of each material source and compare the advantages and disadvantages for each material that available in Thailand.
2. Developing a heavyweight concrete mixture and appropriate use of different material in term of composition and volume used in radiation shielding effectively.
3. Studying mechanical properties behaviour of structural member in heavyweight concrete.

The scope of this research as follow:

1. Mineral and aggregate all the tests to come from domestic sources only, which is in this case only use Barite material in Thailand.
2. Tests the basic properties of fresh concrete and hardened concrete. According to the standards of ASTM.
3. Steps in determining how to design concrete hard according to the standards of ACI.
4. Measuring mineral properties of aggregates include density, mineral contents, and chemical compositions.
5. Measuring gamma rays shielding efficiency only by computing gamma ray attenuation properties of concrete using sources of caesium 137 ( $^{137}\text{Cs}$ ), and cobalt 60 ( $^{60}\text{Co}$ ).
6. Computing mechanical properties include compressive strength, modulus elasticity, and stress-strain relationship.

Benefits expected to be received as follow:

1. Getting information about sources and types of heavyweight material that available in Thailand, both in quantity and quality. Thus, it can be applied as mass production industry.
2. Offering an option in the heavyweight material selection that can be used to mix concrete in certain areas such as gamma irradiation plant, gamma radiography room, and medical treatment room.
3. Effective mix design of heavyweight concrete considered in terms of radiation attenuation and mechanical properties performance.

4. Establishing a relationship between the radiation attenuation coefficients of different mix design heavyweight materials.

### 1.3 Outlines

This research thesis is arranged by reviewing background, heavyweight concrete, radiation transmission, mix design of heavyweight concrete and radiation test in Chapter 2. The basic concepts of mechanical properties in concrete are also featured. Continuing by the sequence of experiment in detail about mixture concrete for gamma rays radiation attenuation and investigation of mechanical properties are showed in Chapter 3. Explanation result summarizes in basic analysis of physical properties each heavyweight material and effective mix design for gamma rays attenuation can be found in Chapter 4. Moreover, all parameters of mechanical properties each mix design is presented in this chapter. At the end, Chapter 5 contains conclusion and outlook of this research thesis, also advice for next researches.

## CHAPTER 2

### Literature Review

#### 2.1 Background

Concrete has been used since ancient times. At that time, producing concrete is easy by mixing all materials then can be used directly. In modern era, increasing of construction led to a surge in concrete demand. These developments urged improvement and enhancement of concrete not only in terms of quantity but also in terms of quality to keep constantly. According to different purposes, sometimes normal concrete cannot meet the required demand. In order to fulfil high performance requirement, new term of concrete have been developed by conform to beyond the standard limits of normal performance range.

Concrete with specific requirement or well-known as high performance concrete (HPC) is concrete which made by combining some proportion of materials with may require special consideration during mixing, transporting, placing, consolidating, and curing so resulting excellent performance concrete that will be used in structure, exposed in environment, and carried loads which subjected its design[4]. Because of using unusual concrete, there some standards as consideration are structural, environmental, loads, materials and mix design, also the construction process. In relation to materials and mix design, concrete which becomes focus on this study is heavyweight concrete. The numbers of research on heavyweight concrete have been carried out due to development of nuclear as renewable energy.

This chapter gives the basic knowledge and ideas to support this thesis research with some experimental and theories research are reviewed. Comprehensive researches with complete investigation in experiments and develop complex mixture

design will exceed the scope of study. Only some material with mixture design will be considered.

## 2.2 Heavyweight Concrete

Heavyweight concrete is the concrete with high density of material's composition. As mentioned ACI Standard 304R-00, special consideration on heavyweight concrete which combines proportion of high specific gravity materials led to an increase in density of concrete. So this is depended on the type of aggregate to be mixed in concrete. Furthermore ACI stated that by using natural aggregates and synthetic aggregates provide typical density of concrete higher than  $3.840 \text{ kg/m}^3$  and  $5.450 \text{ kg/m}^3$ , respectively[4]. For example, by using mineral barite will be achieved density of concrete around  $3.500 \text{ kg/m}^3$  or 45% higher than normal concrete, whilst mineral magnetite, other very heavy minerals with iron, and lead shot can produce  $3.900 \text{ kg/m}^3$  (60%),  $5.900 \text{ kg/m}^3$  (145%),  $8.900 \text{ kg/m}^3$  (270%), respectively, are higher than normal concrete[5].

Developing heavyweight concrete as mass production industry related to availability raw material in nature, costs a lot using imported raw. Strategic location geologically made Thailand has heavyweight material abundant[6]. In fact, heavyweight concrete has been used to construct medical building e.g., x-ray room or combination of counterweight foundation in structure in Thailand, but this application is still measly. In term to application heavyweight concrete as mass production is needed further assessment to check properness of it; both qualities of physical and chemical properties, also amount of it.

**Table 2.1** Characteristics and distribution heavyweight material in Thailand[7]

Material	Formula	Type	Specific Gravity	Characteristic	Location
Barite	BaSO <sub>4</sub>	Non-metal	4.5	high specific gravity; non-magnetic; majority used to weighting agent and filler in paint and plastics; insolubility	Petchaburi; Udonthani; Chiang Mai; Lampun; Lampang; Phea; Meahongson; Tak; Nakorn Sri Thammarat; Suratthani; Kanchanaburi; Uthaithani; Ratchaburi
Galena	PbS	Metal	7.5	Low melting point; natural semiconductor	Kanchanaburi; Phea; Chiang Mai; Tak; Lampang; Meahongson; Sukhothai; Suratthani; Pathalung; Songkhla; Satoon; Nakorn Sri Thammarat
Hematite	Fe <sub>2</sub> O <sub>3</sub>	Metal	5.3	anti-ferromagnetic	Nakorn Sri Thammarat; Lopburi; Uthaithani; Chiang Mai; Suratthani; Sukhothai; Nakornsawan
Ilminite	FeTiO <sub>3</sub>	Metal	3.7	basically weakly magnetic but will have magnetic characteristic when burn	Kanchanaburi; Chantaburi; Trat
Magnetite	Fe <sub>3</sub> O <sub>4</sub>	Metal	5.18	carries dominant magnetic; brittle; dissolves slowly in hydrochloric acid; stabil in high temperature	Lopburi; Nakornsawan; Lai; Chonburi; Rayong; Krabi; Nakorn Sri Thammarat
Zircon	Zr(SiO <sub>4</sub> )	Non-metal	4.68	lustrous, greyish-white, soft, ductile and malleable metal which is solid at room temperature; low neutron-capture cross-section and good resistance to corrosion under normal service conditions	Chantaburi; Trad; Srisakate; Phe

Correlating with improving electricity supply by nuclear energy, Thailand has been done preliminary study to construct nuclear power plant in few years ahead in some areas, and for that reason, it will be needed a lot of resource raw materials. Department of Mineral Resources Thailand[8] as authorized institute has being done for mapping distribution and recorded mineral material which available in Thailand. Dividing into 52 parts of Thailand, It maps available material including heavyweight material. This work excluded computing and calculating amount of material which mining explored or still raw in nature. By resuming those maps, Thailand divided into bigger part to make easier describing distribution heavyweight material then measuring highest amount in each area only to restrict with data needed in this research.

As mentioned before, 52 parts map information about distribution mineral that available in Thailand is summarized becoming five different parts based on geographic location. Moreover, this data is filtered among all economic minerals into mineral that have potentially creating heavyweight mixture. Based on this data, barite mineral is available almost every region in Thailand. It means barite mineral can be used as heavyweight concrete in mass scale. Then, variation of iron mineral is abundant its types especially ilmenite, lead, and fluorite. Those materials are available in all area.

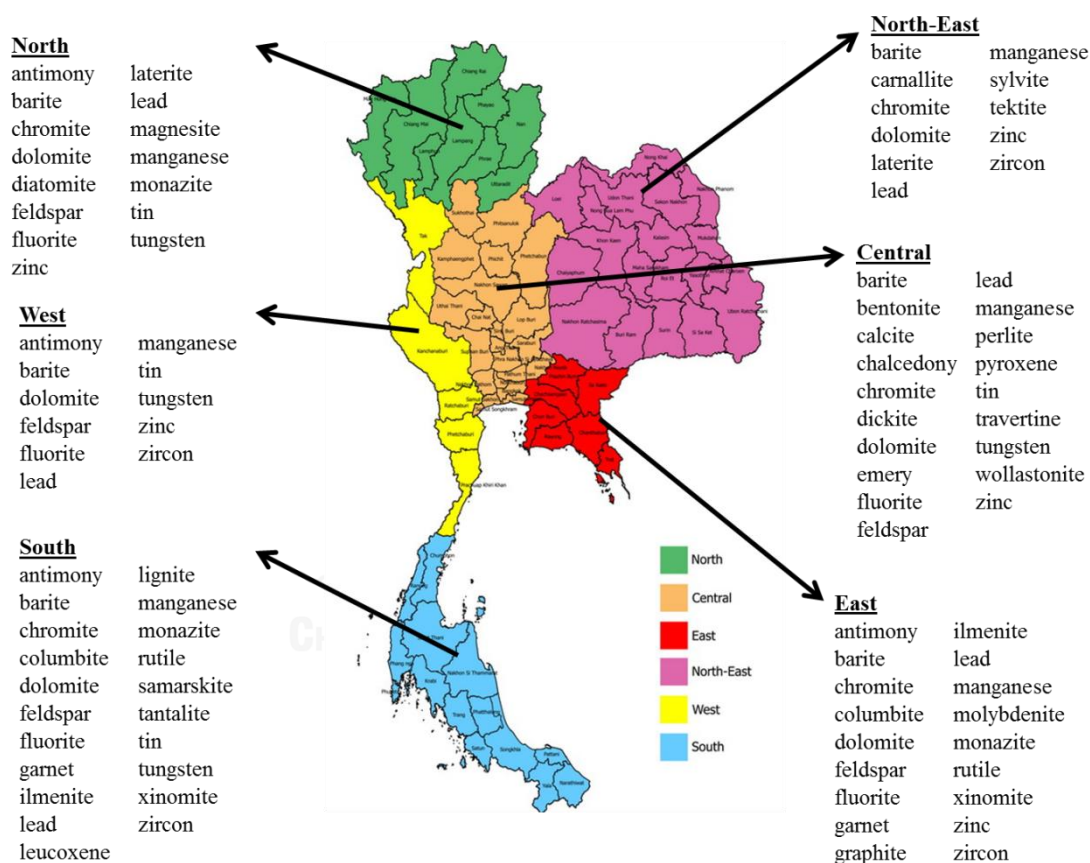


Figure 2.1 Distribution and variation heavyweight concrete in Thailand[8]

Selection of heavyweight material that will be used is not only amount but also physical and chemical characteristics. Heavyweight material especially its density brought important role in protection beside capability in term strength in structure.

### 2.3 Radiation Transmission

Density often associated with the ability to prevent radioactive rays especially gamma rays, so that a higher density of concrete more capable attenuate gamma-rays. Hence, density have main role to absorb gamma rays in heavyweight concrete[9]. Radiation attenuation coefficient ( $\mu$ : attenuation coefficient) is given by Beer's law which the exponential attenuation law as shown in Equation (2.1) and (2.2) to specify linear attenuation coefficient. It shall be written as:

$$I = I_0 e^{-\mu x} \quad (2.1)$$

$$\mu = -\frac{1}{x} \ln \left[ \frac{I}{I_0} \right] \quad (2.2)$$

Where  $I$  is the appearing intensity,  $I_0$  is the radiation intensity from source,  $x$  is the thickness of media absorber (in cm or g/cm<sup>2</sup>), and  $\mu$  is coefficient of gamma-rays attenuation. The resulted unit varies between cm<sup>-1</sup> and cm<sup>2</sup>/g, which called "linear attenuation" and "mass attenuation coefficients", respectively. Linear attenuation coefficient is largely used to compute media absorber with different thickness.

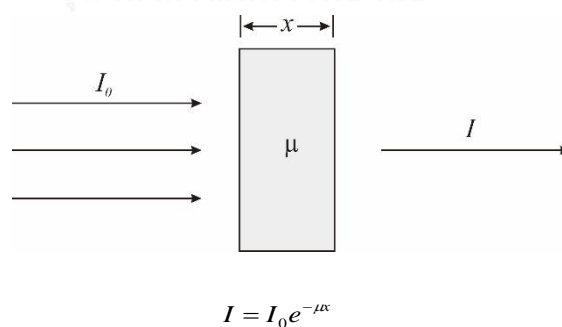


**Figure 2.2** The Exponential Law of Radiation Attenuation[10]

Moreover, we can correlate Equation (2.1) with including density ( $\rho$ ) of the media if it has different density which is defined as mass attenuation coefficient as follows

$$I = I_0 e^{-\left(\frac{\mu}{\rho}\right)(\rho x)} \quad (2.3)$$

Which  $\rho$  is density of media absorber (in  $\text{g}/\text{cm}^3$ ); the ratio  $I/I_0$  is represented propagation of radiation especially for gamma-rays. More detail, Figure 2.2 can be explained the influence of linear attenuation coefficient with applied three types of gamma-ray energies.

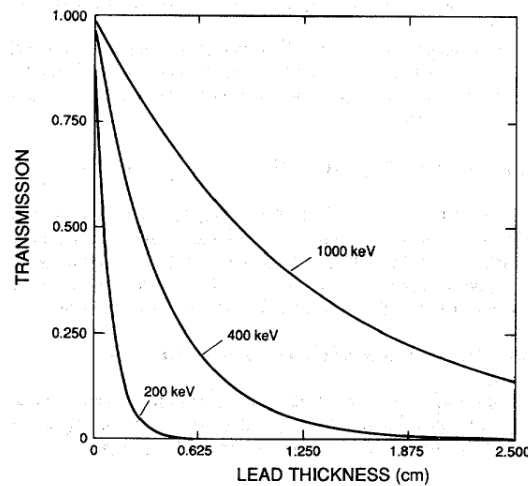


**Figure 2.3** Gamma-rays propagation with different media absorbers and energies[10]

Linear attenuation coefficient is ability of absorbing media properties. As showed in Figure 2.3 that the rising of gamma-rays propagation due to the increasing of radiation energies otherwise will be decreased by thickness of media. Therefore, linear attenuation coefficient can be said the easiest methods in experimental to calculate the absorption of a material only using thickness of media without considering the type of material which is related to density. On the other hand, mass attenuation coefficient considers electron density which is affected by atomic number and mass, also mass density due to interacting of gamma-rays with electrons.

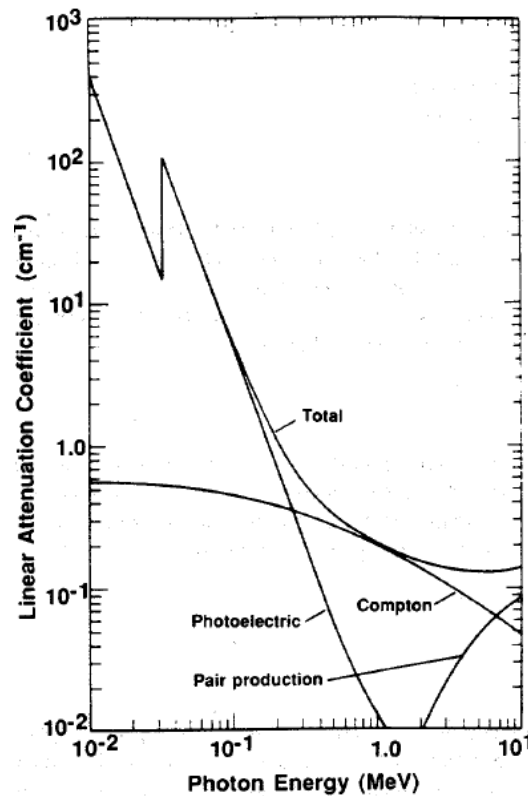


**Figure 2.4** Interaction processes for obtaining Total Attenuation Coefficient[10]

The figure above is calculated contribution of each interaction processes which depends on energy of gamma-rays and media absorber's number of atomic[10, 11]. These interaction are classified into three main processes which are

- Photoelectric absorption is the loss of gamma-rays due to interaction with atomic electron.
- Compton Scattering is the transfer of gamma rays energy process effect of interaction with atomic electron.
- Pair Production is the construction a pair of electron-positron impact of atomic coulomb field in surrounding nucleus that created by gamma-rays energy greater than 1.022 MeV.

Interaction processes also can be shown by defining density into attenuation coefficient that can be seen in Figure 2.5 as follow

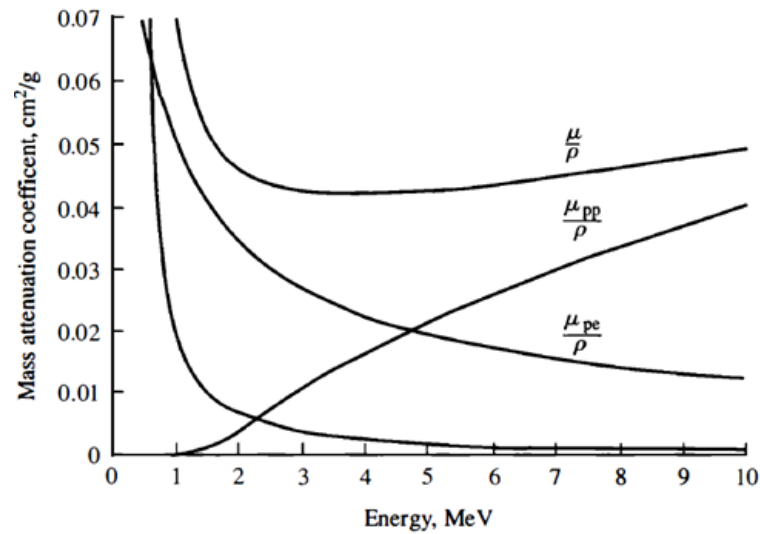


**Figure 2.5** Contribution of each interaction processes due to attenuation coefficient and density of material[11]

Applying three processes into several materials, we concluded that number of atomic is dependent parameter which determines rising of low-energy. This means that photoelectric process is influent interaction among all materials except hydrogen. Above that rises, Compton Scattering process has influent with indicated dropping of mass attenuation value. More detailed value of mass attenuation coefficient some element lead as gamma ray energy can be seen in Figure 2.6 below.

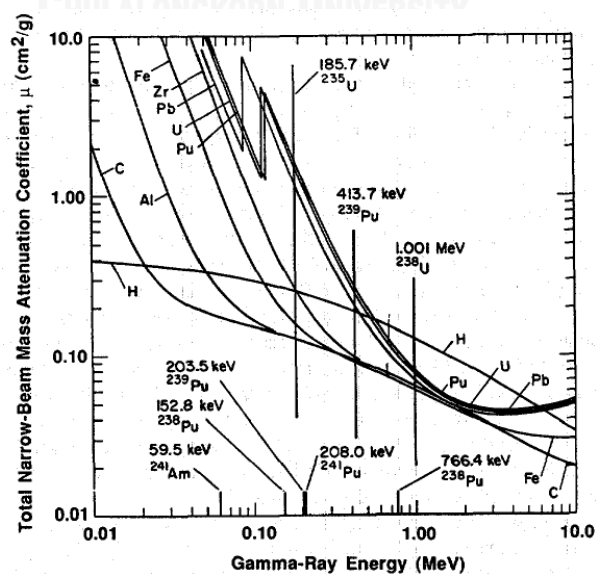


**Figure 2.6** The value of mass attenuation coefficient several elements[10]

## 2.4 Mixed Design of Heavyweight Concrete and Radiation Testing

Development and utilization of heavyweight material in term to density has been used largely. This is associated to development of nuclear energy as a substitute for petroleum which limited amount. As result, we need necessary material that can counteract one of the results of reaction which is harmful radiation. It encourages some research to produce a superior product enhancement either ability to absorb radiation rays or quality and power of the resulting mixture.

### 2.4.1 Mixture of Barium Minerals

These are conducted to look for the best mixed material in term of physical, chemical, and mechanical characteristics. In the past, many researches have done to mix some heavy material obtaining concrete for preventing radioactive rays. Mineral Barite ( $BaSO_4$ ) is usually used for this mixed due to it has high density among other heavy mineral, but it is not adequate amount around the world. I. Akkurt et al[12] observed mineral barite in mixing concrete, both fine aggregate and coarse aggregate also compare with normal aggregate. The purpose this research is contribution investigation of different combination and content on concrete in related to radiation attenuation for this case using 0.66 MeV and 1.33 MeV photons. This research classifies into 3 parameters water ratio—0.65, 0.51, 0.43 that reflected by code 2, 3, and 4, respectively and five series combination materials which are entirety volume of normal aggregate (A), entirety volume of barite (B), half of volume aggregate is normal and the other barite (K), fine aggregate is normal aggregate and coarse aggregate barite (AB) whilst fine aggregate is barite and course aggregate normal aggregate (BA). These can be seen in Table 2.1 below.

**Table 2.2** Combination series of all concrete (kg/m<sup>3</sup>)[12]

	A2	A3	A4	B2	B3	B4	K2	K3	K4	AB2	AB3	AB4	BA2	BA3	BA4
Cement	310	362	425	310	362	425	310	362	425	310	362	425	310	362	425
Water	201	183	183	201	183	183	201	183	183	201	183	183	201	183	183
w/c	0.65	0.51	0.43	0.65	0.51	0.43	0.65	0.51	0.43	0.65	0.51	0.43	0.65	0.51	0.43
Fine normal aggregate	697	697	679	–	–	–	349	349	338	697	697	679	–	–	–
Coarse normal aggregate	1092	1092	1061	–	–	–	545	547	531	–	–	–	1092	1092	1061
Fine Barite aggregate	–	–	–	1113	1114	1083	557	558	542	–	–	–	1113	1114	1083
Coarse Barite aggregate	–	–	–	1700	1701	1653	850	850	826	1700	1701	1653	–	–	–

Producing gamma-rays attenuation is used source material <sup>137</sup>Cs and <sup>60</sup>Co where emitted 0.66 MeV and 1.33 MeV—had been counted from 1 keV to 100 GeV photon energies, respectively with 3 different thicknesses of target (2 cm, 4 cm, and 6 cm). Thereupon comparing with computer software program database—XCOM code the linear attenuation coefficients of each series combinations. This research obtained which differences of w/c ratio have not affected to coefficient of attenuation ( $\mu$ ) significantly either by measurement or by calculation. Moreover, combination coarse aggregate/fine aggregate—Barite/Normal and Normal/Barite with w/c ratio 0.51 and 0.43 respectively, have the highest of linear attenuation coefficient in 0.66 MeV photon energy, similarly for combination whole barite with w/c ration 0.65 in 1.33 MeV photon energy.

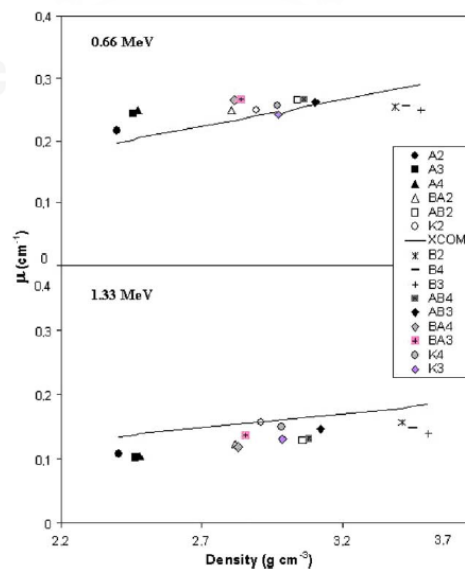


**Figure 2.7** Linear Attenuation Coefficients Result of Combination Series by using photon energies 0.66 MeV and 1.33 MeV[12]

As shown in figure above, distribution combination series of all concrete have same level between experiment and computation program, it apply for whole barite or whole normal aggregate as well as with combination. Rise of attenuation coefficient ( $\mu$ ) parallels with density values. Other thing in this research concluded that barite is recommended as substantial material for radiation shielding.

Continuing this research, I. Akkurt et al[13] compares pure barite 90% with barite concrete and material lead with combination energies—662, 1173, 1332 keV energies from same sources material[12] with constant w/c ratio in 0.5 then evaluated with mass attenuation coefficient ( $\mu/\rho$ ) in XCOM code database. Verifying potency shielding capabilities are used the half value layer (HVL) or the tenth value layer (TVL) method. As estimated before, lead has highest value of linear attenuation coefficient, followed by barite and barite concrete. Furthermore, checking transmission gamma-rays using HVL and TVL indicated lead needs short distance due to thickness compared with barite and barite concrete at the same energy. Accordance to Akkurt et al[13], F. Bouzarjomehri et al[14] investigated barite as concrete in term of density, performance strength, and HVL at different samples that followed by ratio of fine-coarse aggregates (35-65 and 50-50), cement dosage (350 kg/m<sup>3</sup> to 500 kg/m<sup>3</sup> with range 50 kg/m<sup>3</sup>), and w/c ratio (0.40, 0.45, 0.50, 0.60, 0.70) using radiation source <sup>60</sup>Co. The ratio of fine-coarse aggregate 35-65 with cement dosage 350 kg/m<sup>3</sup> and w/c ratio of 0.45 resulted lowest HVL and highest strength of compression as suitable sample for shielding. Similar test also conducted in Thailand[15] to review attenuation coefficient by HVL and TVL with varies ratio of barite as coarse aggregate from 0% to 100% in range 25% and resulted increasing amount 250 kg/cm<sup>2</sup> of compressive strength in 28 days compared with design. In term of attenuation  $\gamma$ -rays, percentage of mineral barite in concrete brought important role resulting attenuation coefficient, beside duration of radiation, distance from source and thickness.

**Table 2.3** Compressive strength and gamma-ray attenuation coefficient from Cobalt-60 of varies percentage barite[15]

Sample	$\mu$ (1/cm)	HVL (cm)	TVL (cm)	Compressive Strength (kg/cm <sup>2</sup> )			
				3 days	7 days	14 days	28 days
Normal Concrete	0.1688	4.105	13.626	191.18	258.74	320.56	353.09
Concrete with Barite 25%	0.1637	4.233	14.050	240.63	305.81	240.94	381.2
Concrete with Barite 50%	0.2017	3.436	11.403	253.89	293.12	363.4	331.96
Concrete with Barite 75%	0.2118	3.272	10.859	277.37	307.75	379.13	381.36
Concrete with Barite 100%	0.2137	3.243	10.763	230.9	290.61	353.56	365.79

Continuing previous research using barite ( $\text{BaSO}_4$ ), Akkurt et al[13] had been done for knowing impact in physical and mechanical properties due to rate of barite[16]. Ideal ratio of barite with dosage of cement became main purpose to be achieved with range of rate 0%, 50%, 60%, 70%, and 100% and water ratio same as research before[12]. The ultrasound pulse velocity (UV), Schmidt hardness (SH) and unit weight (UW) are used as properties parameters to decide ideal ratio of barite aggregates. This research obtained significant results which are UV test and SH test have not impact in 0.51 and 0.65 w/c ratio but tend to drop in w/c ratio 0.43. Moreover unit weight measurement obtained 100% barite aggregates in w/c ratio 0.51 as maximum value of weight—3,507 kg/m<sup>3</sup>. There is no direct impact for durability using barite or normal aggregates, but grading distribution and shapes consideration become main issue as workability in heavyweight concrete. It is also making segregation effect due to density of heavyweight aggregates[17].

An equivalent result has been achieved by İlker Bekir Topçu[18], conducting parameter properties in physical and mechanical of barite with inspecting seven variation of w/c ratio between 0.30 and 0.60 with step 0.05 and two type of cements—PKC 32.5 (type II with specific gravity 2850 kg/m<sup>3</sup>) and PC 42.5(type III with specific gravity 3100 kg/m<sup>3</sup>). This research aimed to reach appropriate water-cement ratio with different type of cement in term of attenuation capability. Using distribution grading of

barite aggregates which following grain size 0.50 – 1 mm, 1 – 2 mm, 2 – 4 mm, 4 – 8 mm, 8 – 16 mm are 12%, 18%, 20%, 20%, 30% respectively. Other tests also had been done for supporting data such as Schmidt hardness by non-destructive test, resonance vibration and ultrasound length.

**Table 2.4** Variation mixture of barite concrete with different w/c ratio[18]

W/c ratio	Amount of water (kg/m <sup>3</sup> )	Amount of cement (kg/m <sup>3</sup> )	Amount of aggregate (kg/m <sup>3</sup> )	Absorbed water (kg/m <sup>3</sup> )	Slump (cm)
0.30	105	350	3038	24.30	0.5
0.35	123	350	2967	23.70	1.0
0.40	140	350	2876	23.00	1.5–2
0.45	158	350	2835	22.65	2.5
0.50	175	350	2756	22.00	4–5
0.55	193	350	2683	21.46	6–7
0.60	210	350	2615	20.92	7.0

Determining cement dosage is first consideration to get suitable mixture. Regarding to another experiment that had been done before this research, appropriate dosage of cement is not more than 350 kg/m<sup>3</sup> if radioactive permeability will carry out[19]. By increasing dosage of cement can reduce void and increase unit weight, but in contrary also increase shrinkage effect then propagate cracks on concrete. This effect can reach up to 70-75% compared with normal concrete[20], and have higher value in w/c low condition while cement dosage more than 500 kg/m<sup>3</sup>[4]. Furthermore, it can affect in preventing radioactive beside thickness of shielding. Another thing that must be considered is amount of coarse aggregate; it might disturb uniformity of mixture. In addition to reduce risk of segregation, this research proposed to add amount of fine aggregates than coarse aggregate and use low duration of mixing.

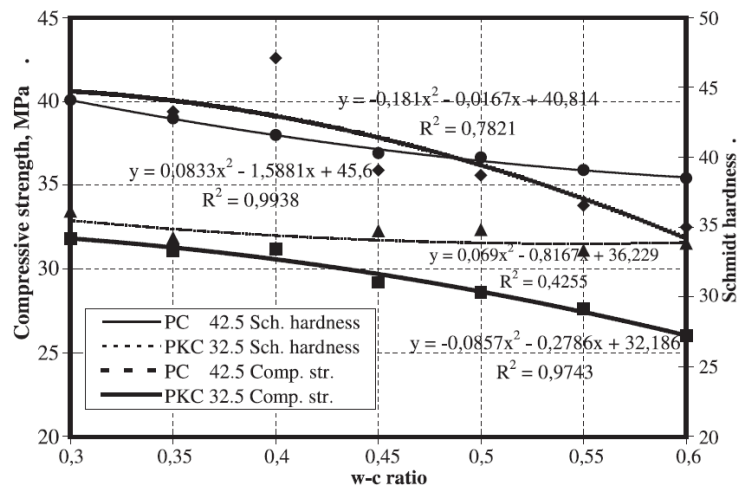


**Figure 2.8** Distribution of compressive strength and Schmidt hardness by different w/c ratio[18]

This research concluded that w/c ratio between 0.30 and 0.50 suitable for heavyweight concrete especially barite material and not suggested to use w/c ratio exceed 0.50. Moreover, using 0.30 w/c ratio could achieve highest strength among other w/c ratio, but it had workability problem when mixing process occurred. Special treatment such as adding plasticizer and using special cement type is needed if w/c ratio of 0.30 is used. In other hand, 0.50 w/c ratio has more advantage in term of workability but it should consider about shrinkage effect that may be occur then propagate cracks. As a solution, w/c ratio of 0.40 can be used and effective to overcome all problems that occurred in w/c ratio of 0.30 or 0.50. It also can be used without any treatments or special cement usage.

#### 2.4.2 Mixture of Combination Barium Mineral with Iron Minerals

As mentioned above, barite is largely used to produce heavyweight concrete due to high density among heavyweight material, easy to maintain crushing process, and less important is high coefficient of thermal expansion[20]. On the other hand, disadvantages of barite concrete product are related to the length of mixing process[21], tardiness of hardening and the setting time on some matter happened in

fine aggregates of barite, and durability problem on exposed concrete[20]. Related to those disadvantages, experiments have been conducted to minimize and improve barite material.

D. Mostofinejad, et al[21] tried to produce effective mix design on attenuation of  $\gamma$ -rays then compare with normal concrete based on some parameter which are water-cement ratio, kind of aggregates, content of aggregates, cement, superplasticizer and silica fume. This experiment investigated impact of those parameters in term of compressive strength and attenuation coefficient of  $\gamma$ -rays. Moreover, the study can be summarized that the value of density and attenuation coefficient increased proportionally, by replacing cement with silica fume reduced attenuation coefficient on heavyweight concrete, rising of cement dosage with constant w/c ratio will reduce attenuation coefficient of  $\gamma$ -rays, w/c ratio above 0.40 will increase compressive strength into same normal concrete, but less than that will apply reverse up to 10%[21].

Identical with experiment before, Ahmed S. Ouda[22] tried to compare barite with other heavyweight material and explore in term of concrete performance, physical and mechanical properties, and also attenuation coefficient of  $\gamma$ -rays. This developed more admixture using not only silica fume, but also granulated blast-furnace slag and fly ash; it also compare barite with magnetite, goethite, and serpentine. Using constant w/c ratio of 0.35 added with superplasticizer and cement dosage 450 kg/m<sup>3</sup> obtained results such as specific gravity from high to low into barite, magnetite, goethite, and serpentine, respectively. For concrete performance, magnetite with 10% silica fume reached highest required compression strength—above 600 kg/cm<sup>2</sup>—and contrarily goethite and serpentine could not reached requirement. In term of physical and mechanical properties, fine aggregate of magnetite showed higher value than barite and goethite. And the last, magnetite also reached highest rank due to  $\gamma$ -rays attenuation coefficient.

In Thailand, similar experiments had been conducted with combining different ratio of admixture in barite material such as smectite powder (SP)[23] and ground natural perlite (GNP)[24]. Both of experiments used constant w/c ratio of 0.40 with different varies of cement dosage and resulted thickness of 15 mm as high attenuation shield, beside that both of it have high strength compressive as well as bonding. Moreover, developing equation in rebound test and ultrasonic pulse velocity (UPV) had been conducted using barite concrete, magnetite-hematite concrete, and combination with fly ash and limestone[25]. Radiation test also conducted using caesium 137 ( $^{137}\text{Cs}$ ), and cobalt 60 ( $^{60}\text{Co}$ ) energies resources to achieve linear attenuation coefficient of samples.

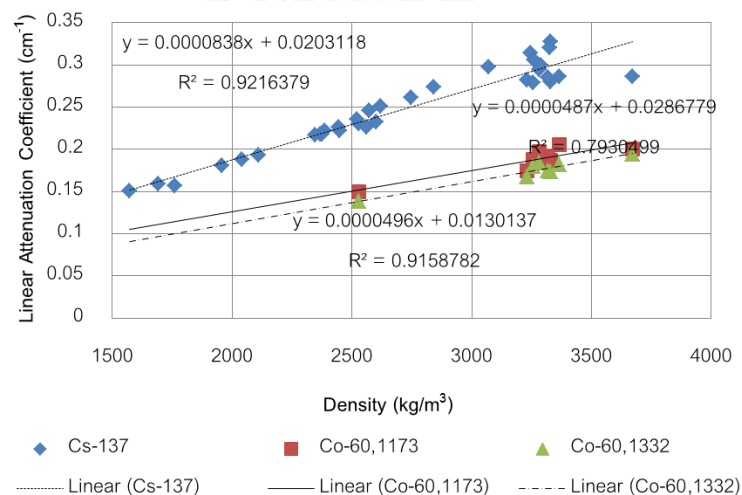


**Figure 2.9** Linear attenuation coefficient of different density of concrete by 0.622 MeV, 1.173 MeV, and 1.332 MeV energy resources[25]

This research obtained proportional w/c ratio for barite concrete is 0.57 with slump 75 mm, this happened because barite aggregate absorbed water more than normal aggregate. Further, adding fly ash in barite concrete mixture did not affect in compressive strength, but in term of workability is significantly. In term of UPV, this research obtained relationship between compressive strength with UPV as follow:

$$f'_{c_{heavy}} = 1.2815(0.024V_{in} - 43.583)^{1.4947} - 40 \quad (2.4)$$

Where  $V_{in}$  is velocity of heavyweight concrete by indirect test in m/s.

Developing more by combining varies ratio of barite material with other heavyweight material as fine or coarse aggregates had been done in relation to attenuate  $\gamma$ -rays. F. Demir examined combination of barite-colemanite as fine aggregates and normal aggregates as coarse one in 0.663 MeV[26], 6 MV and 18 MV[27]. Using constant w/c ratio 0.44, grading distribution maximum 16 mm for coarse aggregates and 4 mm for fine aggregates, this experiments concerned to effect of combination in term  $\gamma$ -rays attenuation. All of energies resulted 100% barite contains have highest density and attenuation coefficient values. In other hand, barite as coarse aggregate combined with varies ratio waste of cathode ray tube (CRT), both crushed (CFG) and treated (TFG) as fine aggregate is conducted. Mixing with constant cement dosage 355 kg/m<sup>3</sup> (type 1) and fly ash with w/c ratio of 0.48 showed reduction value of compressive and tensile strength, but increase density and discharge dry shrinkage. Another thing that should be considered is using barite as coarse aggregate reducing elastic modulus in concrete around 31%[28]; this value is not much different in both type of funnel glass.

#### 2.4.3 Mixture of Iron Minerals

Exploration other heavy materials also largely examined that not only provide capability to attenuate  $\gamma$ -rays but also in term of mechanical properties. Another material can be found in Thailand abundant is Magnetite ( $Fe_3O_4$ ). Many experiments had been conducted to examine this material due to less available information and standard. Keun-Hyeok Yang investigated behaviour of concrete in term of shrinkage combining with fly ash[29] then comparing with calculation equations from CEB-FIB model[30]. Moreover, another experiment also conducted to develop mixture of magnetite concrete in term workability and mechanical properties afterwards compared with modelling from ACI 349[31] and CEB-FIB[30] equations. By three

different water-binder ratios, samples of shrinkage test divided into 3 categories with varies percentage substitution of sand into magnetite fine aggregate with maximum size 5 mm to investigate effect of this substitution and/or fly ash additional. Keeping slump values in 100 mm at first as recommendation made mixture low of workability[32], then required admixture adding at lowest water-binder ratio. In fact, investigation physical properties of aggregate also had been done to study shrinkage effect in magnetite concrete. This research concluded substantially, pore in aggregate lead to shrinkage effect in magnetite concrete. Further, rising of substitution sand percentage and adding of fly ash caused increasing of shrinkage effect to 15%[29]. However, shrinkage effect is almost not affected into water-binder ratio.

Continuing with similar sample, another mixture sample with granite coarse aggregate with maximum size 25 mm added to achieve workability behaviour and mechanical properties in magnetite concrete. Mixture with fly ash is not used in this experiment because it did not give result significantly. Related to mechanical properties, some tests conducted such as direct shear, compressive, and splitting tensile strength, modulus rupture and elasticity, also stress-strain and bond stress-slip relationship. Furthermore, this experiment also investigated effect of granite coarse aggregate ( $R_c$ ) and natural sand ( $R_f$ ) as fine aggregate substitution in magnetite concrete. This experiment obtained by substituting fine aggregate assessed significantly rising in some result such as workability, tensile capacity, shear strength, and bonding compared with substituting coarse aggregate. However, this made dropping of density and impacted to modulus elasticity of magnetite concrete, but it did not impact in compressive strength substantially.

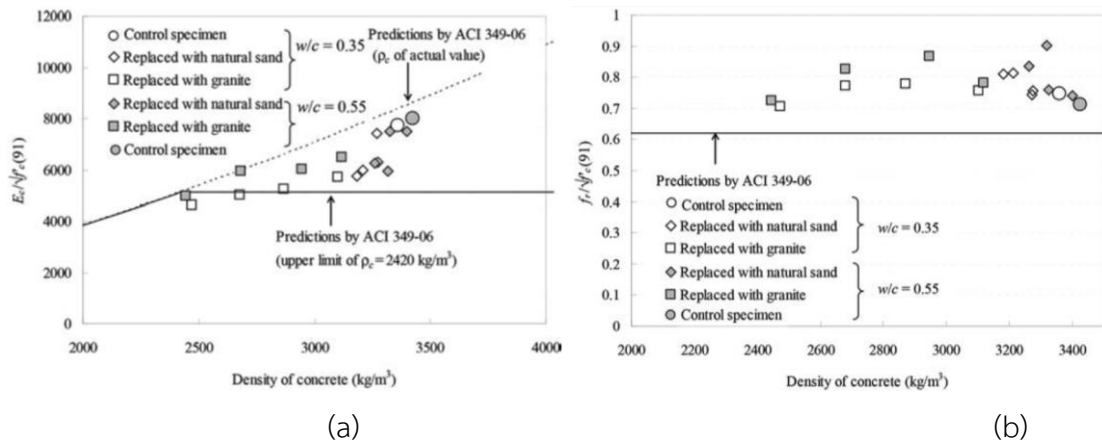


**Figure 2.10** Density impact on (a) modulus of elasticity, and (b) modulus of rupture[17]

Although experiment result of modulus elasticity and rupture greater 1.5 times than model of ACI 349, it can conclude that this commonly conservative result of magnetite concrete.

**Table 2.5** Variation mixture of magnetite concrete with different w/c ratio[17]

Specimen No.	w/c	R <sub>F</sub> , %	R <sub>C</sub> , %	Cement	Water	Unit Weight, kg/m <sup>3</sup>				R <sub>SP</sub> , %				
						Fine Aggregate		Coarse Aggregate						
						Sand	Magnetite	Granite	Magnetite					
1*	0.35	0	0	514.3	180	0	987	0.0	1689	0.5				
2		25	0			171	740	0.0	1689					
3		50				342	494							
4		75				514	247							
5		100					685	0						
6		0	0			25	327.3	180	0		987	237.2	1267	0.0
7						50			474.4		845			
8						75			711.7		422			
9						100			948.9		0			
10*	0			0	0	1077			0.0	1842				
11	0.55	25	0	187	807	0.0	1842							
12		50		374	538									
13		75		561	269									
14		100		747	0									
15		25		0	1077			258.8	1382	0.0				
16		50	517.5	921										
17		75	776.3	461										
18		100	1035.0	0										

\*Concrete specimen 1 and 10, which were made without replacement with conventional NWA, indicate control mixture  
 Notes: w/c is water-cement ratio; R<sub>F</sub> is replacement level by natural sand for magnetite fine aggregates by volume; R<sub>C</sub> is replacement level by granite particles for magnetite coarse aggregates by volume; R<sub>SP</sub> is high-range water-reducing agent-to-cement ratio by weight; 1 kg/m<sup>3</sup> = 0.062 lb/ft<sup>3</sup>.

Modifying usage of material above[17, 29], another experiment conducted with applying three percentage of silica fume—0%, 10%, and 20% of cement weight— in

magnetite coarse aggregate with some parameters such as ratio of coarse aggregate to total aggregate (0.48 and 0.65) and combination magnetite fine aggregate or sand in w/c ratio 0.24 and superplasticizer 3.5% to cement dosage. This experiment aimed to achieve highest concrete strength in 140 MPa (180 days) as a planning beside capability in radiation attenuation[33].

**Table 2.6** Combination mixture magnetite aggregate with silica fume[33]

Mix No.	C	sf/c	w/(c+sf)	SP	SP/(c+sf)	Fine agg.	C/(F+C)	Slump	Density
	kg/m <sup>3</sup>	%		Type	%	Type		mm	t/m <sup>3</sup>
MMO	350	0	0.5			M	0.65	117	4.05
MMC	500	0	0.24	SP6	5	M	0.65	108	3.97
MM1	500	10	0.24	SP6	3.5	M	0.48	120	4
MM11	500	20	0.24	SP6	3.5	M	0.48	125	3.87
MM3	500	10	0.24	SP6	3.5	M	0.65	115	4.01
MM33	500	20	0.24	SP6	3.5	M	0.65	125	3.99
MSO	350	0	0.5			S	0.65	112	3.4
MSC	500	0	0.24	SP6	4	S	0.65	102	3.38
MS1	500	10	0.24	SP6	3.5	S	0.48	100	3.26
MS11	500	20	0.24	SP6	3.5	S	0.48	120	3.28
MS3	500	10	0.24	SP6	3.5	S	0.65	119	3.56
MS33	500	20	0.24	SP6	3.5	S	0.65	128	3.56

From this research, the results are significantly improving compression strength in magnetite concrete. Adding 10% silica fume can improve compression strength of concrete up to 45% using normal sand and 56% by magnetite fine aggregate and reduce thickness of shielding. However, additional of silica fume more than 10% has impacted slightly comparing by 10% added then reduced attenuation of concrete up to 5%. In term of ratio of coarse aggregate, value of 0.65 has highest rank in compression strength and radiation attenuation rather than 0.45 and slightly impact of application in magnetite or sand as fine aggregate. This research is also contradicting with Yang's experiment[17] which adding coarse aggregate is more recommended than fine aggregate.

In case of  $\gamma$ -rays attenuation, another experiment conducted utilizing radiation Californium-252 (<sup>252</sup>Cf)[34] beside an experiment that mentioned before[22]. Using

local fine aggregate from Bangladesh, magnetite and ilmenite are mixed with normal coarse aggregate with w/c ratio 0.50 and radiation test conducted for measuring attenuation in neutron shielding. By comparing with previous similar aggregate experiment[35] and another heavyweight material [35-37] resulted highest attenuation coefficient of ilmenite and magnetite for this local fine aggregate with HVT 7.40 and 7.00 cm, respectively. Even though using same type of heavyweight aggregate, varies compositions and ingredients of concrete, chemical, and physical properties of aggregate had been used affected significantly on attenuation coefficient and compressive strength.

Not only magnetite has been examined largely, but also other iron minerals like serpentine, colemanite, ilmenite, limonite, hematite, etc. has been studied further. But, these studies related to radiation shielding and attenuation only [38-40]. Conducting experiments had done in term of ilmenite aggregate by comparing two ilmenite concrete with different density for producing highest radiation attenuation coefficient in radiation shielding using three varies of gamma rays beam energy—bare , cadmium, and boron carbide filter[39]. Iron punching used to add density in concrete as planning  $4.6 \text{ g/cm}^3$  and  $3.5 \text{ g/cm}^3$  without it by only combined ilmenite as aggregates. Different thickness of ilmenite concrete had been prepared from 15 to 45 cm with increment 10 cm to measure gamma rays attenuation and secondary gamma rays by neutron effect. This research recommended negating utilization of iron punching in mixture with thermal heat propagation effect and economical reason[39].

**Table 2.7** Variation mixture percentage of ilmenite concrete with under investigation ( $\rho=3.5 \text{ g/cm}^3$ ) and previous investigation ( $\rho=4.6 \text{ g/cm}^3$ )[40]

Concrete under investigation		Previously investigated concrete	
Composition	Percentage weight	Composition	Percentage weight
Portland cement	8.3%	Portland cement	9.0%
Ilmenite fine aggregate <sup>1</sup>	38.0%	Ilmenite fine aggregate <sup>1</sup>	18.41%
Ilmenite coarse aggregate <sup>2</sup>	25.0%	Ilmenite coarse aggregate <sup>2</sup>	18.09%
Ilmenite coarse aggregate <sup>3</sup>	23.0%	Iron punchings	50.7%
Water	5.0%	Water	5.0%
1. Fine aggregate grain size (0–0.5 cm)		1. Fine aggregate grain size (0.2–0.47 cm)	
2. Coarse aggregate grain size (1–2 cm)		2. Coarse aggregate grain size (0.47–5.81 cm)	
3. Coarse aggregate grain size (2–3 cm)			

Moreover, this research also brought derivation empiric equation to compute gamma rays flow ( $\phi_\gamma$ , photons/cm<sup>2</sup>s) with varies of thickness as follow:

$$\phi_\gamma = (976077 - 103838\rho)\exp[-(0.001246 + 0.0389\rho)t] \quad (2.5)$$

Where, it applies difference heavyweight concrete density ( $\rho$ , g/cm<sup>3</sup>) and thickness ( $t$ , cm). However, that equation can be used for energy less than 10 keV. Following previous experiment, ilmenite aggregate is used pairs with limonite and compared with combination hematite-serpentine[40].

**Table 2.8** Mixture of hematite-serpentine concrete ( $\rho=2.5 \text{ g/cm}^3$ ) and ilmenite-limonite concrete ( $\rho=2.9 \text{ g/cm}^3$ )[39]

Hematite-serpentine concrete ( $\rho = 2.5 \text{ g/cm}^3$ )		Ilmenite-limonite concrete ( $\rho = 2.9 \text{ g/cm}^3$ )	
Material	Aggregate density (kg/m <sup>3</sup> )	Material	Aggregate density (kg/m <sup>3</sup> )
Hematite ore	1509	Ilmenite ore	1927
Serpentine ore	558	Limonite ore	415
Portland cement	350	Portland cement	350
Water	236	Water	121

Using higher energy range (1.16–6.60 MeV), this experiment obtained development equation (2.4) with calculating gamma-rays flow of hematite-serpentine ( $\phi_{h,s}$ ) by gamma rays flow of ilmenite-limonite ( $\phi_{i,l}$ ) below:

$$(\phi_{h,s})_\gamma = 1.316(\phi_{i,l})\exp(0.018t) \quad (2.6)$$

This had done because linear coefficient attenuation ilmenite-limonite higher than hematite-serpentine; it is related to higher density of ilmenite-limonite than hematite-serpentine.

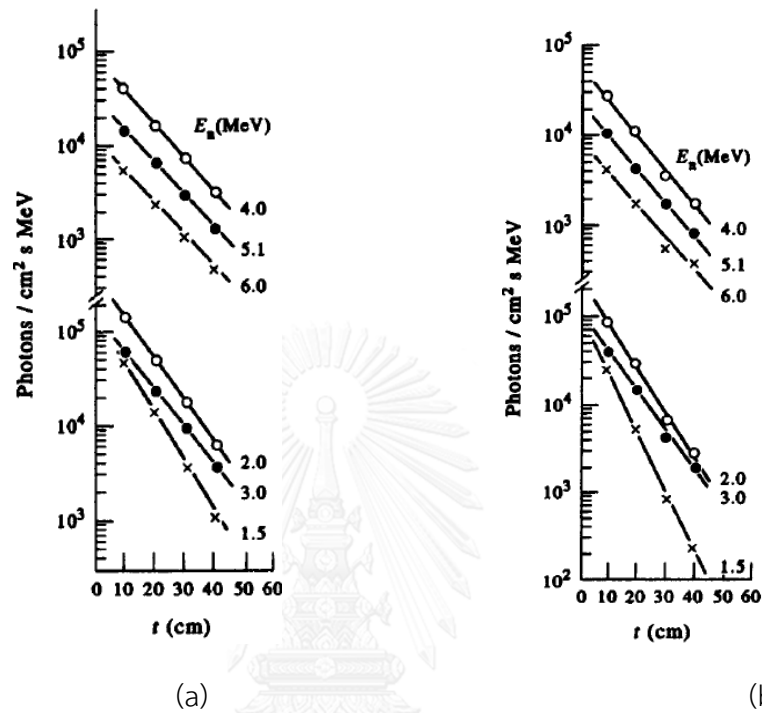


**Figure 2.11** Gamma rays flow in varies energies for (a) hematite-serpentine concrete, and (b) ilmenite-limonite concrete[39].

In another case, combining ilmenite-serpentine with different percentage of steel fibre had conducted to examine heavyweight behaviour in impact effect—method of falling weight with 10 kg applied for measuring energy consuming up to failure[41]. Using constant cement dosage and w/c ratio 0.56 with addition 1.5% of plasticizer, this experiment want to measure impact strength of concrete with ratio 2:1. In term of density, combination ilmenite-serpentine made higher value 25% to 48% than normal concrete. Moreover, ultrasound velocity test recorded more than 2% of additional steel fibre propagated crack or honeycomb in ilmenite-serpentine concrete.

**Table 2.9** Combination different steel fibre in ilmenite-serpentine concrete[41]

No. Specimen	Cement kg/m <sup>3</sup>	Coarse Aggregate, kg/m <sup>3</sup>		Fine Aggregate, kg/m <sup>3</sup>		Water kg/m <sup>3</sup>	Fiber kg/m <sup>3</sup>	S.P. kg/m <sup>3</sup>
		Gravel	Ilmenite	Sand	Serpentine			
1	400	1328	-	664	-	224	0	6
2	400	-	1947	-	541	224	0	6
3	400	-	1947	-	541	224	78	6
4	400	-	1947	-	541	224	156	6
5	400	-	1947	-	541	224	234	6

Mechanical properties from this represented by computing compressive, tensile, flexural, and impact strength of ilmenite-serpentine concrete with steel fibre. Compressive and tensile strength have similar pattern result with ultrasound velocity, it might be honeycomb effect which made by more addition of steel fibre, otherwise different result in flexural and impact strength which increasing of steel fibre has benefit for those two strength up to 10% for flexural and 1.69 times crack failure for impact strength compared with normal concrete.

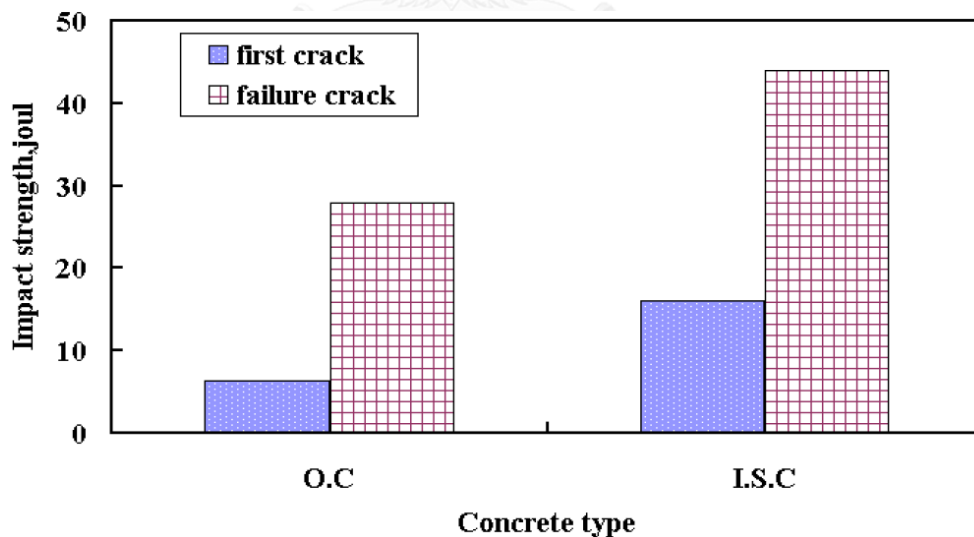


**Figure 2.12** Comparison result of impact strength between normal concrete (O.C) and ilmenite-serpentine concrete (I.S.C)[41]

Different with magnetite and ilmenite that had explained before, colemanite usually uses as coarse aggregate due to need special handling for raw materials and

economical reason. For those reasons too, colemanite is still less exploration in term of radiation shielding and lack information in mechanical properties. By remaining constant of density ( $2,410 \text{ kg/m}^3$ ), colemanite coarse aggregate with varies percentage of colemanite by total aggregate 15% to 75% with increment 15% mixed with highest cement dosage to reduce effect of colemanite mineral itself and resist mechanical properties of concrete and attenuated with neutron energy[42]. This test obtained that using colemanite as coarse aggregate reduce thickness of shielding 13 cm or equals with 14 tons of mass. Further, using 10% percentage colemanite by total aggregate is recommended to achieve effective mixture in term of cost with requiring high amount of cement.

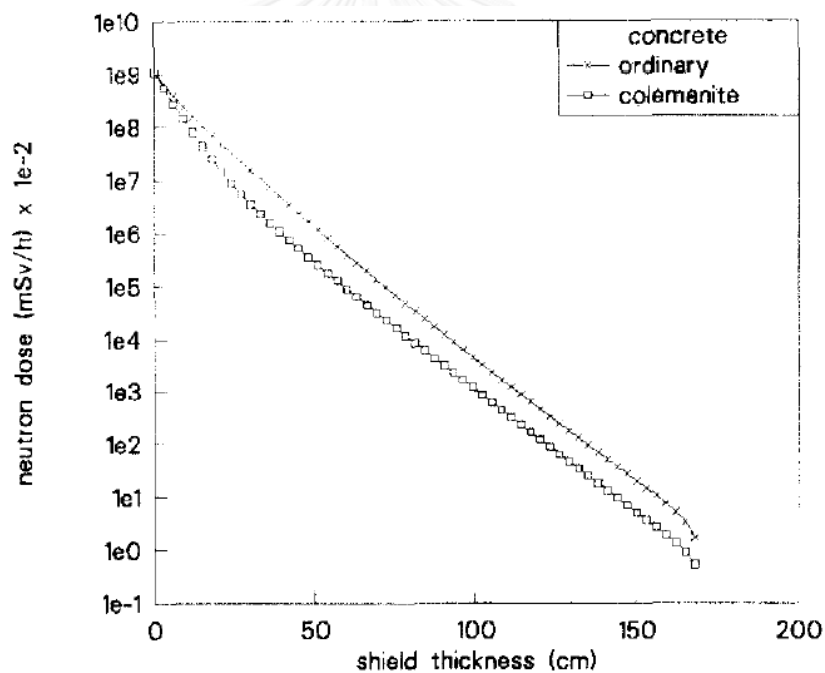


**Figure 2.13** Neutron flow ratio in varies thickness of normal and colemanite concrete[42].

#### 2.4.4 Mixture of Synthetic Aggregate

Heavyweight synthetic aggregate is not popular comparing with barium and iron minerals due to special handling preparation and economical reason. This usage came

up for harness waste disposal by recycling it into aggregate. Similar with experiment before[28], but in this case ferrochromium was used as coarse aggregate[43] with combining application of fly ash. Investigating mechanical properties of concrete with constant cement dosage  $400 \text{ kg/m}^3$  and water-binder ratio 0.40, this research applied combination percentage of fly ash—10, 20, and 30%— and ferrochromium—between 25% and 75% with increment 25%— in concrete and used normal crush stone with two gradation distribution and normal sand as mixing; used superplasticizer to satisfy workability in mixing.

Ferrochromium in this research has significant impact in term of unit weight, slump value, compressive strength, splitting tensile strength, modulus of elasticity, and freeze-thaw, but those matters is contradictive with increasing of fly ash in concrete. However, fly ash has positive effect in workability, porosity, and water absorption of concrete. These results mean ferrochromium applicable in term of mechanical properties heavyweight material and need full-scale experiment for attenuation radiation capability.

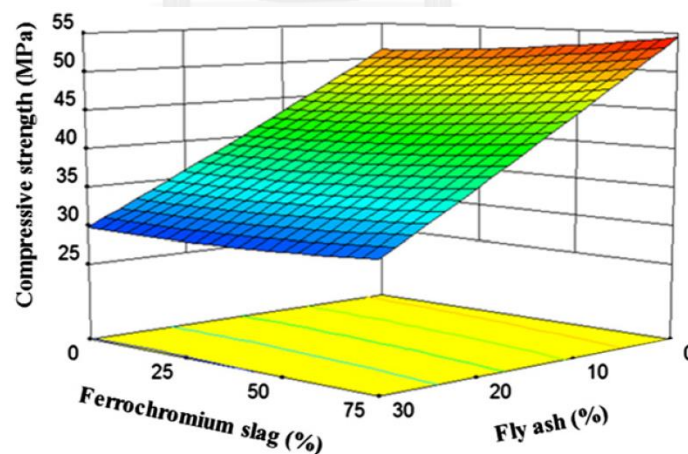


**Figure 2.14** Compressive strength response due to fly ash and ferrochromium[43]

Unlike the previous cases, steel fibre is largely used in concrete technology. Mechanical properties effect of steel fibre is already proven to straighten tension which weakest part of concrete and resist more loads when deflection happened. It also

increased the toughness and reduced brittle on concrete, but in term of application for radiation shielding has not investigated yet. One of study about it had been conducted with using normal concrete adding by steel fibre to examine  $\gamma$ -rays attenuation for radiation shielding. Using energy sources from  $^{60}\text{Co}$ ,  $^{22}\text{Na}$ , and  $^{137}\text{Cs}$ , Constant cement dosage  $350 \text{ kg/m}^3$ , w/c ratio 0.55, and additional admixture 2.5% had used to investigate effect of varies percentage steel fibre on concrete[44]. Compressive and tensile strength are also measured in term of mechanical properties beside density of concrete.

**Table 2.10** Mixture concrete with different percentage of steel fibre[44]

Mixture Fiber Content	Cement (kg)	Sand (kg)	Coarse Aggregate (kg)	Water (kg)	Additives (kg)	Steel Fiber (kg)	Concrete density ( $\text{gm/cm}^3$ )
0	10.432	17.777	35.557	5.737	0.261	0	2.14
1	10.432	17.777	35.557	5.737	0.261	0.698 (1%)	2.17
2	10.432	17.777	35.557	5.737	0.261	1.395 (2%)	2.18
3	10.432	17.777	35.557	5.737	0.261	2.093 (3%)	2.22
4	10.432	17.777	35.557	5.737	0.261	2.790 (4%)	2.11

By adding steel fibre increased compressive strength, tensile strength, and density 1.012 (1% addition), 1.189 (3% addition), and 1.1 (3% addition) times comparing with normal concrete without steel fibre. Furthermore, additional 3% of steel fibre is effective for attenuating  $\gamma$ -rays.

## 2.5 Mixture Based on American Concrete Institute (ACI) and American Society for Testing and Materials International (ASTM)

Lack of information and standard in mechanical properties heavyweight concrete made this type of concrete less development. In fact, application of heavyweight concrete for radiation shielding decreased thickness of shielding wall up to 40%[45]. All standard that have been used is not detailed explaining about planning equation or trusted experiment data. And, some of standard based on normal concrete

which may it be did not significantly appropriate for applying in heavyweight concrete. For example, the common standard[46] did not give specific preference for concrete more than  $2500 \text{ kg/m}^3$  in term of mechanical properties compared with lightweight concrete. Moreover, ACI 349 that special utilities concrete structure in nuclear safety had mentioned density impact related to mechanical properties.

Density of concrete, material cost and workability are main factor to specify mixture ratio in heavyweight concrete. Although compressive strength is not quite important, but structure performance is required for measuring safety element in building. Design mixture must fulfil all requirements to obtain proper performance in radiation shielding. Explanation about heavyweight material can be found in ASTM C637[47] and ASTM C638[48]. It also explained properties and type of each heavyweight aggregate. It classifies heavyweight material based on particle composition such as barium mineral, iron mineral, boron, Ferro-phosphorus. Moreover, it explained detail characteristic of each material e.g., mixing Portland cement with Ferro-phosphorous will lead flammable and possibly toxic gases that can expand high pressures in confined area or detail numbers can be seen in Table 2.9. Though those numbers are not restricted; it can be used as reference for choosing material in concrete. For specific gravity, it may be different depend on composition in each area.

In accordance with those materials, there is needed standard mixture to produce effective ratio mixed design. Practically in mass production, quantity of concrete must consider capacity of mixer, setting time due to transport in construction site. It is needed to prevent segregation, consolidation, and packing on concrete. Further, it stated in ACI 304.3R-96[49].

**Table 2.11** Characteristics heavyweight aggregate[50]

Heavy Aggregate	Composition	Specific Gravity (SSD)		Percent by weight	
		Coarse	Fine	Iron	Fixed water
Ilmenite	Fe, Ti, O, etc.	4.5	4.6	40	0
Limonite-goethite	$2\text{Fe}_2\text{O}_3 \cdot 3\text{H}_2\text{O}$	3.45	3.7	55	11
Magnetite	$\text{Fe}_3\text{O}_4$	4.5	4.55	60	1
Magnetite	Hydrous iron	4.3	4.34	60	2-5
Barite	>92% $\text{BaSO}_4$	4.2	4.24	1-10	0
Barite	>90% $\text{BaSO}_5$	4.28	4.31	<1	0
Ferrophosphorus	$\text{Fe}_3\text{P}$ , $\text{Fe}_2\text{P}$ , $\text{FeP}$	6.3	6.28	70	0
Steel aggregate		7.78		99	0
Iron shot			7.5	99	0

Physical properties of concrete are tend to have high of elastic modulus. In low thermal expansion, concrete will have low elastic and deformation. This also condition applies to determine thickness in heavyweight concrete. In fact, intending high compressive strength usually effect in application low w/c and this will make problem when hardening process happens; it propagates shrinkage and creeps on concrete. Furthermore, special curing treatment should be held; it can do by pre-cooling or post-cooling treatment. This two methods is described detail in ACI 207.2R[51] and ACI 224R[52].

Mix design proportion of heavyweight concrete follows the steps that outlined in ACI 211.1[53]. Producing high compressive strength and density and consider high workability in application, proportion of water, admixture, and all ingredients should be fixed. According to capability concrete for radiation shielding, all requirement is specified in ACI 349.01[31]. Furthermore, detail characteristic mixture of heavyweight concrete is specified in Table 2.10.

Table 2.12 Characteristics mixture ratio of heavyweight concrete[31]

Density (unit weight) kg/m <sup>3</sup>	Compressive strength age 3 months MPa	Cement kg/m <sup>3</sup>	Heavy aggregate (kg/m <sup>3</sup> )				Mix water kg/m <sup>3</sup>	Water content* (kg/m <sup>3</sup> )	
			Fine		Coarse			Minimum	Maximum
4810	34.5	376	Iron shot	3120			192	56	192
			Magnetite	1120					
4810	33.6	386	Ferrophosphorus	1470	Ferrophosphorus	2740	203	58	203
4200	36.9	380	Ferrophosphorus	1120	Ferrophosphorus	1120	205	58	205
			Barite	560	Barite	800			
3720	44.8	389	Magnetite	1380	Magnetite	1760	184	91	216
3560	41.4	309	Barite	1380	Barite	1680	186	46	186
3510	44.8	399	Hydrous iron ore	1310	Hydrous iron ore	1600	192	147	280
3040	39.6	335	Serpentine	800	Magnetite	1700	208	146	304
<b>Pre-placed-aggregate method</b>									
5540	207	330	Magnetite	700	Punchings	4330	181	56	189
4810	34.5	317	Magnetite	670	Magnetite	1070	175	66	192
					Punchings	2560			
4210	41.4	356	Limonite	450	Limonite	960	195	208	351
					Punchings	2240			
4200	33.1	317	Magnetite	670	Magnetite	1950	175	75	202
					Punchings	1070			
3920	-	312	Serpentine	370	Serpentine	769	157	-	-
					Punchings	2320			
3910	34.5	280	Magnetite	590	Magnetite	2880	155	77	191
3440	34.5	364	Limonite	460	Limonite	450	200	175	320
					Magnetite	1950			

\*Maximum water content is water weight when concrete is wet. Minimum water content is amount left after drying to constant weight at 185 F (85 C). Difference between the maximum water content and the amount of mix water added is the water of crystallization held by the aggregate. The difference between the minimum water content and the water of crystallization is the water retained by the hardened cement paste.

## CHAPTER 3

### Research Methodology

#### 3.1 Physical and Mechanical Properties of Aggregates

Deriving heavyweight material from mining must pass requirement uniformity of aggregate. This is done to maintain quality of aggregate. Modifying gradation, size, density of material, and moisture level can impact into feature and outcome of mixture[54]. Material that came from mining usually still in boulder shape, crushing process is needed to simplify in concrete production.

Preliminary study of availability raw heavyweight material must be conducted before all laboratory mechanism happen. This will be done to make sure amount of material in Thailand as mass production. Coordinating with department of mining and mineral resource, feasibility study will be done in term of quality of material itself. Physical, mechanical, and chemical characteristics of heavyweight material in Thailand will be analysed before crushing process. Moreover, these characteristics will be needed for combining each material to produce effective mix design in heavyweight concrete.

Some experiment test is conducted to gain information related to physical characteristics such as specific gravity, water absorption, bulk density, and void of aggregates. Those tests will be conducted at Concrete Laboratory, Department of Civil Engineering, Chulalongkorn University. Analysing composition of elements to investigate chemical characteristics is conducted at Science and Technology Centre, Faculty of Science, Chiang Mai University with X-ray fluorescence (XRF) method and is supported with Energy-dispersive X-ray spectroscopy (EDS) method is conducted at Science and Technological Research Equipment Centre (STREC), Chulalongkorn

University. Besides that, additional information about surface topography is also conducted with Scanning Electron Microscopy (SEM) analysis.

### 3.1.1 Gradation, Wear, and Organic Content

Crushing process is done to acquire material in small pieces, and then that material will be graded using standard sizing sieve aggregate. It is required to measure size distribution for coarse aggregate and fineness modulus for fine aggregate. Coarse aggregate and fine aggregate that is used at least followed requirement ASTM C637[47] which coarse aggregate should through sieve size 19 mm (3/4 in.) and detained to sieve 4.75  $\mu\text{m}$  (No.4) and for fine aggregate should through sieve size 4.75  $\mu\text{m}$  (No.4) and detained to sieve 150  $\mu\text{m}$  (No.100). Moreover, this aggregate is calculated quantity mass and soaked in water for 24 hours to clean it up from the dust.

Other tests are also conducted to measure aggregate quality. Abrasion test is organized to determine worn-out durability and threshold of use coarse aggregate using Los Angeles machine. And then, fine aggregate is checked for organic impurities test; controlling of decay organic substance material that is mixed with fine aggregate estimated.

### 3.1.2 Specific Gravity and Water Absorption

Based on ASTM C127-01[55], relative density is derived from computing 500 grams soak of coarse aggregate in water, then absorbing the surface until dry and pondering it. Further, relative density can be calculated by equation (3.1)

$$\text{Relative density} = \frac{A}{A - B} \quad (3.1)$$

$$\text{Water absorption (\%)} = \frac{C - A}{A} \times 100 \quad (3.2)$$

If A = weight of saturated-surface-dry (SSD) aggregate in air (gram)

B = weight of saturated aggregate in water (gram)

C = weight of dry-oven aggregate in air (gram)

In case of water absorption, drying coarse aggregate in oven with temperature 105<sup>0</sup>-115<sup>0</sup>C for approximately 24 hours then let it cool at room temperature, weigh, and calculate with equation (3.2).

For fine aggregate, measuring relative density is applied on ASTM C128-01[56] using 500 gram SSD aggregate which is dried after soaked into the water for 24 hours approximately 1000 gram of sample. Placing this sample aggregate into volumetric apparatus and filling with water up to bubbles inside apparatus disappear. Further, weigh this apparatus with all content inside then pour fine aggregate and water into pan, dry in temperature 105<sup>0</sup>-115<sup>0</sup>C for approximately 24 hours, and weigh again that aggregate. Calculation for relative density and water absorption can be seen in equation (3.3) and equation (3.4) as follow:

$$\text{Relative density} = \frac{S}{B + S - C} \quad (3.3)$$

$$\text{Water absorption (\%)} = \frac{S - A}{A} \times 100 \quad (3.4)$$

If A = weight of dry-oven aggregate in air (gram)

B = weight of volumetric apparatus with water (gram)

C = weight of volumetric apparatus with fine aggregate and water (gram)

S = weight of saturated-surface-dry (SSD) aggregate in air (gram)

### 3.1.3 Bulk Density (Unit Weight) and Void in Aggregates

In term of bulk density, ASTM C29[57] is used reference for measuring bulk density in dense and slack condition and void gaps of aggregate. This applies for aggregate is not more than 125 mm. Starting with fill up 1/3 of measuring container then compacting 25 times, repeat the process for other 1/3 of part until container full

and measure container capacity. Calculation of bulk capacity can be seen in equation (3.5) and equation (3.6).

$$\text{Unit weight (M)} = \frac{A}{B} \quad (3.5)$$

$$\text{Gross void gaps (\%)} = \left(1 - \frac{M}{C}\right) \times 100 \quad (3.6)$$

If A = weight of aggregate full in container (gram)

B = Measurement container capacity (gram)

C = specific gravity (gram)

### 3.2 Experiment Problems

Verifying capability and availability heavyweight material in Thailand become mass production concrete to fulfil requirement in the future is became main issue of this research held. Many experiments in Thailand had been conducted in heavyweight concrete [15, 23-25, 58] only focused on attenuation capability, less in term of structural matters, and using barite material as main object research. This research will conduct combination percentage of barite aggregates to produce effective mix design. Amount of cylinder specimen will be casted to measure appropriate compressive strength and accommodating workability of heavyweight concrete. In case of radiation shielding, cylinder specimen will be checked in different points to check its homogeneity about attenuating  $\gamma$ -rays. Moreover, heavyweight concrete beam specific reinforcement are made to examine characteristic of mechanical properties in heavyweight concrete.

### 3.2.1 Mix Design and Specimen

#### 3.2.1.1 Material

All concrete mixture used local material from Thailand. For main binder, ordinary Portland cement type I is used. Crushed gravel and natural sand were used as normal concrete coarse and fine aggregate, respectively. In term of heavyweight material, barite aggregate is largely used at this experiment mined from Phrae Province, north of Thailand.



**Figure 3.1** Visualization of aggregates (a) Natural sand (b) Gravel (c) Barite sand, and (d) Barite stone.

Chemical admixture Masterglenium ACE 8320 was chosen for this experiment. It was supplied by liquid dispersible in water that specialized for mix concrete with low water-cement ratio. The compressive strength after 28 days are targeted reaching 30 MPa. It were determined by average value of three cylinder specimen.

In relation with steel reinforcement in the beam, reinforcement bars accord to TIS (Thailand Institute Steel) standard. Deformed bar is tested to gain its mechanical properties. Detailed is shown in Table 3.1 below.

**Table 3.1** Mechanical Properties of Reinforcement Steel

Size	Grade	Cross-section area (mm <sup>2</sup> )	Unit weight (kg/m)	Modulus of Elasticity (MPa)	Yield Strength (MPa)	Ultimate Strength (MPa)
RB6	SR24	28.30	0.222	200,000	235	385
RB9	SR24	63.60	0.499	200,000	235	385
DB16	SD40	201.06	1.578	200,000	522.2	646.6

### 3.2.1.2 Specimen

In this study, specimens that were used are cylinder specimen with dimension 150x300 mm, 4 specimens for each mixture referred for compressive test and radiation test as preliminary sample for appointing the best mixture. Those best mixtures will be continued to be made as beam specimen. Three sample will be tested for 7 days and others in 28 days for compressive test. Besides that, along with processing with beam sample, other 3 cylinder will be made as control strength of concrete.

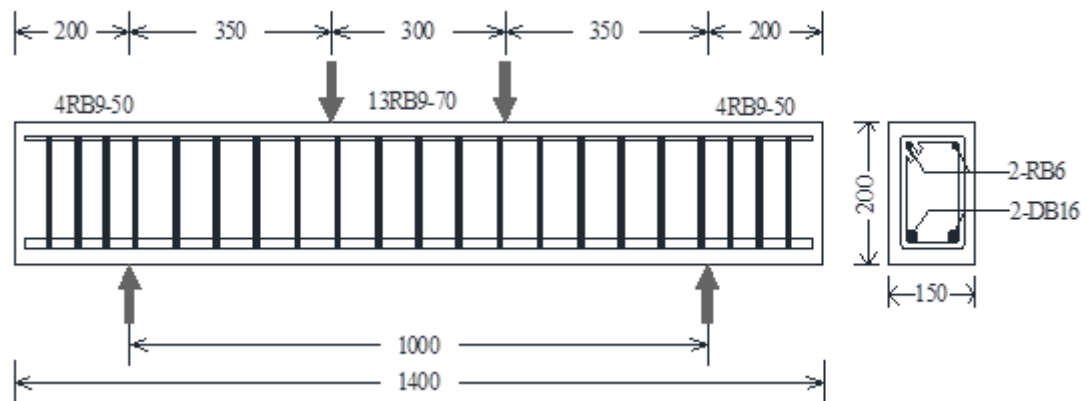


**Figure 3.2** Dimension and Detail of reinforcement steel in beam specimen

In term of structure, beam specimen with length 1,400 mm, width 150 mm, and height 200 mm were prepared a number of eight beams with two different w/c ratio that consisted of two beam as control beam made from normal aggregate, two beam made from barite aggregate, and other are beam that have highest value of compressive strength.

### 3.2.1.3 Mix Design

Modifying mixture design Keun-Hyeok Yang, et al[17] whom designed mixture for magnetite concrete and combined with experiment Ekasit Wongchirung[25] whom designed mixture from local material in Thailand for barite concrete majority, this experiment will use barite from local ores in Thailand. This material will be combined with various percentage of normal aggregate replacement from 0% to 100% with 25% lapse each. The maximum size of coarse aggregate and fine aggregate assigned to 25 mm and 5 mm, respectively. Afterwards, this combination will be divided in two part of water-cement ratio which is 0.35 and 0.55 with constant water content  $180 \text{ kg/m}^3$ . Moreover, this experiment upgrades the volumetric fine aggregate to total aggregate at 45%; this value is enhanced 5% from Keun-Hyeok Yang's design. Keeping low workability, water-reducer admixture will be added in w/c ratio 0.35 and 0.55

approximately 0.8% and 0.4% of cement content respectively. For easy recognizing specimens, the specimen would be named as given in Table 3.2 below.

**Table 3.2** Varies of heavyweight concrete mixture composition with replacement of normal aggregate and different w/c ratio

Specimen Name	w/c	R <sub>F</sub> , %	R <sub>C</sub> , %	Cement	Water	Unit Weight, kg/m <sup>3</sup>				R <sub>SP</sub> , %		
						Fine Aggregate		Coarse Aggregate				
						Sand	Barite	Limestone	Barite			
NN1	0.35	0	0	514	180	511	0	1341	0	0.8		
BB1						0	873	0	1772			
RFA-251						25	654					
RFA-501						50	436					
RFA-751						75	218					
RFA-1001		100	0									
RCA-251		0	25			0	873	0	873		335	1329
RCA-501			50								670	886
RCA-751			75								1006	443
RCA-1001			100								1341	0
NN2	0.55	0	0	327	180	657	0	1341	0	0.4		
BB2						0	1122	0	1772			
RFA-252						25	841					
RFA-502						50	561					
RFA-752						75	280					
RFA-1002		100	0									
RCA-252		0	25			0	1122	0	1122		335	1329
RCA-502			50								670	886
RCA-752			75								1006	443
RCA-1002			100								1341	0

The sequence of mixture heavyweight aggregate is shown detail in Table 3.2 above. Coding the specimen based on type of replacement aggregate, percentage of

replacement, and water-cement ratio. Further, NN and BB are representing control beam made by pure normal aggregate and pure barite aggregate, respectively. Code RFA and RCA represented replacement fine aggregate and coarse aggregate, code 25, 50, 75, and 100 represented percentage of replacement. Finally code 1 or 2 represented w/c ratio in mixture where 1 is w/c 0.35 and 2 is w/c 0.55.

In every mixture, blend coarse aggregate, fine aggregate then cement approximately 2 minutes for dry mixture. After that, pour water along 80% and let mixed for 1.5 minutes then pour the rest of water. Let mixer running gradually until 2 minutes. Preventing from segregation of aggregate is recommended to keep low speed. After all sequence are completed, slump test should be taken to quantify workability of fresh concrete which is based on ASTM C143[59] then casting took a place with tightening with vibrator every 1/3 layer. Moreover, curing process should be done to maintain durability of concrete and achieve anxiety compressive strength.

Mixture process up to compressive strength test will be conducted in Material Testing Laboratory, Department of Civil Engineering Faculty of Engineering Chulalongkorn University. Compressive test is specified in 7 and 28 days at the curing ages using 2000 kN compressive testing machine. A set of cylinder specimen is used to set compressive strength.

### **3.2.2 Radiation Attenuation Test**

The purpose of this test is to determine radiation attenuation coefficient of  $\gamma$ -rays. Using cylinder specimen similar with specimen for compressive test, radiation is penetrated in five different point along the height of cylinder with the thickness 150 mm and interval penetration of radiation 30 mm.

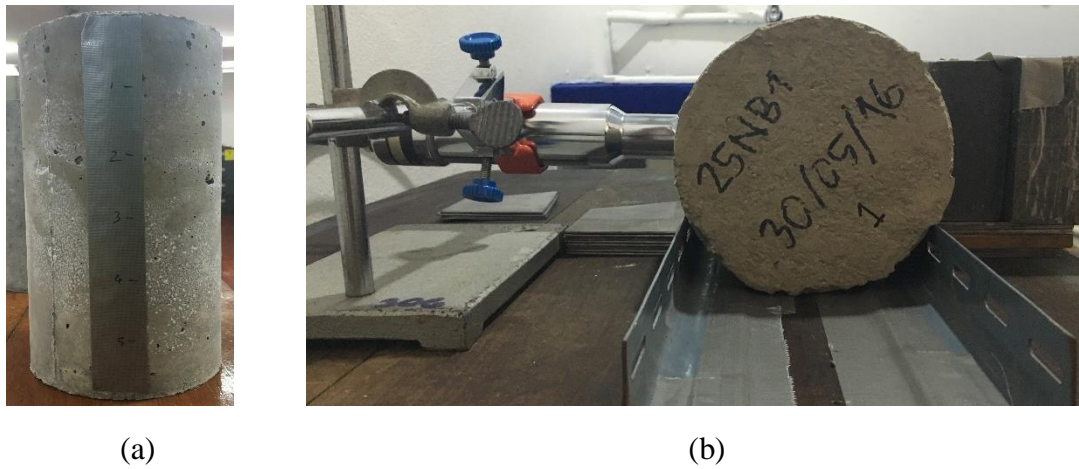


**Figure 3.3** Radiation testing (a) Cylinder sample with penetrated point, (b) Set-up radiation test in laboratory

It will be used sources from caesium 137 ( $^{137}\text{Cs}$ ), and cobalt 60 ( $^{60}\text{Co}$ ) with different energies. This experiment will be conducted in Radiation Measurement Laboratory, Department of Nuclear Engineering Faculty of Engineering Chulalongkorn University.

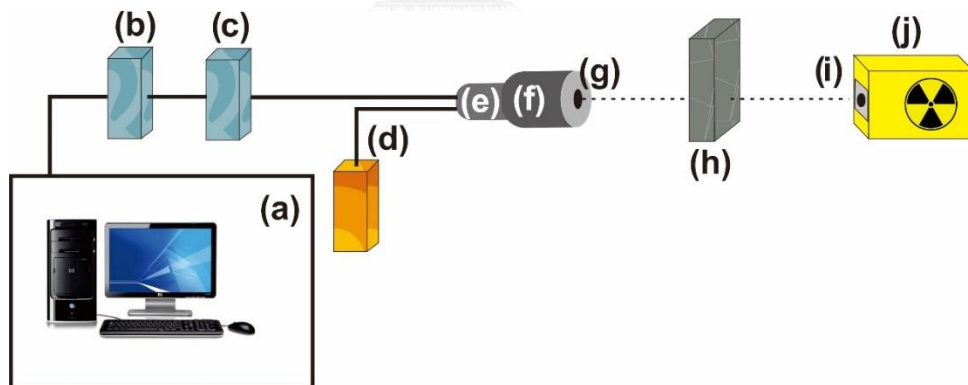


**Figure 3.4** Scheme of set-up  $\gamma$ -rays transmission test[60]

(a) procurement data sample software; (b) signal amplifier; (c) pre-amplifier; (d) high voltage; (e) photomultiplier; (f) NaI(Tl) detector; (g) detector collimator; (h) concrete sample; (i) radioactive source; (j) source collimator.

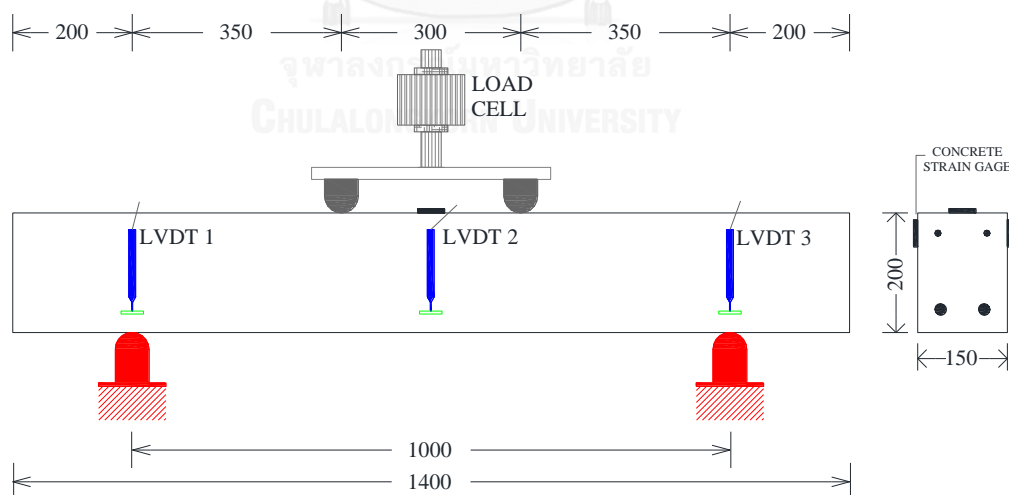
Moreover, various specimens from combination mixing are calculated radiation attenuation coefficient which mentioned in equation (2.1) and equation (2.2) for

different source energies. And then, deciding which combination material has highest capability in  $\gamma$ -rays attenuation.

### 3.2.3 Heavyweight Reinforced Concrete Beam Test

Specimen model approaching by Campione and Mindess[61] is used this experiment. Rectangular cross section beam have width, height, and length at 150, 200, and 1400 mm is made for measuring flexural and shear strength. Two deformed bars possess DB16 as longitudinal tension reinforcement bar, and two RB6 as longitudinal compression reinforcement bar then stirrups with same type at spacing 70 mm. Longitudinal steel reinforcement at upper part is used for forming a framework to keep position of steel. Further, design of beam is planned for flexural failure.

Basically, steel reinforcement for the beam specimens is required to fulfil ACI 349[31]. The test will be conducted first to measure properties of specimen steel reinforcement. The tests are based on ASTM A370[62] about mechanical test of the steel. In this study, the steel reinforcement is constant parameter.



(a)

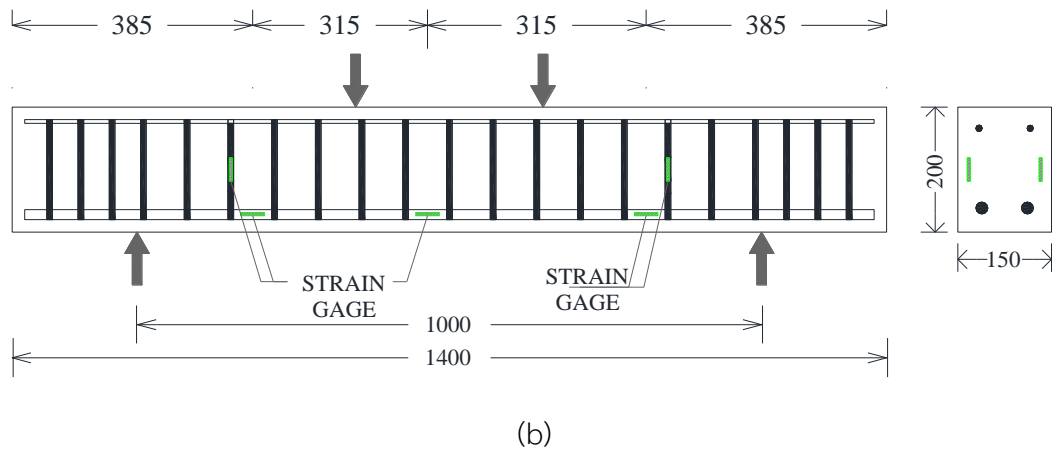


**Figure 3.5** Scheme of set-up beam tested with (a) LVDTs and concrete strain gages, (b) steel strain gages location in beam

Implementation of beam tested is done in Concrete Laboratory, Department of Civil Engineering, Chulalongkorn University by flexural test on beam based on ASTM C78-09[63]. Description of the beam tested can be found in Figure 3.5. The linear variable differential transformation (LVDT) will be applied to measure the deflection at mid-span of the beam as the highest point of bending and upper the support for measuring deflection which is happened in support area. Electrical strain gages will be put at tension bars at quarter and mid-span to measure the stain of the beam. Increment of loading will be utilized 10 kN until failure happened. While flexural test is done, the yields due to shear will propagate cracks opening then every steps of line pattern and opening should be documented.

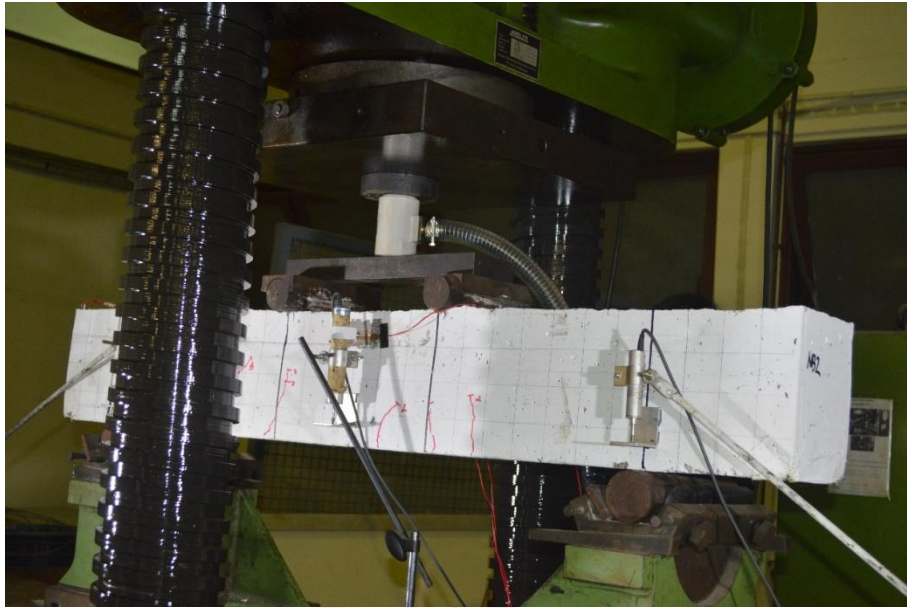


**Figure 3.6** Setting up experiment test with beam sample using four point testing.

After conducting the flexural test for beam is done, the calculation of stress-strain relationship, elastic modulus will be provided by this experiment then compared with ACI 349[31] provision.

## CHAPTER 4

### Result and Discussion

This chapter informs primary results of the experiments which are summarized and analysed by divided into

#### 4.1 Physical and Chemical Properties of Aggregates

The material selection played important roles to produce well mixture of concrete. Furthermore, aggregates are variable that is investigated in this experiment to obtain effective mixture with radiation gamma-ray shielding ability. Some experiments are conducted to inquire properties of aggregates as mentioned in previous chapter.

**Table 4.1** Physical Properties of aggregates

Aggregate	Relative Specific Gravity	Water absorption capacity (%)	Unit weight (g/cm <sup>3</sup> )	Void (%)
Natural sand	2.47	0.55	1.689	31.53
Gravel	2.68	2.08	1.559	41.80
Barite sand	4.21	0.27	2.949	29.96
Barite stone	3.54	0.33	2.071	41.49

In this study, barite were used to produce varies types of heavyweight concrete combine with crushed limestone and natural sand as natural aggregates. In Table 4.1 shows that barite as heavyweight concrete have higher specific gravity and density than normal aggregates, also barite will absorb more water that might me effect in workability of mixture. Then, value of percentage of absorption is needed to control

ratio of water in aggregates and percentage of void is used to design the composition of aggregate to be denser.

Beside physical properties, this study also conducted non-mechanical properties which is part of important characteristics in term structural parameter of heavyweight aggregates[64]. Figure 4.1 showed texture of each aggregate that investigated in this study in microstructure features.

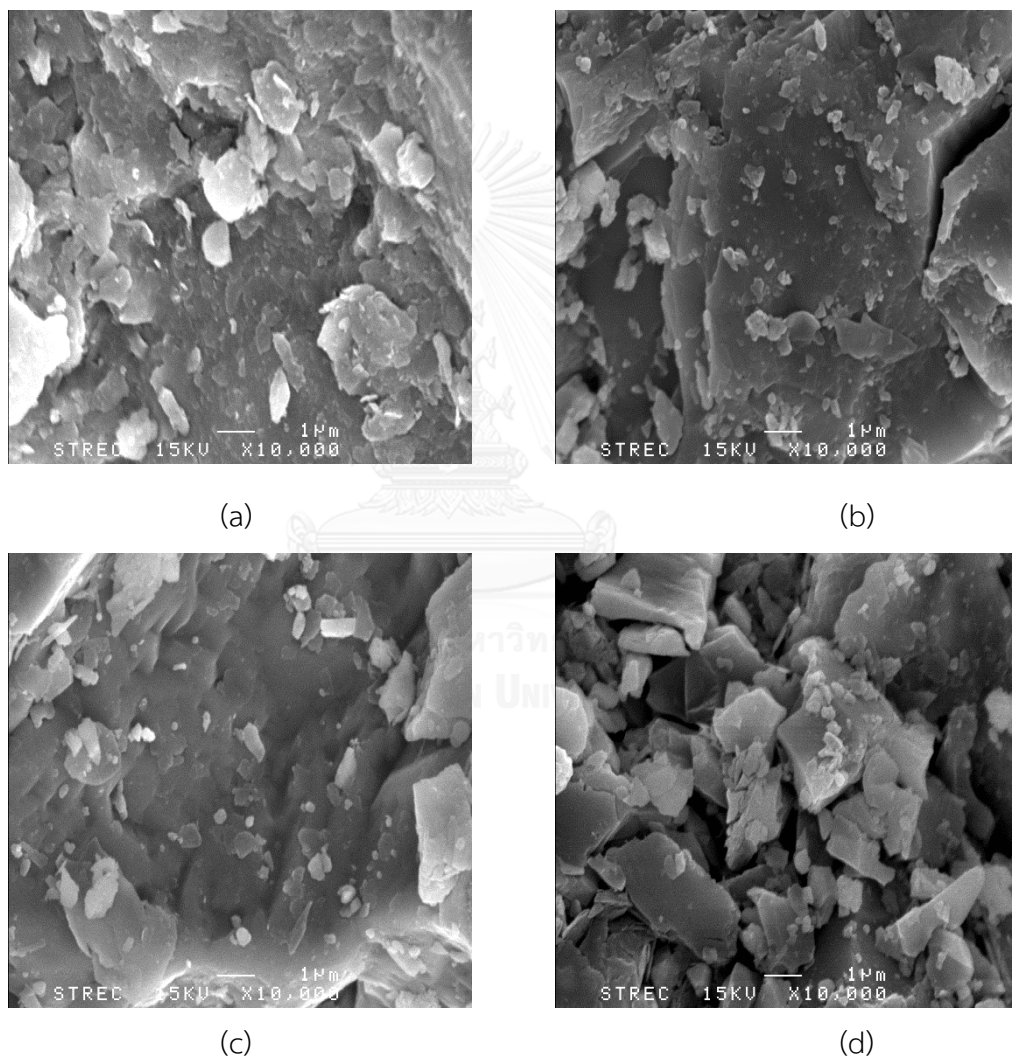
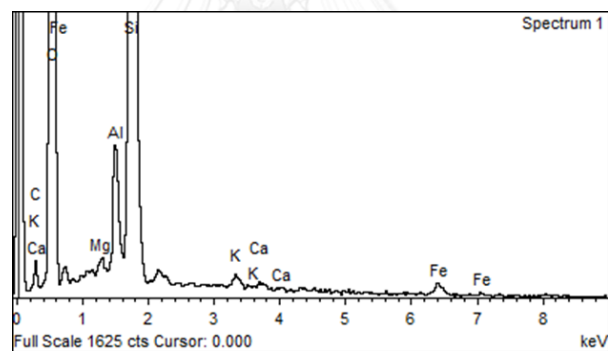


**Figure 4.1** The morphology of aggregates in microstructure by SEM micrograph each aggregates (a) Natural sand (b) Gravel (c) Barite sand, and (d) Barite stone.

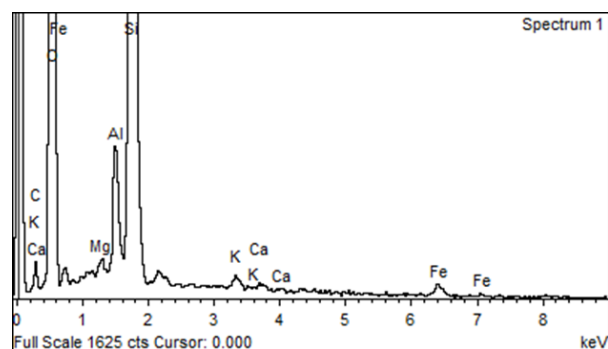
Using Scanning Electron Microscopy (SEM) analysis, morphology of each aggregate are investigated. Surface of aggregates is obtained data about orientation and texture of materials. In figure above, the surface of barite aggregate is rougher and denser than normal aggregate that is used. Furthermore, barite aggregate has layering in it surface, then make cohesion among particles is greater than normal aggregate.

Together with Energy Dispersive X-ray Spectroscopy (EDS) analysis, SEM analysis is used for performing qualitative and semi-qualitative result in chemical composition of materials and determined elements in aggregate. Peak of energy is representing appropriate of various element or particles in aggregates. Detail information of EDS analysis can be shown in Figure 4.2. Peak height of each element represented high percentage of element in those aggregates.



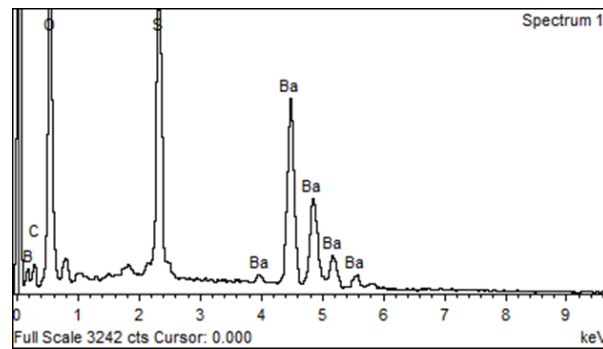
*Normal sand*

(a)

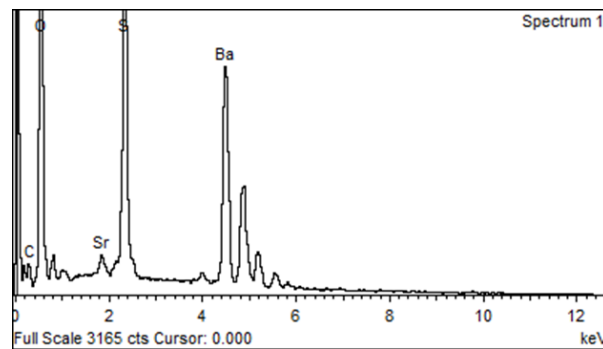


*Gravel*

(b)

*Barite sand*

(c)

*Barite stone*

(d)

**Figure 4.2** Element composition of each aggregate by EDS analysis (a) Natural sand (b) Gravel (c) Barite sand, and (d) Barite stone.

To obtain better average of composition, the EDXRF is used for analysis of the chemical composition in aggregates. Those might be useful for further research if continuing experiment in term of distribution of aggregate in microstructure element. Detail composition element of aggregate can be shown in Table 4.2 and Table 4.3 for normal aggregate and barite aggregate, respectively.

**Table 4.2** Chemical Composition of normal aggregates

Composition	Al <sub>2</sub> O <sub>3</sub>	SiO <sub>3</sub>	K <sub>2</sub> O	CaO	TiO <sub>2</sub>	Fe <sub>2</sub> O <sub>3</sub>
Natural sand	4.60	15.67	3.15	67.06	0.75	8.53
Gravel	8.26	78.84	7.80	2.28	0.27	2.16

**Table 4.3** Chemical Composition of barite aggregates

Composition	BaO	SO <sub>3</sub>	SiO <sub>3</sub>	Fe <sub>2</sub> O <sub>3</sub>	SrO
Barite	61.54	21.10	8.92	3.01	1.43

Based on both analysis, Correlation between EDS graph and EDXRF test showed similarity in result which are high peak of EDS graph representing high percentage of element content in sample.

#### 4.2 Workability of Concrete

In order to radiation gamma-ray shielding requirement, water composition in this study was keeping constant for both w/c ratio which is 180 kg/m<sup>3</sup>. Enhancing low workability in the mixture, superplasticizer was used with different percentage in both w/c ratio.

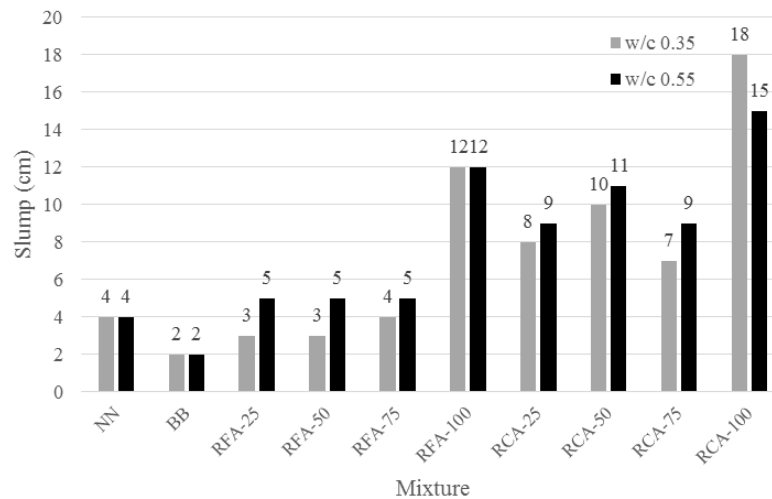


**Figure 4.3** Comparison slump value in varies percentage replacement of aggregate in barite concrete

Based on previous research using magnetite as heavy material[17] showed that workability in heavyweight concrete influenced by replacing fine aggregate especially effected by normal aggregate. From Figure 4.3 above denoted similar result in term of

percentage of replacement normal aggregate. However, present study by barite aggregate indicated that replacement coarse aggregate was most advantageous in term of workability of heavyweight concrete especially barite concrete.

### 4.3 Unit Weight of Concrete

Unit weight of concrete is main characteristics that affected to capability of concrete as radiation gamma-ray shielding. This concrete usually denser and heavier 1.5 times than normal concrete[65]. Correlated with this study, replacement barite aggregate with normal aggregate also had similar trend with previous study despite it is not reaching 1.5 times. Average barite concrete that resulted with some percentage replacement is 1.2 times than normal aggregate as shown in Table 4.4 below.

**Table 4.4** Unit weight of barite concrete and comparison each sample with normal concrete

Specimen	w/c 0.35		w/c 0.55	
	$\rho_b$ (g/cm <sup>3</sup> )	$\rho_b/\rho_n$	$\rho_b$ (g/cm <sup>3</sup> )	$\rho_b/\rho_n$
NN	2.54		2.43	
BB	3.12	1.23	3.19	1.31
RFA-25	3.02	1.19	3.14	1.29
RFA-50	3.02	1.19	2.99	1.23
RFA-75	2.97	1.17	2.87	1.18
RFA-100	2.85	1.12	2.80	1.15
RCA-25	3.04	1.20	3.11	1.28
RCA-50	3.01	1.19	3.06	1.26
RCA-75	2.91	1.15	2.99	1.23
RCA-100	2.79	1.10	2.84	1.17

There was no doubt that pure barite mixture have highest unit weight among the mixture, but table above also showed that both water-cement ratio with replacement 25% in fine and coarse normal aggregate still produced high unit weight compared with other percentage replacement. It is affected by number of barite aggregate in the mixture still high, then it might influence to unit weight of concrete.

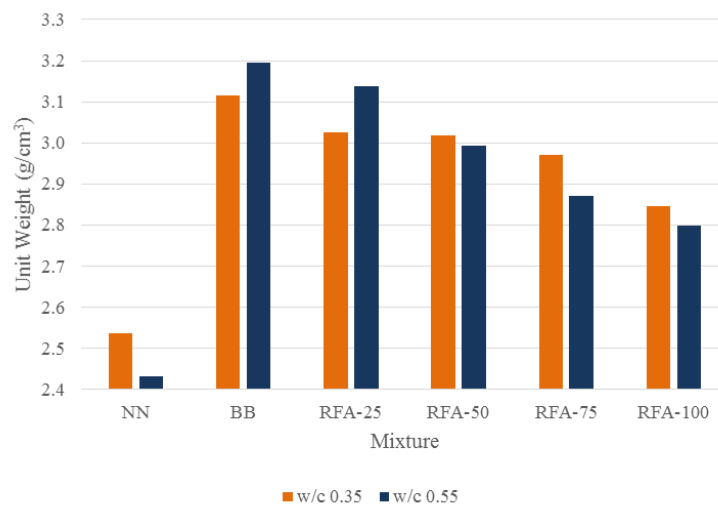


**Figure 4.4** Comparison unit weight in varies percentage replacement of fine aggregate in barite concrete

More detail, those also were be seen in Figure 4.4 above that tendency decreasing of unit weight due to increasing percentage replacement fine aggregate to natural one. Furthermore, percentage fine aggregate total aggregate and fixed amount of used water in mixture may impact to number of fine aggregate and cement in paste, then value of unit weight for w/c 0.55 was less than w/c 0.35.

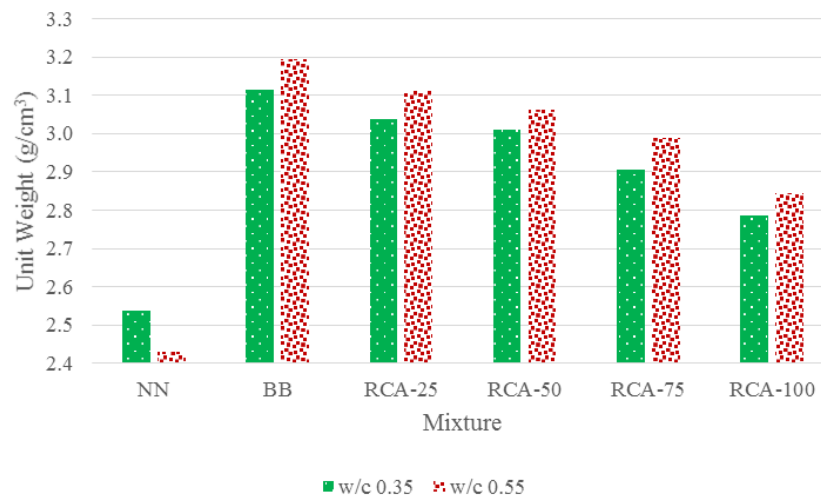


**Figure 4.5** Comparison unit weight in varies percentage replacement of coarse aggregate in barite concrete

Contrary with unit weight value by fine aggregate, replacement coarse aggregate in concrete w/c 0.55 is higher than concrete w/c 0.35, but same tendency which are increasing percentage replacement with normal aggregate will make decreasing value of unit weight in concrete.

#### 4.4 Mechanical Properties of Barite Concrete

##### 4.4.1 Compressive Strength

Compressive strength of barite concrete is summarized in Table 4.5. It is predictable that mixture with w/c 0.35 has higher compressive strength than w/c 0.55, but this experiment showed that barite concrete had higher compressive strength comparing with normal aggregate. This is contrary with previous study with barite aggregate[28], but it shows similarity when comparing with previous experiment that is conducted in Thailand [15, 25].

**Table 4.5** Compression strength for 7 days and 28 days of cylinder concrete

Specimen	w/c 0.35		w/c 0.55	
	fc'(7) (MPa)	fc'(28) (MPa)	fc'(7) (MPa)	fc'(28) (MPa)
NN	51.017	63.475	26.283	26.425
BB	59.412	63.701	35.515	38.033
RFA-25	64.130	59.979	59.412	42.243
RFA-50	64.066	56.551	34.728	41.495
RFA-75	57.038	68.994	35.176	39.461
RFA-100	63.911	69.797	37.133	38.876
RCA-25	57.709	59.278	30.220	33.039
RCA-50	59.749	62.355	31.262	34.089
RCA-75	54.055	47.755	26.764	23.810
RCA-100	40.932	51.687	25.131	30.459

Moreover, Table 4.5 showed that barite concrete with replacement of fine aggregate slightly have higher compressive strength than replacement of coarse aggregate. Then, it can be correlated with unit weight in previous discussion. Increasing unit weight of concrete was not prominently accompanied increased following by increasing of compressive strength of concrete. Detailed comparison can be seen in Figure 4.6 below.

Those values will be used to choose the mixture and performed in beam specimen. Compressive strength became main major to decide mixture that used in beam specimen beside their workability. Concrete with w/c 0.35 were picked specimen code RFA-251 and RFA-501 mixture which replacement of fine aggregate 25% and 50% respectively. Both mixtures are chosen because among other mixture, it had highest compressive strength but lesser workability. On other hand, concrete with w/c 0.55 were picked specimen code RFA-752 and RCA-1002 mixture which replacement of fine

aggregate 75% and replacement of coarse aggregate 100%. Those were picked due to high workability but have average value in compressive strength.

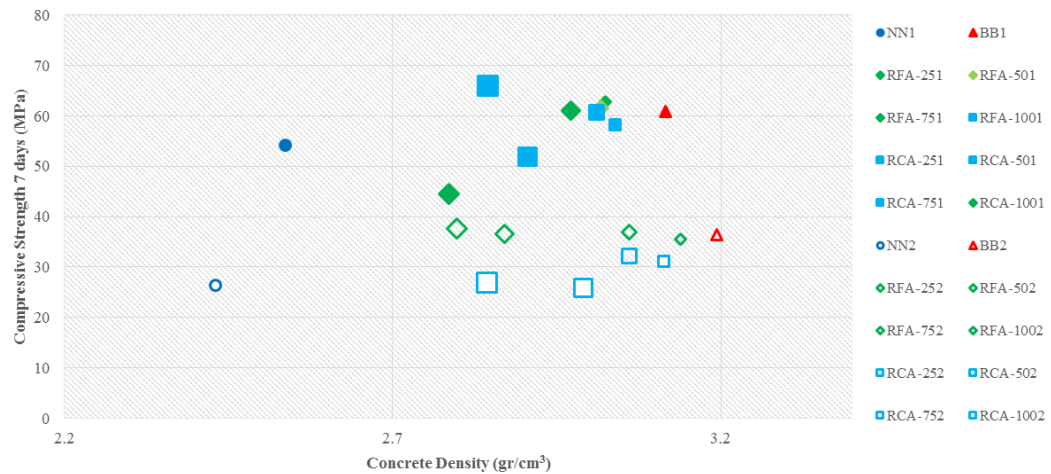


**Figure 4.6** Distribution of unit weight in barite concrete comparing with compressive strength

Figure above showed that despite having similar unit weight replacement fine aggregate produced higher compressive strength comparing with replacement of coarse aggregate for both w/c ratio. Enhancement of compressive strength by replacing fine aggregate compared with coarse aggregate are 7% and 14% for w/c 0.35 and 0.55 respectively.

#### 4.4.2 Stress-Strain Relationship

Because heavyweight concrete was special concrete due to its uniqueness in term of weight, it was interesting to investigate properties of material by stress-strain relationship of concrete. One 28 days cylinder specimen was tested to measure stress and strain of barite concrete. Further, two strain gages were attached to cylinder specimen vertically and horizontally.

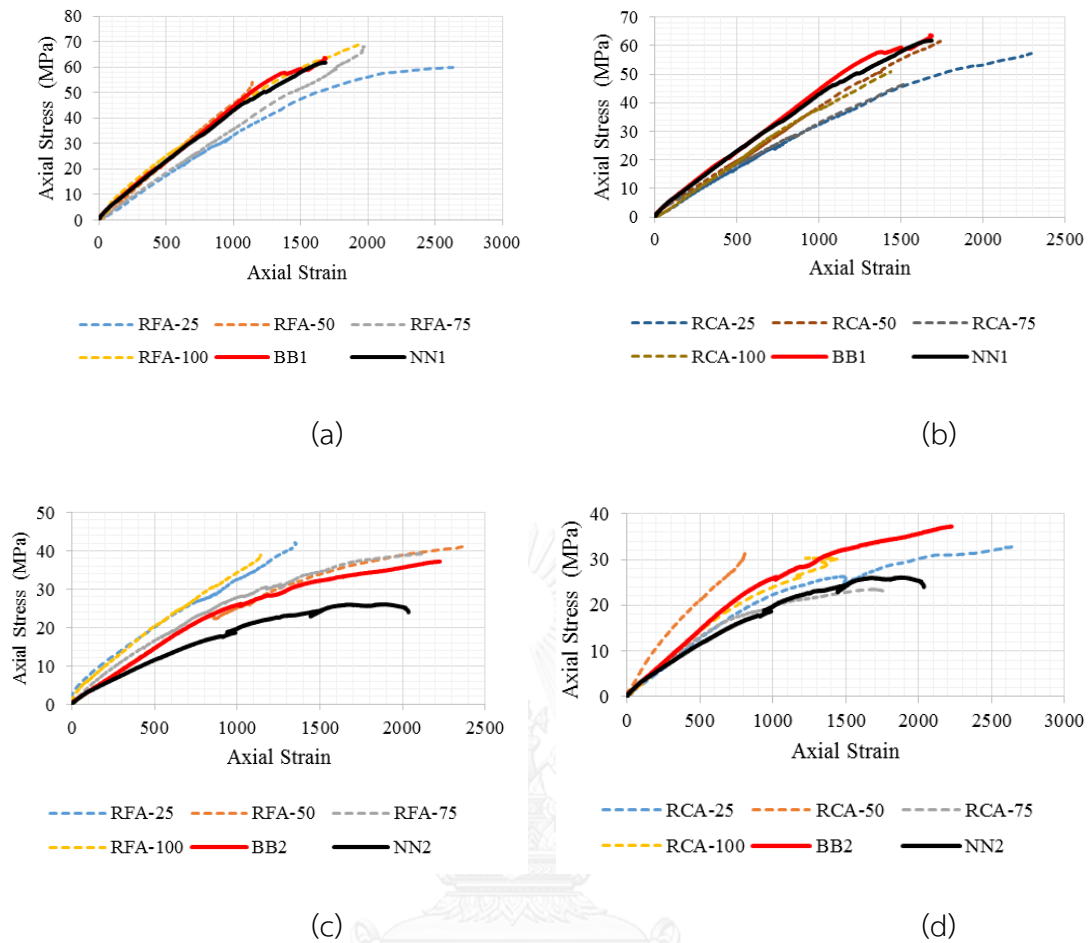


**Figure 4.7** Stress-strain relationship curvature barite mixture with (a) w/c 0.35 and replacement fine aggregate, (b) w/c 0.35 and replacement coarse aggregate, (c) w/c 0.55 and replacement fine aggregate (d) w/c 0.55 and replacement coarse aggregate

Plotted stress-strain curve of barite concrete showed in Figure 4.7. As comparison, normal concrete and pure barite concrete are provided in the same graph. Impact of compressive strength on the stress-strain relationship of barite concrete was slightly identical to trend for normal concrete. Slope is higher in climbing branch and sudden drop for concrete with w/c 0.35 than concrete with w/c 0.55.

Different with characteristic in magnetite[17], behaviour of stress-strain curve of barite concrete were affected by replacement of aggregates. Increasing percentage

replacement aggregate made climbing branch more abrupt, then proceeded smaller strain at the peak stress.

#### 4.4.3 Modulus of Elasticity and Poisson's Ratio

##### 4.4.3.1 Modulus of Elasticity

From stress-strain relationship curve, modulus of elasticity barite concrete can be achieved. Moreover, ASTM C469-02[66] guided to obtain nearest value based on the curve as follow:

$$E_{\text{exp}} = \frac{(S_2 - S_1)}{(\epsilon_2 - 0.00005)} \quad (4.1)$$

Where E is Modulus of Elasticity;  $S_2$  is stress at 40% ultimate load;  $S_1$  is stress at longitudinal strain, and  $\epsilon_2$  is longitudinal strain. Then, experimental modulus of elasticity will be compared with estimation calculation from ACI provision using following equation:

$$E_{\text{est}} = w_c^{1.5} 0.043 \sqrt{f_c'} \quad (4.2)$$

Where  $w_c$  is unit weight of concrete and  $f_c'$  is compressive strength of concrete. Moreover, ACI stated that this equation is used for unit weight of concrete is not more than  $2420 \text{ kg/m}^3$ . For calculation modulus elasticity for normal concrete, ACI provision suggested to use this following equation in computation:

$$E_n = 4730 \sqrt{f_c'} \quad (4.3)$$

Calculation result modulus elasticity of barite concrete is summarized in Table 4.6. Then, comparison normalized modulus elasticity with estimation from ACI provision for normal concrete can be seen in Figure 4.8. Further, comparison between normalized modulus of elasticity with unit weight of concrete is shown in Figure 4.9.

**Table 4.6** Comparison modulus elasticity of barite concrete from experiment and estimation of ACI standard in varies of w/c ratio

Specimen	w/c 0.35			w/c 0.55		
	$(E_c)_{exp}$	$(E_c)_{est}$	$(E_c)_{exp}/(E_c)_{est}$	$(E_c)_{exp}$	$(E_c)_{est}$	$(E_c)_{exp}/(E_c)_{est}$
	(MPa)	(MPa)		(MPa)	(MPa)	
NN	46224.73	43634.70	1.06	23396.27	27315.71	0.86
BB	44346.86	60160.12	0.74	28375.11	47687.00	0.60
RFA-25	34731.24	56540.09	0.61	42913.51	48746.03	0.88
RFA-50	45514.01	52597.15	0.87	29268.61	45589.82	0.64
RFA-75	35933.26	57287.00	0.63	32387.26	41484.05	0.78
RFA-100	49186.71	55760.94	0.88	39279.76	38754.63	1.01
RCA-25	33787.18	55722.91	0.61	25466.93	42935.26	0.59
RCA-50	37502.49	58682.23	0.64	51103.24	43316.37	1.18
RCA-75	36573.54	46006.23	0.79	26306.40	33940.67	0.78
RCA-100	38851.69	46085.58	0.84	28411.46	36254.01	0.78

In this experiment found that modulus elasticity barite concrete with replacement of coarse aggregate have lower modulus elasticity than replacement of fine aggregate. It means that barite concrete with replacement with gravel is more ductile. For pure barite concrete, modulus elasticity is higher than normal concrete. In relation with provision standard, ACI 349-06 equation for normal concrete in modulus elasticity showed that distribution of experiment result mostly have higher modulus elasticity in term of normal concrete. In relation with replacement aggregate, trend replacing coarse aggregate increases modulus elasticity of barite concrete.

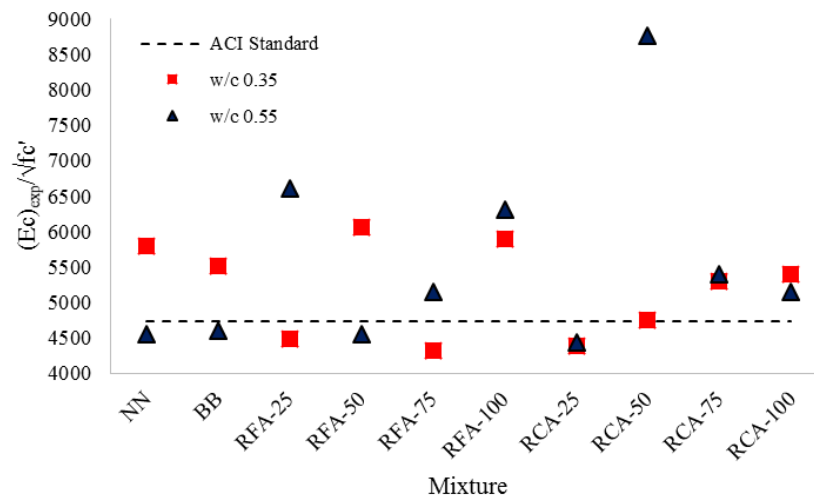


**Figure 4.8** Distribution normalized modulus of elasticity of barite concrete parallel with ACI 349-06 standard.

By linear rise branch of stress-strain curve, normalized modulus of elasticity shows unit weight increased by replacement fine aggregate than coarse aggregate. When unit weight reached on range  $2500 \text{ kg/m}^3$  to  $3000 \text{ kg/m}^3$ , modulus elasticity of barite concrete from experiment had higher value than estimation in ACI349-06 standard. For higher than  $3000 \text{ kg/m}^3$ , modulus elasticity had lower value even from upper limit of unit weight for ACI standard. This was influenced by modulus elasticity of aggregate[67]. Barite aggregate is more brittle than normal gravel and sand. In addition, ACI provision is only limited calculation for concrete with unit weight  $2420 \text{ kg/m}^3$ , then estimation of calculation become inconsistent depend on unit weight of concrete.

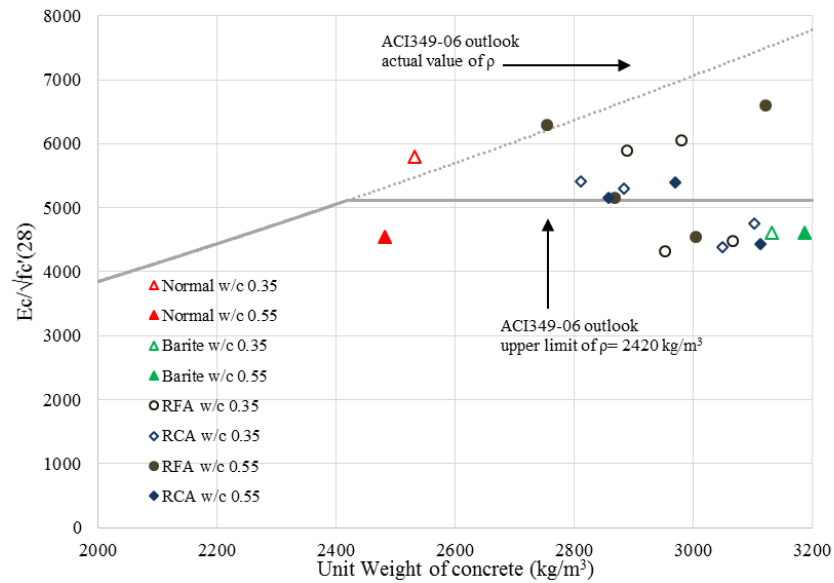


**Figure 4.9** Influence of unit weight concrete on normalized modulus of elasticity compared with ACI 349-06 standard

#### 4.4.3.2 Poisson's Ratio

From cylinder specimen, Poisson's ratio is obtained from computation longitudinal strain gage and transversal strain gage at 40% ultimate load with equation based on ASTM C469-02[66] as follow

$$\mu = \frac{(\varepsilon_{t2} - \varepsilon_{t1})}{(\varepsilon_2 - 0.00005)} \quad (4.4)$$

Where  $\mu$  is Poisson's ratio;  $\varepsilon_{t2}$  is transversal strain corresponding to 40% ultimate load;  $\varepsilon_{t1}$  is transversal strain corresponding to longitudinal strain, and  $\varepsilon_2$  is longitudinal strain. Detailed calculation is presented with comparison with normal concrete in varies of replacement aggregate of barite concrete in Table 4.7.

**Table 4.7** Poisson's ratio and maximum stress of barite concrete with different w/c ratio

Specimen	w/c 0.35		w/c 0.55	
	$\mu_b$	$\mu_b/\mu_n$	$\mu_b$	$\mu_b/\mu_n$
NN	0.250		0.071	
BB	0.242	0.970	0.119	1.680
RFA-25	0.175	0.700	0.308	4.334
RFA-50	0.261	1.044	0.139	1.952
RFA-75	0.167	0.669	0.173	2.437
RFA-100	0.278	1.115	0.250	3.527
RCA-25	0.196	0.783	0.164	2.311
RCA-50	0.180	0.721	0.426	5.996
RCA-75	0.218	0.873	0.077	1.089
RCA-100	0.277	1.109	0.181	2.545

#### 4.5 Attenuation of Gamma-ray

Linear attenuation coefficient (LAC), mass attenuation coefficient (MAC), half value layer (HVL), and tenth value layer (TVL) of barite concrete are set up. Those were measured at 0.662 MeV photon energy for Cs-137 and mean of two photon energies of 1.173 MeV and 1.337 MeV (1.250 MeV) for Co-60. Both energy were emitted 85% and 100% for Cs-137 and Co-60, serially. Analysis result are summarized in Table 4.8.

Barite concrete with 25% replacement coarse aggregate for both w/c ratio indicated had highest coefficient using energy 0.662 MeV. From energy 1.250 MeV, 25% replacement coarse aggregate and 50% replacement fine aggregate had highest attenuation coefficient among other mixture.

The thickness of concrete shielding is becoming main role attenuating radiation beside material that was used for build it. Half value layer is qualitative factor that frequently used to represent ability of penetration in specific radiation and through object[68]. It expressed by distance units (cm or mm). HVL and TVL can be calculated using the following equations

$$x_h = \frac{\ln 2}{\mu} \quad (4.5) \quad \text{and} \quad x_t = \frac{\ln 10}{\mu} \quad (4.6)$$

Where:  $\mu$  is linear attenuation coefficient,  $x_h$  is HVL thickness and  $x_t$  is TVL thickness.

**Table 4.8** Analysis result of radiation test using sources Caesium-137 (0.662 MeV) and Cobalt-60 (1.250 MeV)

Sample Name	LAC		MAC		HVL		TVL	
	Cs-137	Co-60	Cs-137	Co-60	Cs-137	Co-60	Cs-137	Co-60
	(cm <sup>-1</sup> )	(cm <sup>-1</sup> )	(cm <sup>2</sup> /gr)	(cm <sup>2</sup> /gr)	(cm)	(cm)	(cm)	(cm)
NN1	0.140	0.139	0.055	0.055	4.959	4.973	16.475	16.519
BB1	0.225	0.168	0.072	0.054	3.087	4.131	10.254	13.722
RFA-251	0.244	0.171	0.080	0.056	2.839	4.045	9.430	13.438
RFA-501	0.233	0.168	0.078	0.056	2.978	4.127	9.891	13.711
RFA-751	0.231	0.169	0.078	0.057	2.997	4.096	9.957	13.607
RFA-1001	0.203	0.151	0.070	0.052	3.418	4.604	11.355	15.295
RCA-251	0.247	0.175	0.081	0.057	2.807	3.968	9.326	13.181
RCA-501	0.238	0.170	0.077	0.055	2.918	4.067	9.692	13.509
RCA-751	0.244	0.161	0.084	0.056	2.846	4.299	9.453	14.282
RCA-1001	0.202	0.152	0.072	0.054	3.438	4.545	11.419	15.099

Sample Name	LAC		MAC		HVL		TVL	
	Cs-137 (cm <sup>-1</sup> )	Co-60 (cm <sup>-1</sup> )	Cs-137 (cm <sup>2</sup> /gr)	Co-60 (cm <sup>2</sup> /gr)	Cs-137 (cm)	Co-60 (cm)	Cs-137 (cm)	Co-60 (cm)
NN2	0.139	0.135	0.056	0.054	4.984	5.132	16.555	17.048
BB2	0.221	0.165	0.069	0.052	3.143	4.214	10.440	13.997
RFA-252	0.244	0.180	0.078	0.058	2.844	3.844	9.447	12.771
RFA-502	0.244	0.181	0.081	0.060	2.840	3.837	9.434	12.746
RFA-752	0.224	0.163	0.078	0.057	3.088	4.258	10.257	14.145
RFA-1002	0.197	0.151	0.071	0.055	3.527	4.585	11.717	15.233
RCA-252	0.253	0.172	0.081	0.055	2.741	4.032	9.105	13.394
RCA-502	0.228	0.168	0.074	0.054	3.038	4.123	10.093	13.697
RCA-752	0.235	0.169	0.079	0.057	2.948	4.107	9.794	13.642
RCA-1002	0.199	0.150	0.070	0.053	3.481	4.610	11.565	15.314

Even though radiation in small energy is very useful, it is still dangerous if it exposure too much. In addition, there is limitation for human exposure to radiation that regularly 1 mSv per year for general public space or uncontrolled area and 50 mSv per year for radiation workers[2]. The number of HVL in some materials means ability those materials to reduce half of radiation level. Using HVL and TVL eased determination of radiation ability into thickness of material.

This experiment showed that combination barite aggregate with normal aggregate with varies percentage produced preferable material for shielding with less thickness rather than 100% combination. Figure 4.10 showed replacement both fine aggregate and coarse aggregate with percentage 25, 50, and 75 needed less thickness compared with 100% combination barite aggregate and normal aggregate or even pure barite concrete when concrete penetrated with energy 0.662 MeV. Then, result from this experiment is compared to previous experiment[15] and average HVL for Co-60 which is 6.05 cm[69] More, specimen with 25% replacement aggregate has less

thickness to reduce half of radiation energy. In term of comparison with average HVL from NDT resource, experiment result is less HVL means that obtaining result gave good benchmark. Then, similar result also showed if compared with Sainet's experiment result except for value normal concrete and replacement 100% aggregate exhibited less result for photon energy 0.662 MeV using source Cobalt-60.

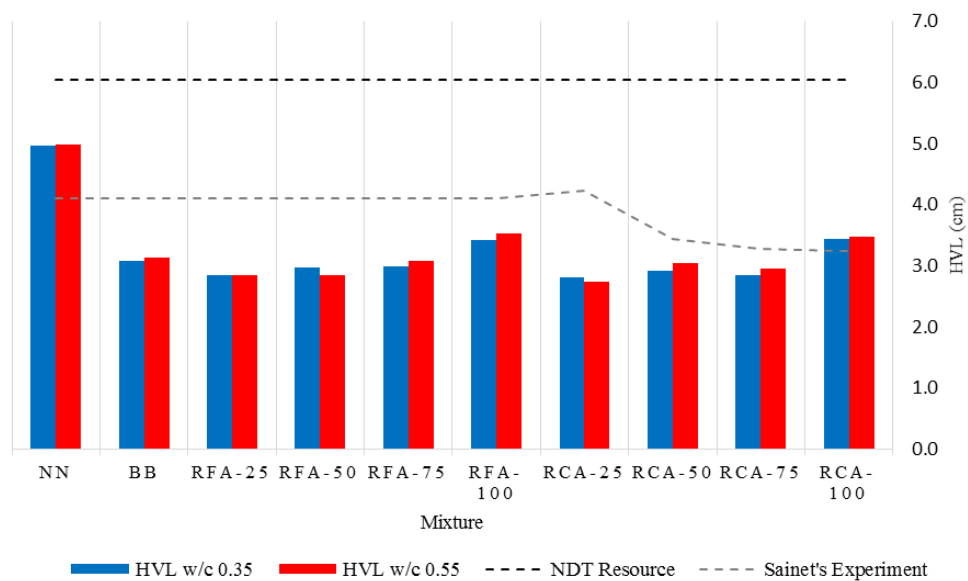


**Figure 4.10** Comparison Half-Value Layer (HVL) at energy 0.662 MeV in varies percentage replacement aggregate for w/c 0.35 and w/c 0.55

Performing similar trend, HVL for energy 1,250 MeV in Figure 4.11 need to thicker due to high energy that is used. Concrete with 25% replacement aggregate performed less thickness to absorb 50% radiation energy. In relation with TVL, both are have similar concept. If HVL showed capability to absorb 50% radiation, then TVL showed capability to absorb 90% of radiation.

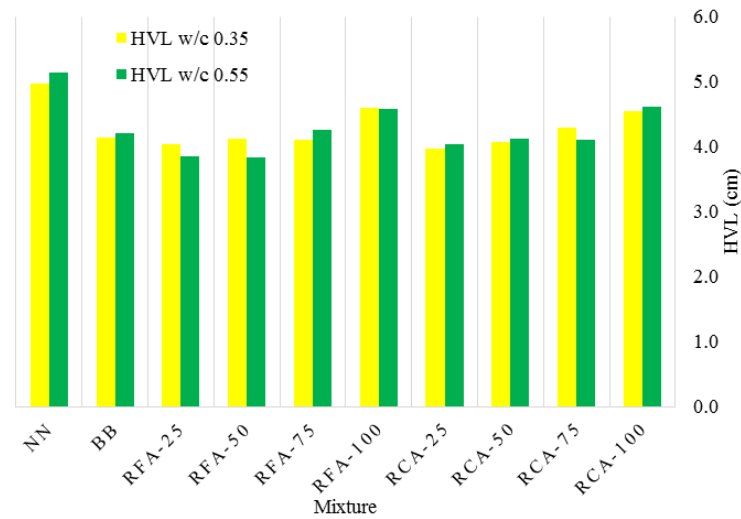


**Figure 4.11** Comparison Half-Value Layer (HVL) at energy 1.250 MeV in varies percentage replacement aggregate for w/c 0.35 and w/c 0.55

According the thickness of sample is 150 mm and average HVL for energy 0.662 MeV and 1,250 MeV are 30.54 mm and 41.94 mm, then using 150 mm barite concrete as shielding wall, respectively can reduce radiation gamma-ray intensity by 96.9% and 93.8% for energy 0.662 MeV and 1.250 MeV.

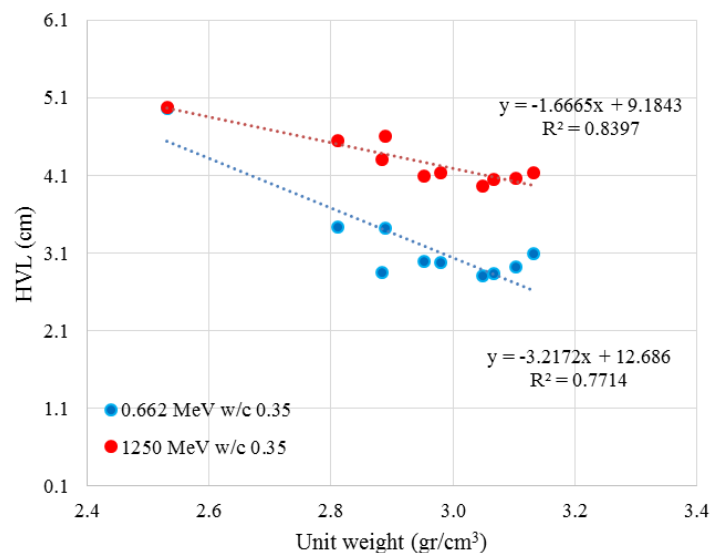


**Figure 4.12** Influence of unit weight concrete on HVL for both energies emitted in concrete w/c 0.35

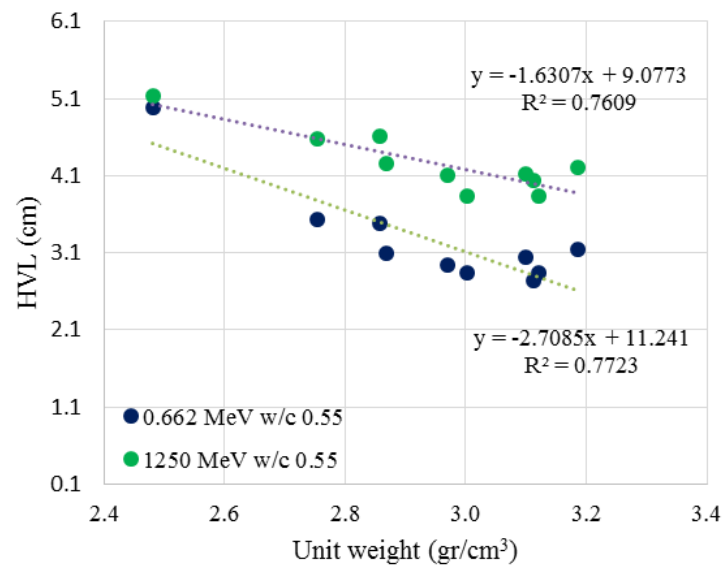


**Figure 4.13** Influence of unit weight concrete on HVL for both energies emitted in concrete w/c 0.55

In accordance to unit weight-HVL, both energy and w/c ratio indicated similar tendency. Increasing of unit weight in concrete is affected to decrease value of HVL in every photon energy. Detail result analysis influence of unit weight due to thickness of HVL can be seen in Figure 4.12 and Figure 4.13.

## 4.6 Heavyweight Reinforcement Concrete Beam

### 4.6.1 Failure Mode and Load-Deflection Characteristic

#### 4.6.1.1 Load-Deflection Behaviour

Similarly with normal RC beam, load-deflection characteristic of barite reinforced concrete beam estimated tri-linear response explained by concrete cracking, steel yielding and post-yielding stage up to failure as shown in Figure 4.14.

Normalized stress resulted from modifying load that was obtained from experimental then compared with compressive strength of control cylinders. Modifying load to bending strength for four-point bending was computed as follows:

$$\sigma_{beam} = \frac{3 \times P(L - L_i)}{2 \times b \times d} \quad (4.7)$$

In this equation  $P$ ,  $L$ ,  $L_i$ ,  $b$ ,  $d$  are load, effective length span, length of load span, width of beam, height of beam, respectively. After that, bending strength is divided by compressive strength of control concrete cylinders. This issue is taken to minimize distinction of combination mixture that might affect in load of beam.

**Table 4.9** Beam test result for all specimens

Specimen Name	Crack state		Yielding state		Ultimate state		Failure Mode
	Load (kN)	$\Delta$ (mm)	Load (kN)	$\Delta$ (mm)	Load (kN)	$\Delta$ (mm)	
NN1	9.42	0.18	73.59	3.67	88.78	8.61	Concrete crushing
BB1	16.55	0.36	70.31	4.57	82.98	7.59	Concrete crushing
RFA-251	19.57	0.71	87.79	5.07	93.93	8.01	Concrete crushing
RFA-501	13.04	0.45	72.93	4.00	79.22	5.75	Concrete crushing
NN2	11.51	0.33	83.58	4.07	86.70	6.79	Concrete crushing
BB2	9.05	0.16	73.84	4.02	77.13	4.32	Concrete crushing
RFA-751	13.48	-0.17	72.05	4.32	82.17	6.29	Shear failure
RCA-1001	7.40	0.13	69.94	4.16	77.48	6.47	Concrete crushing

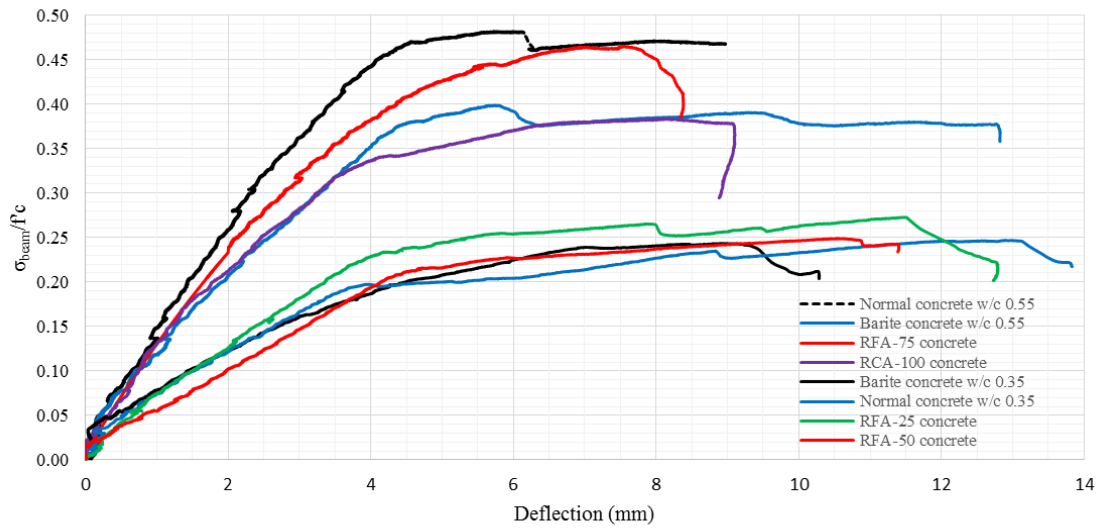


**Figure 4.14** Normalized stress-deflection at mid span characteristics for all beam specimens

In term of normalized stress-deflection, behaviour of beam with w/c ratio is similar. Stiffness of each beam are linear with low neutralized stress compared with w/c 0.55.

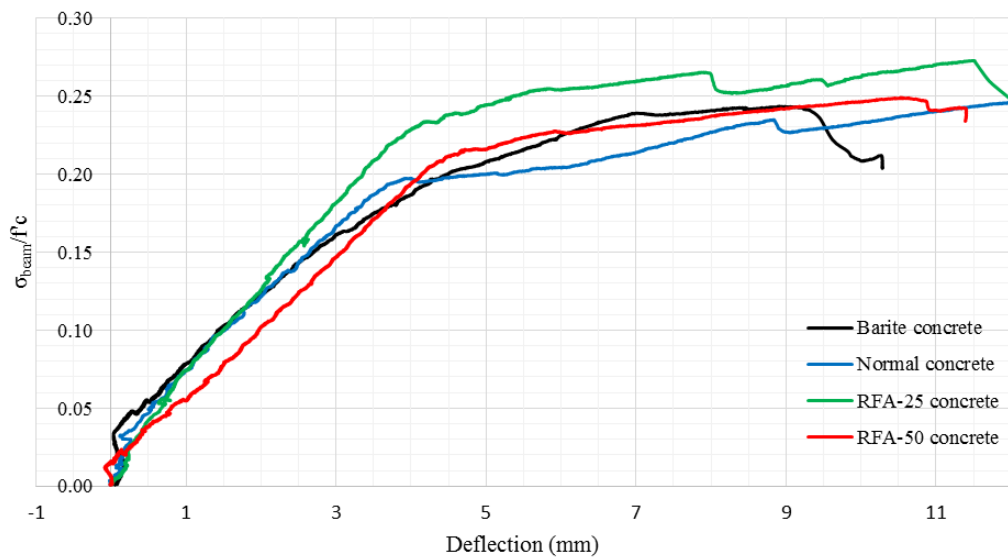


**Figure 4.15** Normalized stress-deflection at mid span characteristics of concrete with w/c ratio 0.35

Normal concrete with w/c 0.55 shows less deflected among to other beam. Then, comparing to all beam specimen NN2 give more ductile and capable to resist load more.

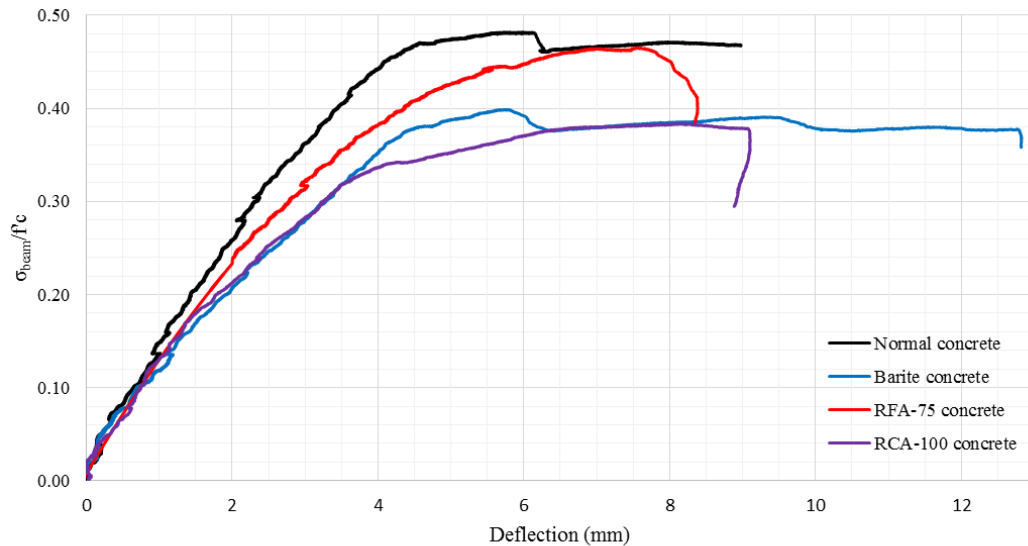


**Figure 4.16** Normalized stress-deflection at mid span characteristics of concrete with w/c ratio 0.55

#### 4.6.1.2 Reinforcement Bar Behaviour

Relating to investigate effect of replacement aggregate in barite concrete, tension bar in all specimen are exploring more. Generally, tension bar in all specimen have similar movement in strain, where in mid span has higher value of strain due to receive higher moment compare with strain in shear span.

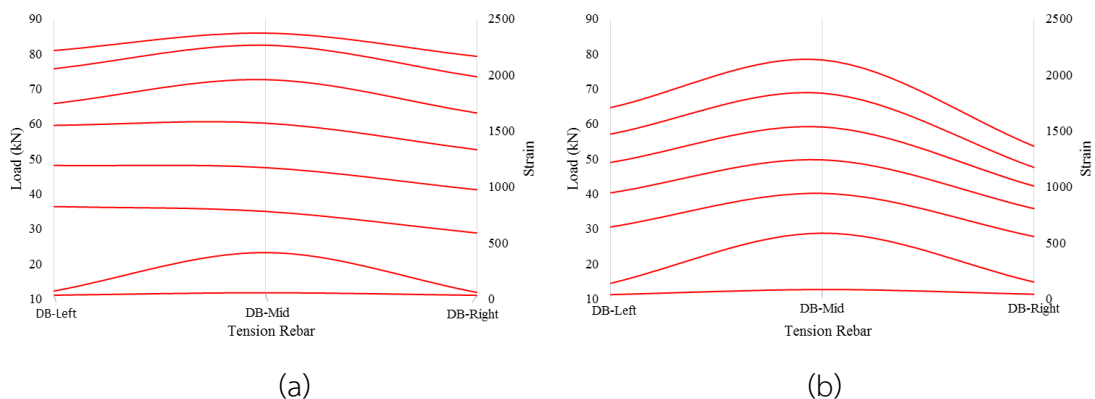


**Figure 4.17** Load-strain at tension rebar of normal concrete with (a) w/c ratio 0.35 and (b) w/c ratio 0.55

Normal concrete w/c 0.35 shows similar behaviour with w/c 0.55 in same strain value. Although different w/c ratio, load capacity both beam are similar.

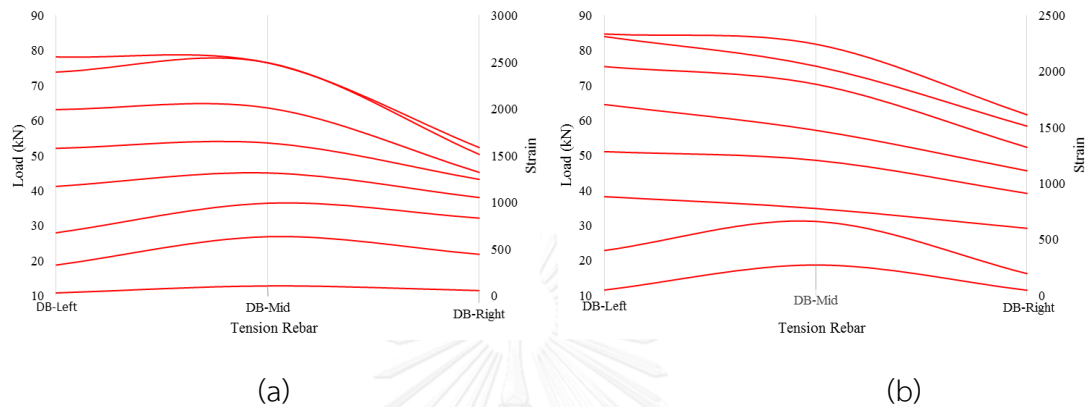


**Figure 4.18** Load-strain at tension rebar of barite concrete with (a) w/c ratio 0.35 and (b) w/c ratio 0.55

In term of barite concrete, w/c 0.35 provided more strain compare with w/c 0.5.

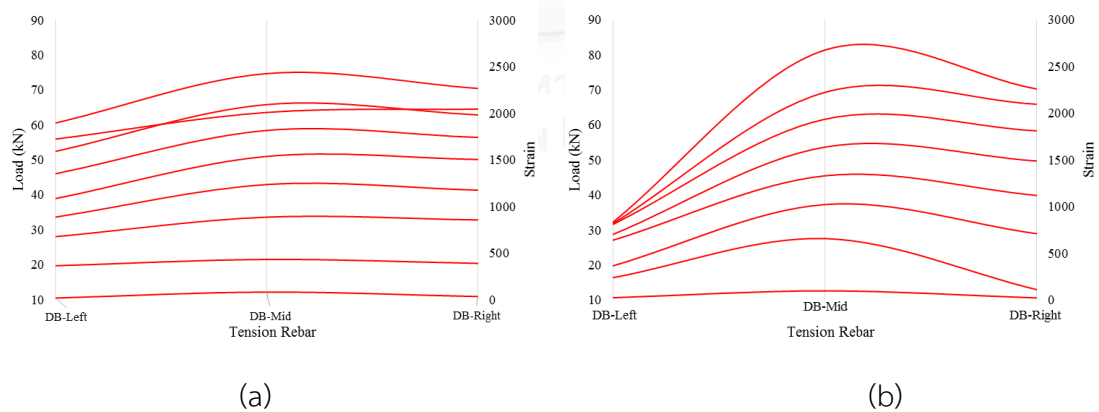


**Figure 4.19** Load-strain at tension rebar of barite concrete for w/c 0.35 with (a) replacement fine aggregate 25% and (b) replacement fine aggregate 50%

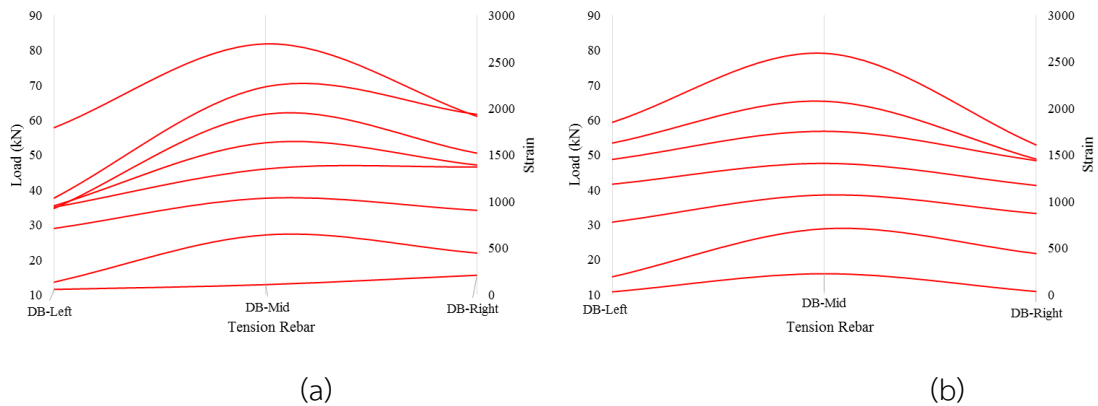


**Figure 4.20** Load-strain at tension rebar of barite concrete for w/c 0.55 with (a) replacement fine aggregate 75% and (b) replacement coarse aggregate 100%

Correlated with nominal strength, contribution of stirrup played important role to avoid failure by shear. Nominal strength by steel controverted with nominal strength by concrete in this relationship. Displaying contribution both nominal strength can be seen in figure below.

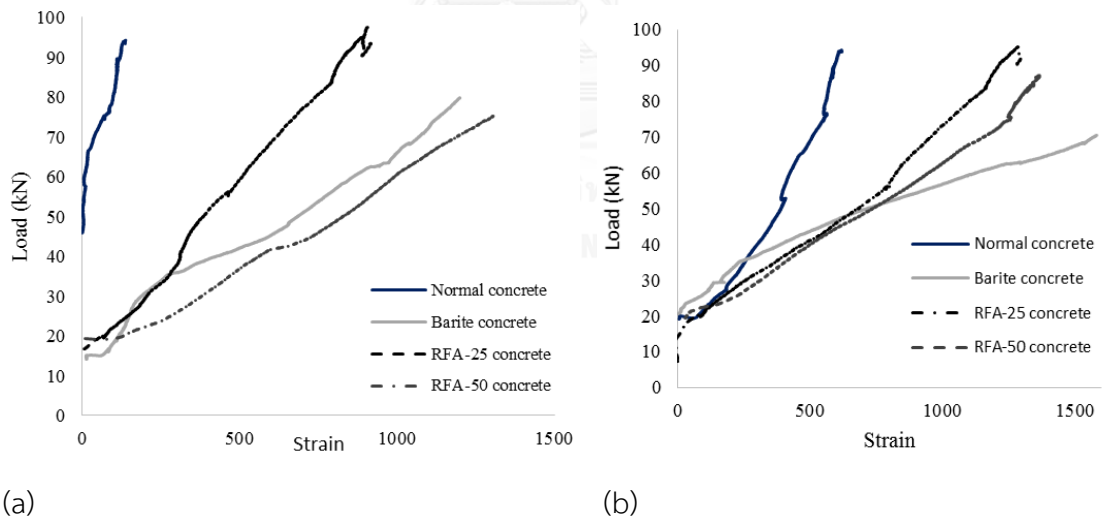


**Figure 4.21** Load-strain at stirrup of barite concrete for w/c 0.35 at (a) left hand side and (b) right hand side

Both concrete in w/c ratio 0.35 and 0.55 showed that contribution strength in barite concrete dominated by strength from concrete. It shows that strain in some point less if compare with normal concrete. Then, concrete with w/c 0.35 can resist more shear

force than w/c 0.55. It related with compressive strength of w/c 0.35 is higher than w/c 0.55.

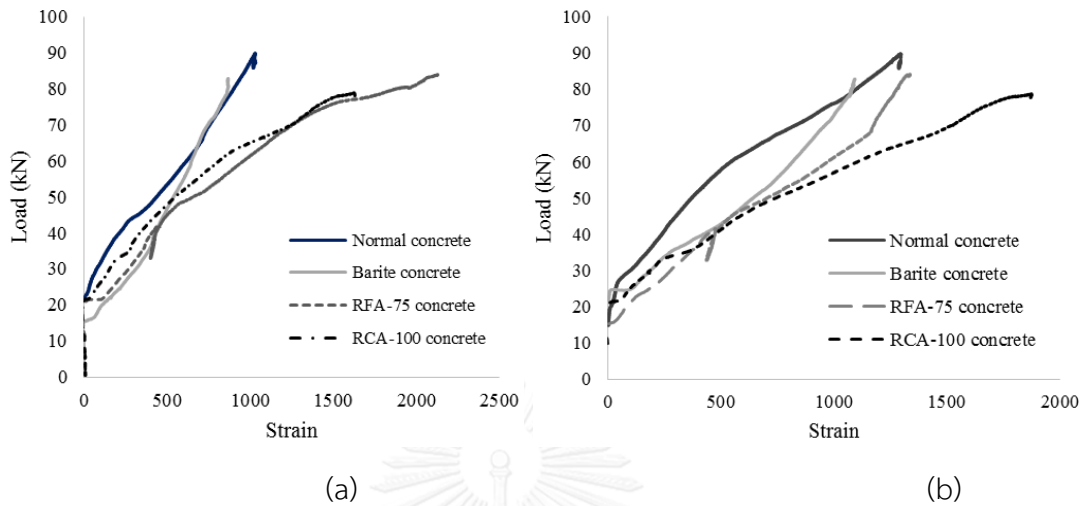


**Figure 4.22** Load-strain at stirrup of barite concrete for w/c 0.55 at (a) left hand side and (b) right hand side

#### 4.6.2 Flexural Stiffness

Similar consideration in computing modulus elasticity and Poisson's ratio, this study assumed that elastic stage occurred when load reached 40% from ultimate load. Then, using correlation deflection-stiffness in simple beam with four point load, stiffness at elastic stage are calculated as shown in equation (4.8) below

$$\Delta_{40u} = \frac{Pa}{24EI} (3L^2 - 4a^2) \quad (4.8)$$

Where  $\Delta_{40u}$  is deflection that occurred at load reached 40% (mm); P is loading at 40% from ultimate load (KN); a is distance shear span of the beam to support (mm); L is length of beam (mm).

From that equation, flexural stiffness based on experimental was achieved, then those result compared with normal concrete beam for each w/c ratio.

Flexural stiffness of the barite RC beam approximately closed to normal aggregate. Contribution replacement normal sand in mixture is affected in stiffness of the beam. Increasing replacement fine aggregate by normal sand in mixture impacted by decreasing value of stiffness for almost 25%. Detailed analysis result of flexural stiffness of barite concrete is summarized in Table 4.10

**Table 4.10** Analysis beam test result of flexural stiffness at elastic stage

Specimen Name	40% ultimate load (KN)	deflection at 40% ultimate load (mm)	Stiffness at elastic stage (kN.mm <sup>2</sup> )	EI/EI <sub>n</sub>
NN1	35.51	1.47	8.84E+11	1.00
BB1	33.19	1.37	8.87E+11	1.00
RFA-251	37.57	1.58	8.68E+11	0.98
RFA-501	31.69	1.76	6.61E+11	0.75
NN2	34.68	1.33	9.52E+11	1.00
BB2	30.85	1.25	9.06E+11	0.95
RFA-751	32.87	1.72	6.99E+11	0.73
RCA-1001	30.99	1.20	9.46E+11	0.99

#### 4.6.3 Ductility Index

Ductility described the deformation capacity of structures after yielding or its ability to dissipate energy. Computation of ductility factor ( $\mu$ ) can be analysed by factor of maximum deflection ( $\Delta_u$ ) to the deflection at yield stage ( $\Delta_y$ ) for inelastic structure.

**Table 4.11** Displacement ductility factor

Specimen Name	Maximum deflection (mm)	Deflection at yield stage (mm)	Displacement ductility factor	
			$\mu = \Delta_U / \Delta_y$	$\mu / \mu_n$
NN1	13.83	7.29	1.90	1.00
BB1	10.29	7.65	1.35	0.71
RFA-251	12.79	8.81	1.45	0.77
RFA-501	11.03	5.99	1.84	0.97
NN2	8.98	5.14	1.75	1.00
BB2	12.83	12.82	1.00	0.57
RFA-751	8.38	4.36	1.92	1.10
RCA-1001	9.11	4.35	2.09	1.20

There were tendency of inclination due to decreasing of percentage replacement of normal aggregate. For Pure barite concrete mixture, reduction of ductility factor reached 29% and 43% in both w/c ratio 0.35 and 0.55, respectively if comparing with ductility factor of normal concrete. Percentage barite in the mixture had main role in ductility factor and not correlated with number of w/c ratio and type of replacement aggregate in the mixture. By increasing percentage of normal aggregate ductility factor increased 20% average ductility factor with increment replacement 25% for both fine aggregate and coarse aggregate. Moreover, escalation trend showed in specimen BN2 by replacement coarse aggregate. It can increase ductility factor around 20%.

#### 4.6.4 Crack Pattern

##### 4.6.4.1 Crack Pattern at Load 40 kN

Behaviour of cracking is recognized by concrete crack prism with mid span bar that subjected to tension. For measuring aggregate effect in concrete, analysis is investigated in same loading for all beam. Some parameter are proposed to explain clearly comparison among the beam. In this study, number of crack, crack angle and crack spacing became parameter that should be investigated in loading 40 kN. Load 40 kN is chosen due to midpoint load to ultimate load for beam.

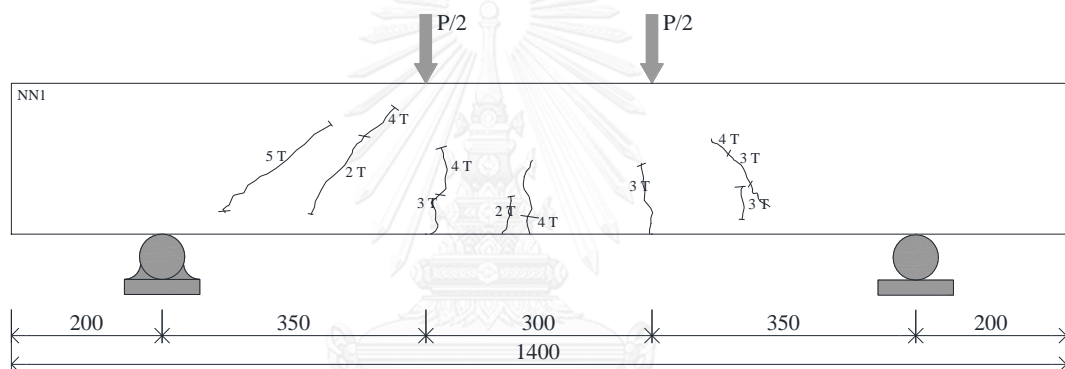


Figure 4.23 Crack pattern of beam NN1 at load 40kN

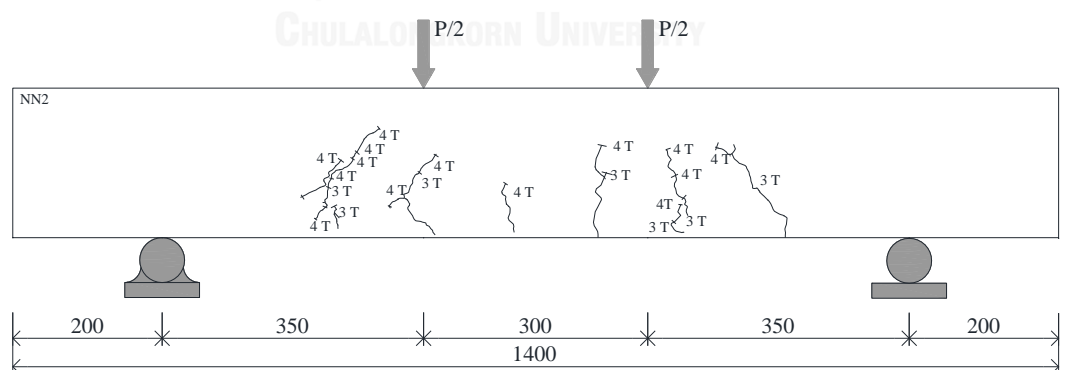
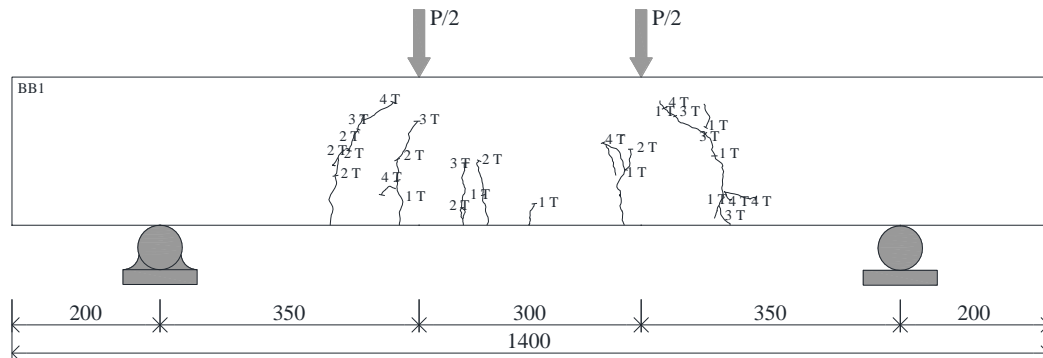


Figure 4.24 Crack pattern of beam NN2 at load 40kN

For normal beam NN1 and NN2 in term of load 40 kN propagate 6 cracks in 3 flexural shear crack and 3 flexural crack with average angle  $62^\circ$  and spacing crack between each other 120 mm for beam NN1. Then, for beam NN2 propagated 7 cracks

that consisted of 4 flexural shear crack and 3 flexural crack in mid span with average spacing 110 mm.



**Figure 4.25** Crack pattern of beam BB1 at load 40kN

Similarly with normal concrete, barite concrete propagated 7 cracks that continuously happen in every load level, and produced longer crack compared with normal beam. Spacing crack between normal concrete and pure barite concrete is slightly same but wider with space 150 mm and 120 mm for BB1 and BB2, respectively. In term of crack angle, barite concrete generated more perpendicular angle to centreline of mid span which are  $67^\circ$  and  $59^\circ$ .

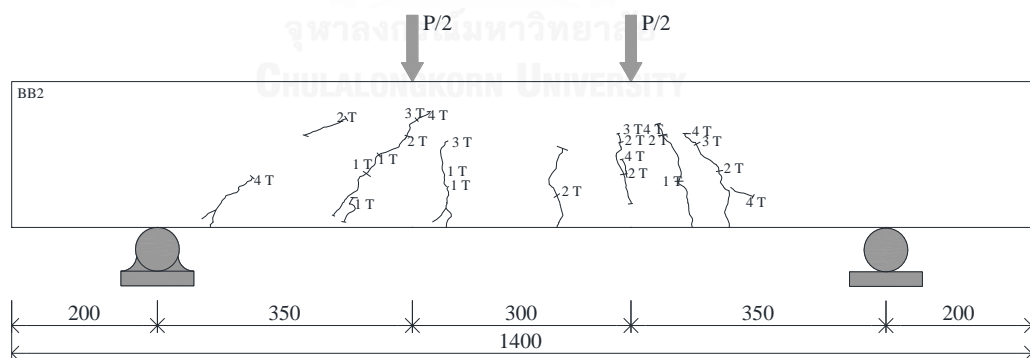


**Figure 4.26** Crack pattern of beam BB2 at load 40kN

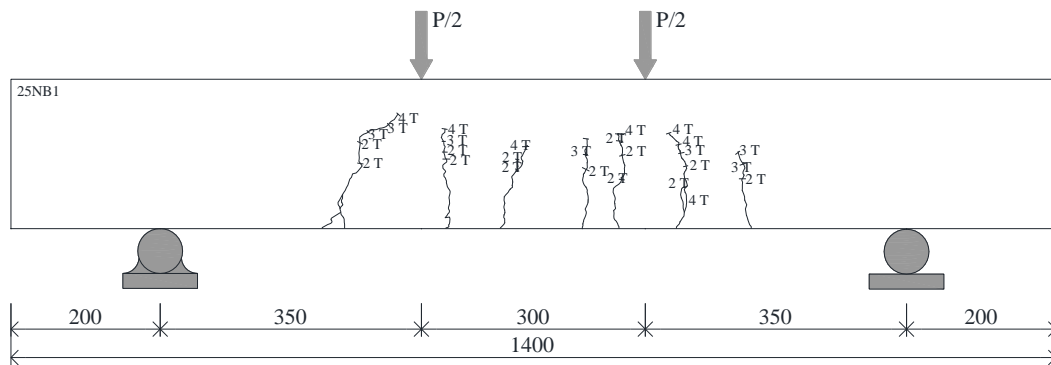


Figure 4.27 Crack pattern of beam RFA-251 at load 40kN

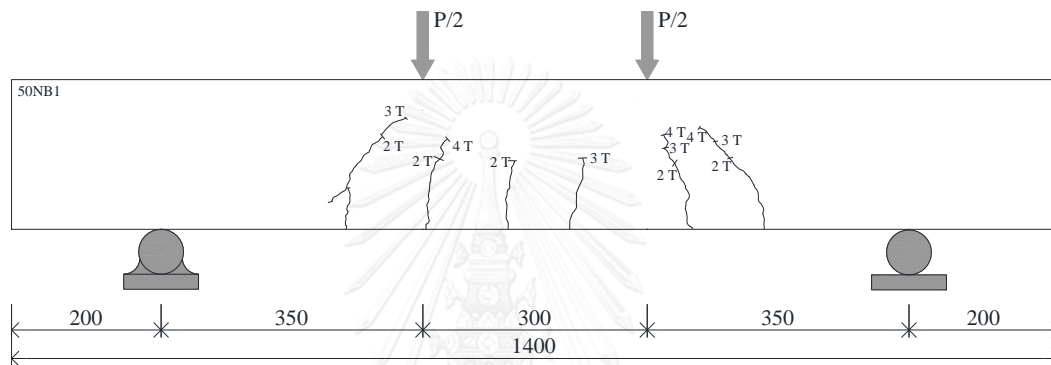


Figure 4.28 Crack pattern of beam RFA-501 at load 40kN

Beam type RFA-251 and RFA-501 which beam with replacement sand in w/c ratio 0.35 generated 7 crack and 6 crack respectively with more perpendicular for angle crack. More vertically, both beam produce  $78^\circ$  and  $85^\circ$  with spacing crack 90 mm and 85 mm respectively. Characteristic for this beam mixture is known that crack that is propagated is long length of crack and is happened in sudden high load.

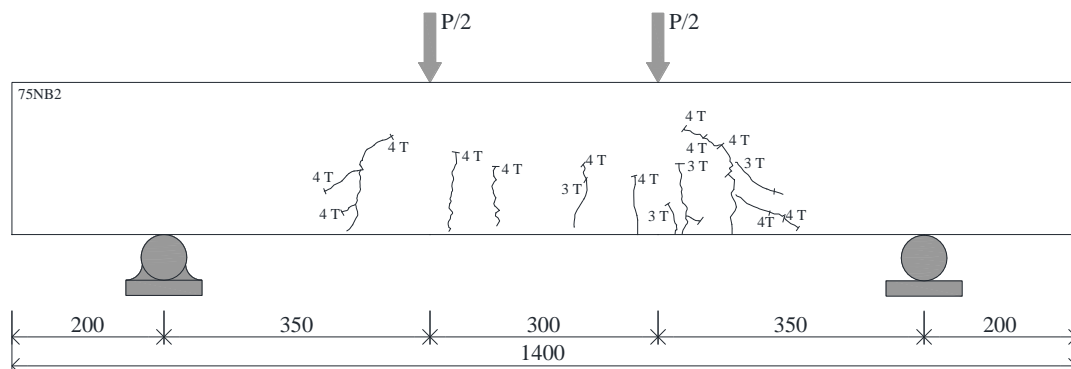
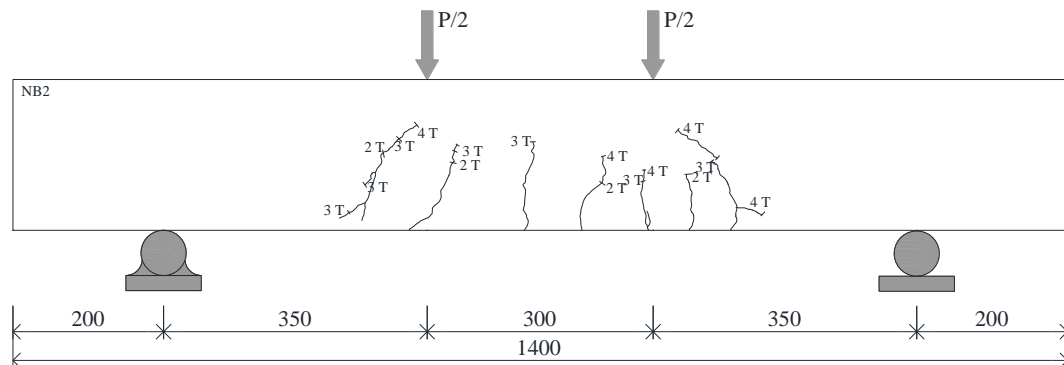


Figure 4.29 Crack pattern of beam RFA-752 at load 40kN



**Figure 4.30** Crack pattern of beam RCA-1002 at load 40kN

For beam with replacement aggregate with w/c 0.55, showed same 7 cracks happened with similar crack angle  $82^\circ$  but different spacing crack 67 mm and 61 mm, respectively. Beam RFA-752 that failed by shear failure is seen also that flexural shear crack already happened started from 30 kN.

Even though those experiment are quite similar each other, but can be seen that effect replacing of aggregate impacted to spacing of crack. Then, replacement of normal aggregate made beam is more brittle.

#### 4.6.4.2 Crack Pattern at Ultimate Load

Crack pattern for normal concrete NN1 and NN2 presented slightly similar behaviour. Flexural crack and flexural shear crack happened symmetrically in both side. There have seven major crack with three crack in both side and one crack in the middle of load span. Further, three crack is occurred in load span area and other two crack in shear span area. Elongation flexural crack developed vertically. First crack is occurred when load reached 30 kN for both beam then it extended vertically. At the end of test, crushing concrete is developed failure.

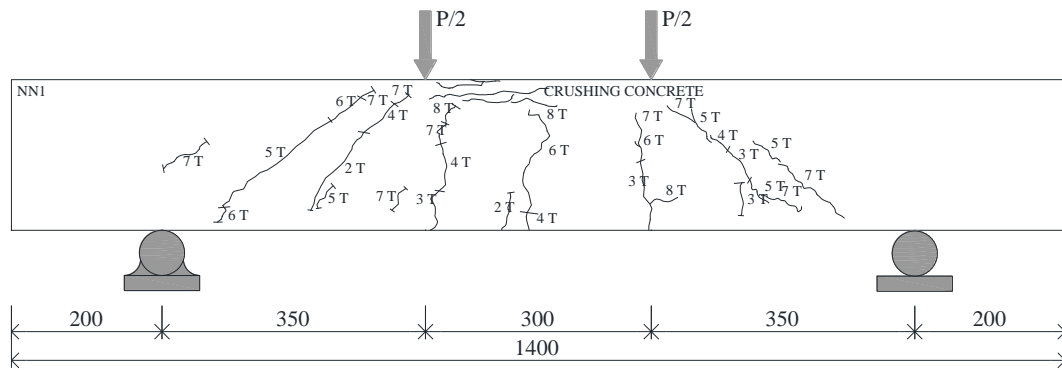


Figure 4.31 Crack pattern of beam NN1 at ultimate load

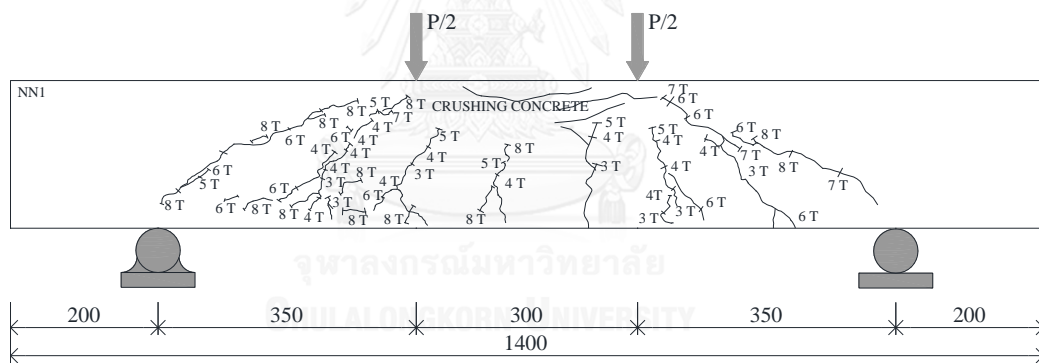
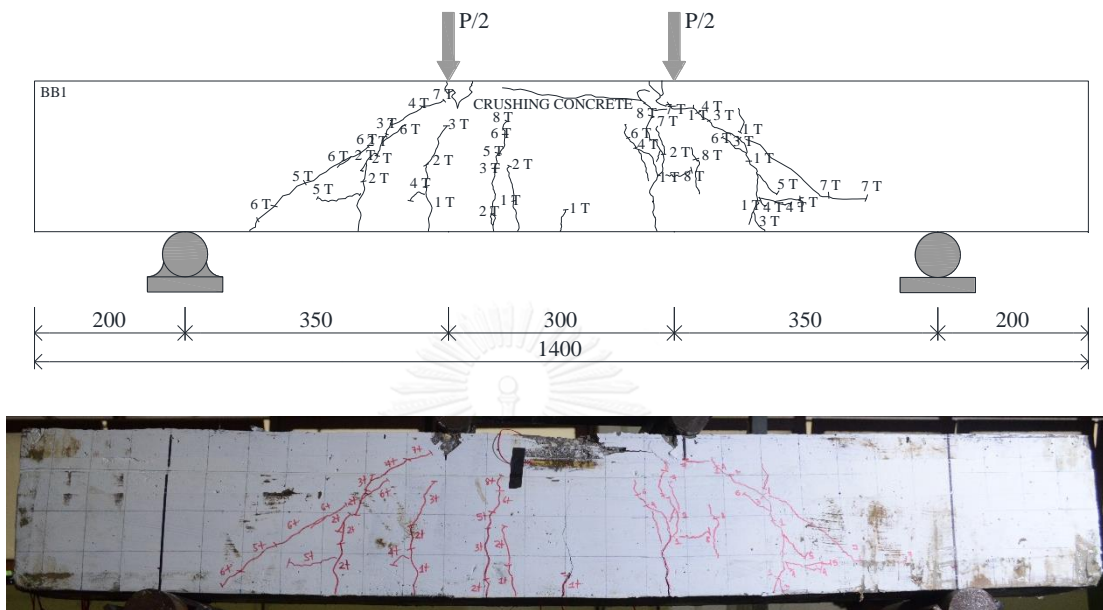


Figure 4.32 Crack pattern of beam NN2 at ultimate load

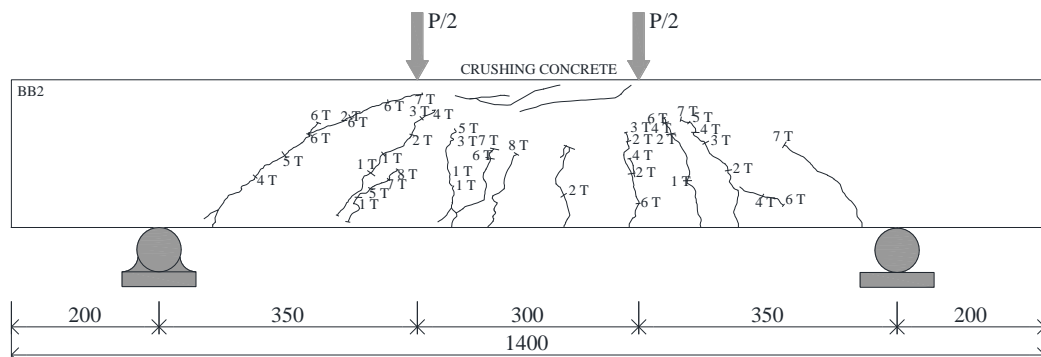
Forward to pure barite concrete BB1, two type of crack is happened. Flexural crack firstly happened in 30 KN in load span area then propagate perpendicularly. Flexural shear crack occurred in 50 KN diagonally in right hand side shear span area continued with left hand side in 60 KN in shear span area. In total, there were five

major crack, which are three flexural crack in load span area and each at one side flexural shear crack in shear span area. Failure occurred due to crushing concrete in compression area.



**Figure 4.33** Crack pattern of beam BB1 at ultimate load

For BB2, there are ten crack occurred with majority flexural crack is developed perpendicularly in load span area. First crack is occurred in 10 KN. Inclining flexural shear crack developed in left hand side of beam started at 40 KN. Final failure is happened due to crushing concrete.



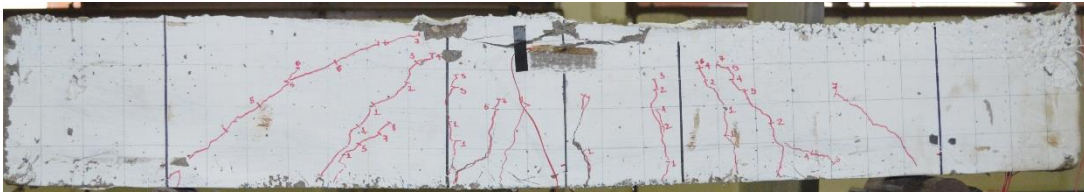


Figure 4.34 Crack pattern of beam BB2 at ultimate load

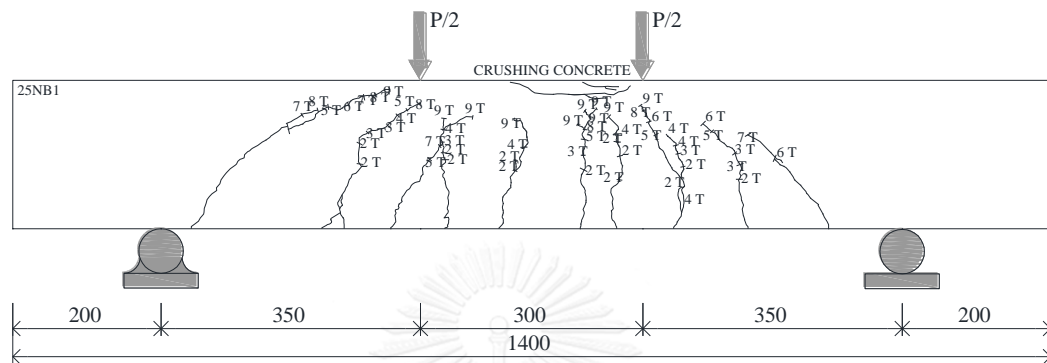
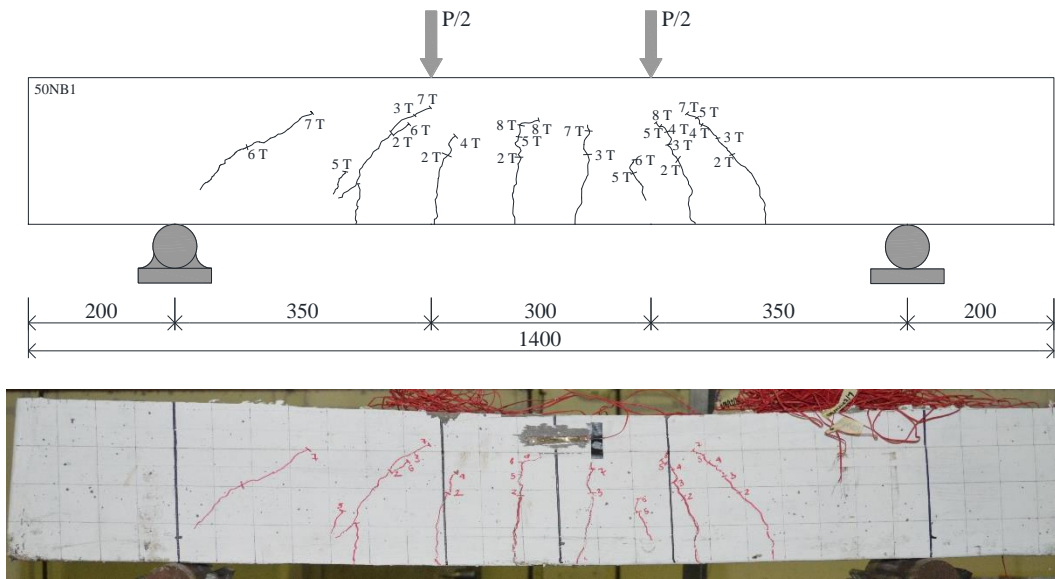


Figure 4.35 Crack pattern of beam RFA-251 at ultimate load

Concrete with 25% replacement fine aggregate showed ten major cracks that largely perpendicular in load span area started at 20 KN. Flexural shear crack is happened diagonally in left hand side of beam from shear span area to support part. This beam is failed due to crush in concrete.

Small cracks observed in beam RFA-501 with seven flexural crack that occurred in load span area. Each two cracks occurred in shear span and other three in load span area. Crack developed at load 20 KN and beam fail due to flexural crack.



**Figure 4.36** Crack pattern of beam RFA-501 at ultimate load

Beam RFA-752 is designated failure by flexural, but in fact it beam failed by shear failure. First 30 KN crack occurred in shear span area in right hand side perpendicularly. Then propagate first flexural shear crack at load 40 KN. Nine major crack with two of it were flexural shear crack diagonally.

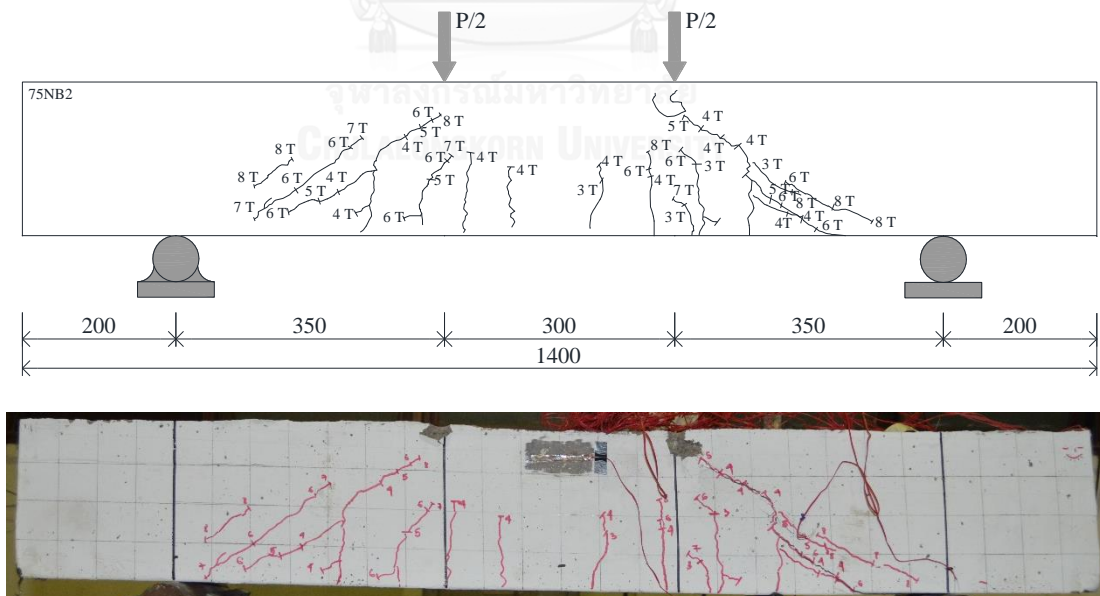


**Figure 4.37** Crack pattern of beam RFA-752 at ultimate load

Beam RCA-1002 had four flexural cracks in load span area that started at load 20 KN. Then, two flexural shear cracks firstly occurred at load 40 KN inclined to compression area beam. This beam continued to propagate crack until load 70 KN and crushing concrete made this beam failed.

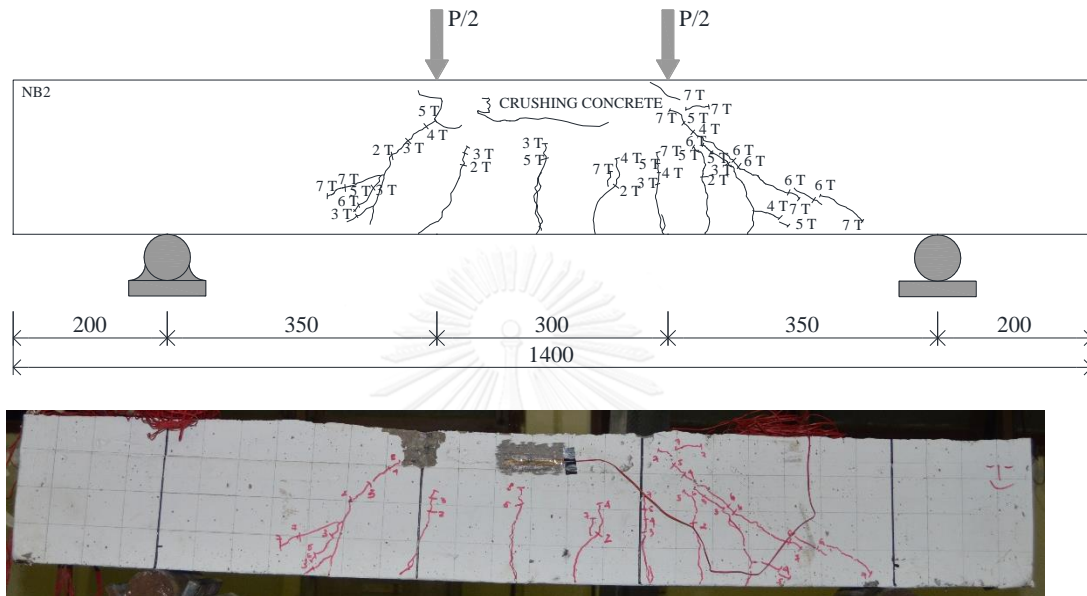


Figure 4.38 Crack pattern of beam RCA-1002 at ultimate load

## 4.7 Design Analysis ACI 349-06

### 4.7.1 Design for Flexural Strength of Barite Concrete

#### 4.7.1.1 Basic Consideration

Design checking for flexural behaviour with special material like heavyweight concrete is necessary to reassure reliability of standard that is used. There are main consideration in flexural analysis as follow:

1. In compatibility condition, any cross section of the beam will remain plane and perpendicular with longitudinal axis while deflection happen.
2. In equilibrium condition, at any point of strain, both concrete and steel are same stage.

3. In constitutive relationship of linear material, any stress can achieve by stress-strain relationship curve for both concrete and steel.

#### 4.7.1.2 Flexural Behaviour

Approaching to compare the result experimental with design standard ACI provision is being done for this study. From experimental result is concluded that barite concrete failed by flexure compression stage. It can be shown with presence of concrete crush in compression area of beam.

By stress-strain relationship curve, calculation compression area of concrete used Hognestad's approaching equation. Assuming parabolic curve with zero stress to the compressive strength of concrete  $f_c'$ , then achieved highest point on that curve representing strain  $\epsilon_0$ . Or simplify with equation as follow

$$f_c = f_c' \left[ 2 \left( \frac{\epsilon_c}{\epsilon_0} \right) - \left( \frac{\epsilon_c}{\epsilon_0} \right)^2 \right] \quad (4.9)$$

Facilitating equation with parabolic curve, stress block equation is introduced in this calculation with using coefficient  $\beta_1$ . Due to this experiment using different value of  $f_c'$  then, it is necessary to compute  $\beta_1$  in term of value of  $f_c'$  as follow:

$$\beta_1 = \left\{ \begin{array}{l} 0.85 \text{ for } f_c' \leq 28 \text{ MPa} \\ 0.85 - 0.05 \frac{(f_c' - 28)}{7} \text{ for } 28 \text{ MPa} < f_c' < 56 \text{ MPa} \\ 0.65 \text{ for } f_c' > 56 \text{ MPa} \end{array} \right\} \quad (4.10)$$

In tension area, reinforcement steel will be regarded as elastic-plastic model with steel modulus of elasticity  $E_s$  is 200,000 MPa. Then, steel rebar model is identify as:

$$f_s = \begin{cases} E_s \epsilon_s & 0 \leq \epsilon_s \leq \epsilon_y \\ f_y & \epsilon_s \geq \epsilon_y \end{cases} \quad (4.11)$$

#### 4.7.1.3 Design Calculation

All computation design for flexural strength followed ACI 349-06 standard for nuclear safety related to concrete structure. Approaching to real situation in experiment result, flexural compression failure at ultimate load is chosen.

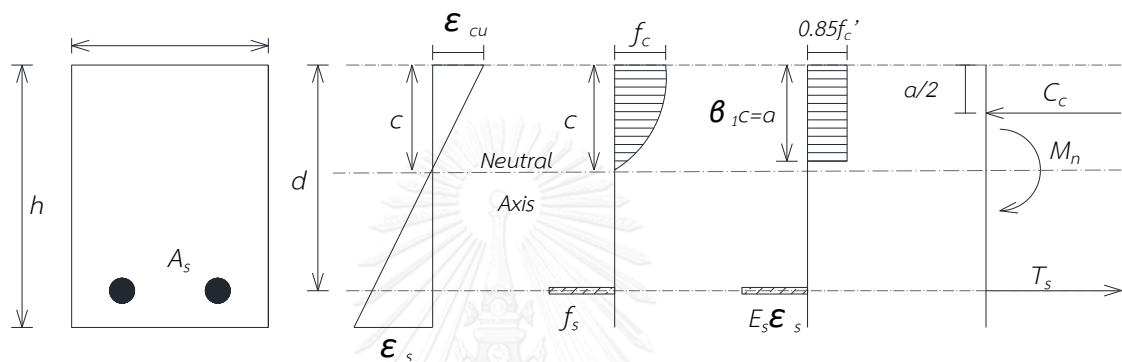


**Figure 4.39** Distribution of stress-strain at ultimate stage

Due to requirement in computational, specification beam that is used for this design is provided as follow:

Beam width (b)	: 150 mm
Beam height (h)	: 200 mm
Flexural depth (d)	: 172 mm
Shear span (a)	: 350 mm
Tension rebar area ( $A_s$ )	: 402 mm <sup>2</sup>
Yield strength rebar ( $f_y$ )	: 522.2 MPa
Modulus of elasticity ( $E_s$ )	: 200,000 MPa
Strain at yield point ( $\epsilon_s$ )	: 2,611 $\mu\text{m/m}$

More, result of compressive strength for this calculation depend on type of mixture in the beam. Information related with compressive strength of each beam is shown in Table 4.12

### Calculation of cracking load

Modulus of rupture in deflection calculation are stated in ACI code as

$$f_r = 0.62\sqrt{f'_c} \quad (4.12)$$

The cracking moment is assigned at the moment due to the stress in the extreme tension to obtain modulus of rupture.

$$M_{cr} = \frac{f_r I_g}{y_t} \quad (4.13)$$

$$P_{cr} = \frac{2M_{cr}}{a} \quad (4.14)$$

**Table 4.12** Varies of cracking load for specimens

Specimen Name	$f'_c$ (MPa)	$f_r$ (MPa)	$M_{cr}$ (kN.mm)	$P_{cr}$ (kN)
NN1	66.81	5.07	5067.9061	28.96
BB1	60.84	4.84	4836.0685	27.63
RFA-251	62.73	4.91	4910.578	28.06
RFA-501	61.35	4.86	4856.0408	27.75
NN2	32.60	3.54	3540.2425	20.23
BB2	36.35	3.74	3738.2505	21.36
RFA-752	31.67	3.49	3488.8747	19.94
RCA-1002	35.96	3.72	3717.834	21.24

### Calculation of ultimate flexural capacity

Using strain distribution in Figure 4.30, equation can be derived as follow:

$$\frac{\varepsilon_y}{d-c} = \frac{\varepsilon_c}{c} \quad (4.15)$$

$$c = \frac{\varepsilon_c d}{\varepsilon_s + \varepsilon_c} \quad (4.16)$$

Then, compression force,  $C_c$  is equal with volume under stress block using Whitney stress block simplification.

$$C_c = 0.85 f'_c b \beta_1 c \quad (4.17)$$

In this experiment, ultimate stage happen due to concrete crushing when steel strain has not reached the yield strain. Then, stress  $f_s$  in tension reinforcement equal with strength in stage  $E_s \varepsilon_s$ . Tension force in steel become

$$T_s = A_s f_s \quad (4.18)$$

Calculating moment in centroid of beam based on force area generate equation as follow:

Moment due to concrete compression force:

$$C_{est} = C_c \left[ \frac{h}{2} - \frac{a}{2} \right] \quad (4.19)$$

Moment due to steel tension force

$$T_{est} = T_s \left[ d - \frac{a}{2} \right] \quad (4.20)$$

Related with flexure compression failure happened in experimental beam, calculated nominal moment strength of beam derived from equation (4.15) and (4.17) become

$$M_{est} = 0.85 f'_c b \beta_1 c \left[ \frac{h}{2} - \frac{a}{2} \right] \quad (4.21)$$

Obtained result from experiment and calculation estimation using ACI 349-06 are summarized in Table 4.13

**Table 4.13** Comparison ultimate load of estimation provision and experimental results

Specimen Name	$M_{est}$ (kN.m)	$M_{exp}$ (kN.m)	$M_{exp}/M_{est}$
NN1	20.25	15.54	0.77
BB1	24.18	14.52	0.60
RFA-251	31.68	16.44	0.52
RFA-501	29.78	13.86	0.47
NN2	19.26	15.17	0.79
BB2	10.84	13.50	1.25
RFA-751	15.60	14.38	0.92
RCA-1002	18.33	13.56	0.74
<b>mean</b>			<b>0.76</b>

#### 4.7.2 Design for Shear Strength of Barite Concrete

In relation with one specimen of this study subjected failed by shear, then it is considered to investigate and compare with design provision standard. Using ACI 349-06 code for designing shear strength in barite concrete, calculation based on failure in yielding stirrup.

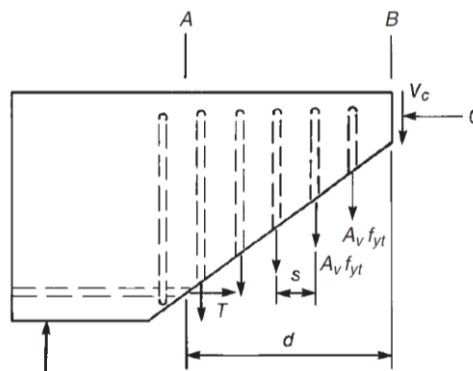


**Figure 4.40** Shear resistant of stirrup

Nominal shear strength carried by concrete based on ACI 349-06 equation (11-3) as follow:

$$V_c = 0.17\sqrt{f'_c}b_w d \quad (4.22)$$

Nominal shear strength carried by shear reinforcement based on ACI 349-06 equation (11-15) as follow:

$$V_s = \frac{A_v f_{yt} d}{s} \quad (4.23)$$

Finally, nominal shear strength can be computed

$$\Phi V_n = \Phi(V_s + V_c) \quad (4.24)$$

Then for specimen RFA-752, give information:

Stirrup yield strength ( $f_y$ ) : 235 MPa

Total stirrup area ( $A_v$ ) : 127 mm<sup>2</sup> (2RB9)

Stirrup spacing(s) : 70 mm

Specified compressive strength of concrete ( $f'_c$ ) : 31.67 MPa

Nominal strength carried by concrete:

$$V_c = 0.17\sqrt{(31.67)} \times 150 \times 172 = 24,682.7(N)$$

Nominal strength carried by steel:

$$V_s = \frac{(127)(235)(172)}{(70)} = 73,333.43(N)$$

Nominal shear strength:

$$\Phi V_n = (0.85)(24,682.7 + 73,333.43) = 83,313.7(N)$$

Ultimate load for shear in estimation of ACI 349-06:

$$P(V)_{est} = 2V_n = 2 \times 83,313.7 = 166,627.4(N) = 166.63(kN)$$

Ultimate load from experimental result:

$$P(V)_{\text{exp}} = \frac{P_u}{2} = \frac{82.17}{2} = 41.085(kN)$$

Result from ACI provision shows that the estimation result is deviating with experimental result. It might be caused equation that is used in ACI 349 is based on normal concrete. For example, the value of  $\lambda$  as parameter unit weight restricted to normal aggregate and lightweight concrete. Then, it need to develop some parameter that can be used for calculation in heavyweight concrete especially in term of structural member. Based on this experiment calculation design from ACI 349-06 provide less than 76% in flexural strength and increasing around 25% in shear strength.



## CHAPTER 5

### Conclusion and Recommendation

#### 5.1 Conclusion of Experimental Result

There is no acknowledgement from previous research that investigating this kind of topic in term of structural members is made present experiment being conducted. Heavyweight concrete is potential development in construction especially Thailand that have abundant raw materials. Some experimental is done to investigate mechanical properties of heavyweight concrete especially barite concrete in term of structural and materials, then this study tried to compare with existing provision code. From some experimental result, the following conclusion can be made:

1. Replacement coarse aggregate with normal aggregate deemed most advantageous in term of workability of concrete. Further, combination fine aggregate-coarse aggregate where one of aggregate use barite and other normal sand or gravel is higher workability compare to any replacement method. However, special treatment by adding superplasticiser considered as necessary due to low workability to make easier when working with reinforcement steel bars.
2. Unit weight of combination replacement of barite concrete resulted 1.2 times concrete that denser and heavier than normal concrete. Then, replacement 25% of aggregate for both w/c ratio generated higher unit weight compared other percentage replacement concrete. By increasing percentage replacement of aggregate will affect in decrease of unit weight.
3. Replacement fine aggregate produced higher compressive strength comparing with replacement of coarse aggregate for both w/c ratio. Enhancement of

compressive strength by replacing fine aggregate compared with coarse aggregate are 7% and 14% for w/c 0.35 and 0.55 respectively.

4. Modulus elasticity barite concrete with replacement of coarse aggregate have lower modulus elasticity than replacement of fine aggregate. It means that barite concrete with replacement with gavel is more ductile. For pure barite concrete, modulus elasticity is higher than normal concrete. In relation with provision standard, ACI 349-06 equation is not applied for barite concrete due to underestimated.
5. Replacement both fine aggregate and coarse aggregate with percentage 25, 50, and 75 needed less thickness compared with 100% combination barite aggregate and normal aggregate or even pure barite concrete when concrete penetrated with energy 0.662 MeV and 1.250 MeV. This experiment resulted that specimen with 25% replacement aggregate has less thickness to reduce half of radiation. More, comparing to previous experiment and average HVL value for normal concrete, present experiment gives good approval in term of HVL for photon energy 0.662 MeV using source Cobalt-60.
6. Flexural stiffness of the barite RC beam approximately closed to normal aggregate. Contribution replacement normal sand in mixture is affected in stiffness of the beam. Increasing replacement fine aggregate by normal sand in mixture impacted by decreasing value of stiffness for almost 25%.
7. Percentage barite in the mixture had main role in ductility factor and not correlated with number of w/c ratio and type of replacement aggregate in the mixture. By increasing percentage of normal aggregate ductility factor increased 20% average ductility factor with increment replacement 25% for both fine aggregate and coarse aggregate.

8. Comparison between estimation design from ACI and experimental result shows that differ each other. It is related to material that used and there is no further provision for heavyweight concrete in term of structural member. Existing standard still used normal concrete as approaching in design of heavyweight. Design of estimation ACI in this study gives less than 62% of experimental result. Developing parameter of unit weight in term of design flexural and shear strength are required for design heavyweight in future.

## 5.2 Recommendation for Future Work

Complementing the present study, there are some recommendations that might be considered to accomplish for future study as follow:

- a. Enriching mixture with different kind of heavyweight material with still considering to workability of concrete.
- b. Measure heavyweight reinforced concrete with shear capacity.
- c. Modelling analysis is needed to perform some parameter that is not shown in ACI standard for heavyweight concrete.
- d. Gaining mechanical properties of heavyweight concrete by including tensile strength.
- e. In term of radiation test, investigate behaviour of concrete using higher energy.

## REFERENCES

- [1] G. H. Brundtland, *Report of the World Commission on environment and development: "our common future."*: United Nations, 1987.
- [2] IAEA. (2014). *Nuclear Share of Electricity Generation in 2014* Available: <https://www.iaea.org/PRIS/WorldStatistics/NuclearShareofElectricityGeneration.aspx>
- [3] K. F. Sozai. (2012, 12 January). *Characteristic of Radiation*. Available: <http://contest.japias.jp/tqj14/140054/etokusei.html>
- [4] ACI, "Guide for Measuring, Mixing, Transporting, and Placing Concrete (ACI 304R-00)," in *Chapter 11 - Heavyweight and Radiation Shielding Concrete*, ed: American Concrete Institute, 2009, p. 41.
- [5] T. C. Society. *Heavyweight Concrete*. Available: [http://www.concrete.org.uk/fingertips\\_nuggets.asp?cmd=display&id=785](http://www.concrete.org.uk/fingertips_nuggets.asp?cmd=display&id=785)
- [6] Departement\_of\_Mineral\_Resources. (2 June). *Geology of Thailand*. Available: [http://www.dmr.go.th/main.php?filename=GeoThai\\_En](http://www.dmr.go.th/main.php?filename=GeoThai_En)
- [7] S. Suthisuntarin, T. Thamkeaw, and W. Pansuk, "Heavyweight Concrete for Radiation Shielding Mixing with aggregate in Thailand " Chulalongkorn University, Thailand2007.
- [8] D. o. M. resources. (2002, 15 June). *Mineral resource maps scale 1:250,000* Available: [http://www.dmr.go.th/ewtadmin/ewt/dmr\\_web/main.php?filename=Map\\_En](http://www.dmr.go.th/ewtadmin/ewt/dmr_web/main.php?filename=Map_En)
- [9] S. Pihlajavaara, "Preliminary Recommendation for Design, Making and Control of Radiation-Shielding Concrete Structures," *ACI Special Publication*, vol. 34, 1972.
- [10] G. Nelson and D. Reilly, "Gamma-ray interactions with matter," *Passive Nondestructive Analysis of Nuclear Materials, Los Alamos National Laboratory, NUREG/CR-5550, LAUR-90-732*, pp. 27-42, 1991.
- [11] J. R. Lamarsh and A. J. Baratta, *Introduction to nuclear engineering* vol. 3: Prentice Hall Upper Saddle River, 2001.
- [12] I. Akkurt, C. Basyigit, S. Kilincarslan, B. Mavi, and A. Akkurt, "Radiation shielding of concretes containing different aggregates," *Cement and Concrete Composites*, vol. 28, pp. 153-157, 2006.
- [13] I. Akkurt, H. Akyildirim, B. Mavi, S. Kilincarslan, and C. Basyigit, "Gamma-ray shielding properties of concrete including barite at different energies," *Progress in Nuclear Energy*, vol. 52, pp. 620-623, 2010.
- [14] F. Bouzarjomehri, T. Bayat, M. Dashti, J. Ghisari, and N. Abdoli, "60 Co  $\gamma$ -ray attenuation coefficient of barite concrete," 2006.
- [15] N. Sainet and N. Toobpuchagron, "Preliminary Study Barite Concrete for Radiation Shielding Gamma-rays," Bachelor, Department of Civil Engineering, King Mongkut's University of Technology North Bangkok, Bangkok, Thailand, 1998.

- [16] S. Kilincarslan, I. Akkurt, and C. Basyigit, "The effect of barite rate on some physical and mechanical properties of concrete," *Materials Science and Engineering: A*, vol. 424, pp. 83-86, 2006.
- [17] K.-H. Yang, J.-S. Mun, and H. Lee, "Workability and Mechanical Properties of Heavyweight Magnetite Concrete," *ACI Materials Journal*, vol. 111, 2014.
- [18] İ. B. Topçu, "Properties of heavyweight concrete produced with barite," *Cement and Concrete Research*, vol. 33, pp. 815-822, 2003.
- [19] Y. Gürsoy, "Investigation of Comparison with Heavyweight Concretes Produced with Dogu Karadeniz Aggregate Deposits and Usual Normal Concrete, MSc, KTU, Institute of Science and Technology, Trabzon, Turkey, 1997," ed: Turkish.
- [20] A. M. Neville, *Properties of concrete*, 1981.
- [21] D. Mostofinejad, M. Reisi, and A. Shirani, "Mix design effective parameters on  $\gamma$ -ray attenuation coefficient and strength of normal and heavyweight concrete," *Construction and Building Materials*, vol. 28, pp. 224-229, 2012.
- [22] A. S. Ouda, "Development of high-performance heavy density concrete using different aggregates for gamma-ray shielding," *HBRC Journal*, 2014.
- [23] D. Tonayopas and W. Nogkaew, "Radiation Shielding of Barite Aggregate Concrete Containing Smectite," in *Engineering Symposium 7th Prince Songkhla University*, Bangkok, Thailand, 2009.
- [24] D. Tonayopas, W. Nogkeaw, and C. Iadpan, "Characteristics of Gamma Radiation Shielding Concrete Containing Barite Aggregate and Ground Raw Perlite," in *Engineering Symposium 6th Prince Songkhla University*, Bangkok, Thailand, 2008.
- [25] E. Wongchirung, "Experimental Investigation of Heavyweight Concrete Properties by Non-Destructive Testing," Master Degree, Department of Civil Engineering, Chulalongkorn University, Bangkok, Thailand, 2011.
- [26] F. Demir, G. Budak, R. Sahin, A. Karabulut, M. Oltulu, and A. Un, "Determination of radiation attenuation coefficients of heavyweight-and normal-weight concretes containing colemanite and barite for 0.663 MeV  $\gamma$ -rays," *Annals of Nuclear Energy*, vol. 38, pp. 1274-1278, 2011.
- [27] F. Demir, G. Budak, R. Sahin, A. Karabulut, M. Oltulu, K. Şerifoğlu, *et al.*, "Radiation transmission of heavyweight and normal-weight concretes containing colemanite for 6MV and 18MV X-rays using linear accelerator," *Annals of Nuclear Energy*, vol. 37, pp. 339-344, 2010.
- [28] T.-C. Ling and C.-S. Poon, "Feasible use of recycled CRT funnel glass as heavyweight fine aggregate in barite concrete," *Journal of Cleaner Production*, vol. 33, pp. 42-49, 2012.
- [29] K.-H. Yang, J.-S. Mun, and H.-J. Shim, "Shrinkage of heavyweight magnetite concrete with and without fly ash," *Construction and Building Materials*, vol. 47, pp. 56-65, 2013.
- [30] F. i. d. béton, *Structural Concrete: Textbook on Behaviour, Design and Performance: Updated Knowledge of the CEB-FIP Model Code 1990*: FIB-Féd. Int. du Béton, 1999.
- [31] A. Committe, "Code Requirements for Nuclear Safety Related Concrete Structures," in *ACI-349*, ed, 1990.

- [32] T. Fujiwara, "Effect of aggregate on drying shrinkage of concrete," *Journal of Advanced Concrete Technology*, vol. 6, pp. 31-44, 2008.
- [33] M. Mahdy, P. Speare, and A. Abdel-Reheem, "Shielding Properties of Heavyweight, High Strength Concrete," in *2nd Material Specialty Conference of the Canadian Society for Civil Engineering*, 2002.
- [34] A. Mollah, G. Ahmad, and S. Husain, "Measurements of neutron shielding properties of heavy concretes using a Cf-252 source," *Nuclear engineering and design*, vol. 135, pp. 321-325, 1992.
- [35] R. Jaeger, "Engineering compendium on radiation shielding. Volume II. Shielding materials," 1975.
- [36] S. Bhuiyan, F. Ahmed, A. Mollah, and M. Rahman, "Studies of the neutron transport and shielding properties of locally developed shielding material: poly-boron," *Health Physics;(USA)*, vol. 57, 1989.
- [37] S. Gujrathi and J. D'auria, "The attenuation of fast neutrons in shielding materials," *Nuclear Instruments and Methods*, vol. 100, pp. 445-452, 1972.
- [38] I. Bashter, "Calculation of radiation attenuation coefficients for shielding concretes," *Annals of nuclear Energy*, vol. 24, pp. 1389-1401, 1997.
- [39] I. Bashter, A. Makarious, and A. E.-S. Abdo, "Investigation of hematite-serpentine and ilmenite-limonite concretes for reactor radiation shielding," *Annals of Nuclear Energy*, vol. 23, pp. 65-71, 1996.
- [40] A. Makarious, I. Bashter, A. E.-S. Abdo, M. S. A. Azim, and W. Kansouh, "On the utilization of heavy concrete for radiation shielding," *Annals of Nuclear Energy*, vol. 23, pp. 195-206, 1996.
- [41] E. Eltehawy, "Behavior of heavy weight concrete under impact effect," in *13th International Conference on Aerospace Sciences & Aviation Technology, Cairo, Egypt*, 2009.
- [42] Y. Yasar and A. Bayülken, "Investigation of neutron shielding efficiency and radioactivity of concrete shields containing colemanite," *Journal of nuclear materials*, vol. 212, pp. 1720-1723, 1994.
- [43] O. Gencil, F. Koksak, C. Ozel, and W. Brostow, "Combined effects of fly ash and waste ferrochromium on properties of concrete," *Construction and Building Materials*, vol. 29, pp. 633-640, 2012.
- [44] F. Ikraiam, J. Ali, A. Abd El-Latif, and A. Abd ELazziz, "Effect of Steel Fiber Addition on Mechanical Properties and gamma-Ray Attenuation for Ordinary Concrete Used in El-Gabal El-Akhdar Area in Libya for Radiation Shielding Purposes," 2009.
- [45] J. O. Henrie, "Magnetite iron ore concrete for nuclear shielding," in *ACI Journal Proceedings*, 1955.
- [46] A. Committee, "Building code requirements for structural concrete (ACI 318-05) and commentary (ACI 318R-05)," 2005.
- [47] A. C637, "Standard Specification for Aggregates for Radiation-Shielding Concrete," ed: Annual Book of ASTM standards, 2003.
- [48] A. C638, "Standard Descriptive Nomenclature of Constituents of Aggregates for Radiation-Shielding Concrete," ed: Annual Book of ASTM standards, 2002.
- [49] A. Committee, "Heavyweight Concrete: Measuring, Mixing, Transporting, and Placing (ACI 304.3R-96)," ed: American Concrete Institute, 2004, p. 8.

- [50] *Nucleonics*. New York: McGraw-Hill Publishing Co., 1955.
- [51] A. Committe, "207.2R-07 Report on Thermal and Volume Change Effects on Cracking of Mass Concrete," ed, 2007, p. 28.
- [52] A. Committe, "224R-01: Control of Cracking in Concrete Structures (Reapproved 2008)," ed, 2001, p. 46.
- [53] A. Committee, "Standard Practice for Selecting Proportions for Normal, Heavyweight, and Mass Concrete (ACI 211.1-91)," ed: American Concrete Institute, 2002, p. 38.
- [54] G. Seegebrecht. *The Role of Aggregate in Concrete*. Available: <http://www.concretenetwork.com/aggregate/>
- [55] A. C127-01, "Standard Test Method for Specific Gravity and Absorption of Coarse Aggregate," ed. Philadelphia, PA: American Society for Testing and Materials 2001.
- [56] A. C128-01, "Standard Test Method for Density, Relative Density (Specific Gravity), and Absorption of Fine Aggregate," ed. Philadelphia, PA: American Society for Testing and Materials 2001.
- [57] A. C29, "Standard Test Method for Bulk Density ("Unit Weight") and Voids in Aggregate," ed: PA: American Society for Testing Materials West Conshohocken, 2009.
- [58] D. Tonnyopas and W. Kamwicha, "Influence of Rice Husk Ash on Strength and Radiation Shielding of Hematite-Ilminite Aggregate Mortar," Bangkok, Thailand, 2010.
- [59] A. C143, "Standard Test Method for Slump of Hydraulic Cement Concrete," ed: ASTM International West Conshohocken, PA, 2004.
- [60] A. C. Moreira, C. R. Appoloni, and C. P. Fernandes, "Gamma ray transmission technique applied to porous phase characterization of low-porosity ceramic samples," *Materials and structures*, vol. 46, pp. 629-637, 2013.
- [61] G. Campione, A. Monaco, and G. Minafò, "Shear strength of high-strength concrete beams: Modeling and design recommendations," *Engineering Structures*, vol. 69, pp. 116-122, 2014.
- [62] A. A370, "Standard Methods and Definitions for Mechanical Testing for Steel Products," ed: American Society for Testing and Material, 1977.
- [63] A. C78-09, "Standard test method for flexural strength of concrete (using simple beam with third-point loading)," in *ASTM International*, ed, 2009.
- [64] S. Özen, C. Şengül, T. Erenoğlu, Ü. Çolak, İ. A. Reyhancan, and M. A. Taşdemir, "Properties of Heavyweight Concrete for Structural and Radiation Shielding Purposes," *Arabian Journal for Science and Engineering*, vol. 41, pp. 1573-1584, 2016.
- [65] A. B. A. Kahtan S. Mohammed, A.M. Mustafa Al Bakri, Kamarudin Hussin, Azmi B. Rahmat, "The Effect of Barite Content on Anti Radiation. Properties of Geopolymer Fly Ash Concrete. Incorporated Natural Rock Ores of Hematite.," *International Journal of Science and Research (IJSR)*, vol. Vol. 3, p. 1818, 2014.
- [66] A. C469-02, in *Standard test method for static modulus of elasticity and Poisson's ratio of concrete in compression* ed. West Conshohocken, Pennsylvania: American Society for Testing and Materials, 2001.

- [67] A. M. Neville, *Properties of concrete*, 1995.
- [68] A. Akkaş, "Determination of the Tenth and Half Value Layer Thickness of Concretes with Different Densities," *Acta Physica Polonica A*, vol. 129, pp. 770-772, 2016.
- [69] N. R. Center. (21 July). *Half-Value Layer*. Available: <https://www.nde-ed.org/EducationResources/CommunityCollege/Radiography/Physics/HalfValueLayer.htm>





APPENDICES

จุฬาลงกรณ์มหาวิทยาลัย  
CHULALONGKORN UNIVERSITY

## VITA

Pamuko Aditya Rahman was born in Pati, Central Java, Indonesia on September 3rd, 1988. He completed his Bachelor Degree in Transportation Planning, Department of Civil Engineering at Sebelas Maret University (UNS) Surakarta, Indonesia in April 2010. Then, he published his research work in journal paper entitled Model Estimation of Distribution Movement from Traffic Count Data with Steepest Descent Method by Software Application EMME/3.

He awarded Academic Achievement Scholarship by PT. Wijaya Karya (Persero), Tbk in 2009 and has been a Junior Engineer in Department of Power Plant and Energy, where he made Smart Entry System for cost budgeting of power plant tender as his innovation for the company. In 2014, he awarded ASEAN Countries Scholarship from Chulalongkorn University, Thailand for pursuing his Master Degree in Structural Engineering, Department of Civil Engineering at Chulalongkorn University, Thailand. Continuing his interest in power plant structure system, his research is related to development special material concrete for structure that is needed radioactive prevention. His current research work is development of effective mixture using local material for gamma-ray attenuation.